



UNIVERSITY OF <sup>TM</sup>  
**KWAZULU-NATAL**

---

**INYUVESI  
YAKWAZULU-NATALI**

## Low-cost Sensory Glove for Human-Robot Collaboration

Submitted By:

Tyrone Bright

(BScEng, UKZN)

215024209

December 2020

Prof. Sarp Adali and Mr. Avern Athol-Webb

Submitted in fulfilment of the academic requirements for the degree of Master of Science in Mechatronic Engineering at the School of Mechanical Engineering, College of Agriculture, Engineering and Science, University of KwaZulu-Natal

## DECLARATION - PLAGIARISM

### Declaration by Author

I, Tyrone Bright, declare that

- i.) The research reported in this dissertation, except otherwise indicated, is my original work.
- ii.) This dissertation has not been submitted for any other degree or examination at any other university.
- iii.) This dissertation does not contain other persons' data, pictures, graphs, or other information unless specifically acknowledged as being sourced from other persons.
- iv.) This dissertation does not contain other persons' writing unless specifically acknowledged as being sourced from other researchers. Where other written sources have been quoted then:
  - a) their words have been rewritten but the general information attributed to them has been referenced;
  - b) where their exact words have been used, their writing has been placed inside quotation marks, and referenced.
- v.) This dissertation does not contain text, graphics, or tables copied and pasted from the internet unless specifically acknowledged, and the source being detailed in the dissertation and in the References sections.

Signed: \_\_\_\_\_

Date: 2 December 2020  
\_\_\_\_\_

Mr. T Bright

### Declaration by Supervisor

As the candidate's Supervisor I agree to the submission of this dissertation.

Signed: \_\_\_\_\_

Date: 2 December 2020  
\_\_\_\_\_

Professor S. Adali

### Declaration by Co-Supervisor

As the candidate's Co-Supervisor I agree to the submission of this dissertation.

Signed: \_\_\_\_\_

Date: 2 December 2020  
\_\_\_\_\_

Mr. A. Athol Webb

## DECLARATION - PUBLICATIONS

DETAILS OF CONTRIBUTION TO PUBLICATIONS that form part and/or include research presented in this thesis (include publications in preparation, submitted, *in press* and published and give details of the contributions of each author to the experimental work and writing of each publication)

**Publication 1:** SAUPEC/R.obMECH/PRASA 2020 (Accepted)

Bright, T. Adali, S and Bright, G. "*A Control System for a Six Degree of Freedom Sensor Glove for Close Human Robot Collaboration*", IEEE, 12th Robotics and Mechatronics Conference of South Africa.

Tyrone Bright was the lead author of this paper and conducted all research while under the supervision of Professor Sarp Adali and Professor Glen Bright.

**Publication 2:** 8th Annual International Conference on Industrial, Systems and Design Engineering 2020 (Accepted)

Bright, T. Adali, S and Bright, G. "*Close Human Robot Collaboration by Means of a Smart Sensory Glove for Advanced Manufacturing Systems*", ATINER, 8th Annual International Conference on Industrial, Systems and Design Engineering.

Tyrone Bright was the lead author of this paper and conducted all research while under the supervision of Professor Sarp Adali and Professor Glen Bright.

Signed:



Mr. T Bright

Date: 2 December 2020

---

## ACKNOWLEDGEMENTS

I would first like to acknowledge my mother (Lizell Bright), my father (Glen Bright), my grandmother (Salome Currin), my partner (Jessica Du Preez), Mrs Miep and Polly for the love and support that they provided me through this research project. A special thanks needs to be given to my supervisors Prof. S Adali and Mr A Athol-Webb for the opportunity to further my research career in the field of Engineering. I would like to thank them for the academic support that they provided me through this journey. I would like to thank Mr G Loubser, Senior Electronic Technician at the University of Kwa-Zulu Natal for his guidance and assistance throughout my project.

“If you get up in the morning and think the future is going to be better, it is a bright day.”

~ Elon Musk ~

## ABSTRACT

Human Robot Collaboration (HRC) is a technique that enables humans and robots to co-exist in the same environment by performing operations together. HRC has become a vital goal for industry to achieve progress towards the fourth industrial revolution (Lotz, Himmel, & Ziefle, 2019) as it focuses on creating advanced production/manufacturing plants that have high levels of productivity, efficiency, quality and automation. Sensory gloves can be used to enhance the Human Robot Collaboration environment in order to achieve progress towards Industry 4.0. It can provide a safe environment where humans and robots can interact and work in conjunction. However, challenges exist in terms of cost, accuracy, repeatability and dynamic range of such devices.

The project researched and developed a low-cost sensory glove to enable a user to collaborate with an industrial robot in a production environment. The sensory glove was used to provide a process whereby humans could collaborate with the robot through physical interaction under safe conditions. The sensory glove used IMU sensors in order to track the orientation of the user's hand accurately. An algorithm was developed and designed to extract the data from the glove and create a simulated three-dimensional render of the hand as it moved through free space. This involved the design and development of an electronic system architecture that powers the glove. A control system was developed to enable the extraction of data and create the simulated three-dimensional hand model. It produced the image that the robot would sense when interacting with the worker. Testing was conducted on the cost, accuracy, dynamic range, repeatability and potential application of the system.

The results showed that it was an innovative and low-cost method for humans and robots to collaborate in a safe environment. The apparatus established a process whereby humans and robots could perform operations together.

**Keywords:** Human-Robot Collaboration, Industry 4.0, Low-cost Sensory Glove, Flexible Manufacturing

## ACRONYMS

AMS	Advanced Manufacturing Systems
BMW	Bayerische Motoren Werke
BMP	Beats per Minute
CAD	Computer-aided Design
CMC	Carpometacarpal
DIP	Distal Interphalangeal
DH	Denavit & Hartenberg
DOF	Degree of Freedoms
EKF	Extended Kalman Filter
EU	European Union
FIR	Finite Impulse Response
FMS	Flexible Manufacturing Systems
HRC	Human Robot Collaboration
HRI	Human-Robot Interaction
ICC	Intra-Class Correlation
IFT	Inverse Fourier Transform
IMU	Inertial Measurement Unit
IP	Interphalangeal
I2C	Inter-Integrated Circuit
KF	Kalman Filter
LED	Light Emitting Diode
MARG	Magnetic, Angular Rate and Gravity
MCP	Metacarpophalangeal
MEMS	Micro Electro-Mechanical System
PCB	Printed Circuit Board

---

PIP	Proximal Interphalangeal
PLA	Polylactic Acid
SCL	Serial Clock Line
SDA	Serial Data Line
SMME	Small, Medium and Micro Enterprises
TOF	Time of Flight
VW	Volkswagen
WiFi	Wireless Fidelity
3D	Three Dimensional

## NOMENCLATURE

A	Ampere
$g$	Acceleration of gravity
K	kilo
Hz	Hertz
m	milli
M	Mega
T	Time (Second)
V	Voltage
$\theta$	Theta
$\phi$	Phi



## TABLE OF CONTENTS

DECLARATION – PLAGIARISM.....	i
DECLARATION – PUBLICATIONS .....	ii
ACKNOWLEDGEMENTS .....	iii
ABSTRACT.....	iv
ACRONYMS.....	v
NOMENCLATURE .....	vii
TABLE OF CONTENTS.....	viii
LIST OF FIGURES .....	xii
LIST OF TABLES.....	xiv
1. INTRODUCTION .....	1
1.1 Wearable Technology .....	1
1.2 Research Question and Objectives.....	2
1.3 Conclusion .....	7
2. LITERATURE REVIEW .....	8
2.1 Introduction.....	8
2.2 Mechatronics & Link to Wearable Devices .....	8
2.3 Sensory Glove.....	11
2.4 Mathematical Modelling.....	14
2.4.1 Quaternions .....	15
2.4.2 Euler Rotation Theorem.....	16
2.5 Filters .....	17
2.5.1 Kalman Filters.....	18
2.5.2 Averaging Filter .....	18
2.6 Current Sensory Gloves .....	19
2.7 Human-Robot Collaboration Environments .....	23
2.8 Conclusion .....	28
3. MECHATRONIC DESIGN APPROACH .....	30
3.1 Introduction.....	30

---

3.2	Proposed Mechatronic Design Approach.....	30
3.3	Design and Performance Specifications.....	32
3.3.1	Sensors .....	32
3.3.2	Microcontroller .....	33
3.3.3	Software .....	33
3.3.4	Filter Design.....	33
3.3.5	Glove and Structural Components .....	34
3.3.6	System Integration .....	34
3.4	Concept Design.....	35
3.4.1	Design Concept 1 .....	35
3.4.2	Design Concept 2.....	36
3.4.3	Design Concept 3.....	37
3.4.4	Decision Matrix.....	38
3.5	Final Mechatronic Design.....	39
3.5.1	The Mechanical Hand Model.....	40
3.5.2	An Averaging Filter Design.....	42
3.5.3	Data Acquisition and Post-processing Algorithm.....	44
3.5.4	Circuitry .....	45
3.5.5	Glove Structure .....	46
3.6	Conclusion .....	47
4.	MANUFACTURING & ASSEMBLY OF SENSORY GLOVE .....	50
4.1	Introduction.....	50
4.2	Manufacturing and Assembly Process of the Sensory glove .....	51
4.2.1	The Electrical & Electronic System.....	51
4.2.2	The Computer System.....	56
4.2.3	The Control System .....	60
4.2.4	Mechanical System.....	68
4.3	Conclusion .....	70
5.	TESTING & RESULTS OF SENSORY GLOVE.....	73

---

5.1	Introduction.....	73
5.2	Accuracy Test .....	74
5.3	Dynamic Range Test.....	77
5.4	Repeatability Test .....	80
5.5	Application Test.....	82
5.6	Conclusion .....	86
6.	DISCUSSION AND FURTHER DEVELOPMENTS.....	88
6.1	Introduction.....	88
6.2	Technology & Methodologies .....	88
6.3	Human Robot Collaboration .....	90
6.4	Design and Development of Sensory Glove .....	91
6.5	Testing and Validation of Sensory Glove .....	93
6.6	Conclusion .....	95
7.	CONCLUSION.....	97
8.	REFERENCES .....	100
9.	APPENDIX.....	104
A	Arduino® Code and Results .....	104
A.1	Arduino® Code for Data Extraction (MPU6050).....	104
A.2	Results for Single MPU6050 from Arduino® IDE.....	108
B	Data Sheets.....	109
B.1	Data Sheet pages for MPU6050 (TexasInstruments, 2016).....	109
B.2	Pinout Diagram of the Arduino® Due (Components101, 2018) .....	112
C	Solidwork® CAD Drawings .....	113
C.1	Human Hand Model.....	113
C.2	Palm Model.....	114
C.3	Index Finger Assembly .....	115
C.4	Sensor Holder.....	116
D	MATLAB® Code .....	117
D.1	Simulink® Write Function.....	117

---

D.2	Simulink <sup>®</sup> Read Function.....	117
D.3	Roll and Pitch Estimation Function .....	117
D.4	Frequency Spectrum Analysis Function .....	118
D.5	Cleaning Function.....	118
D.6	Data Prep Function.....	119

## LIST OF FIGURES

Figure 2-1: Concept of a mechatronic System (Silva, 2005) .....	9
Figure 2-2: A four-stage model of human information processing (Liu & Wang, 2018).....	10
Figure 2-3: Different types of Sensory Technology .....	10
Figure 2-4: Skeleton Structure of the Human Hand (Nanayakkara, et al., 2017) .....	13
Figure 2-5: Simplified kinematic structure of the human hand .....	14
Figure 2-6: Euler Angle Rotation Diagram A, B and C (Weisstein, 2020) .....	16
Figure 2-7: Prime Xsens Glove (Manus VR, 2020).....	20
Figure 2-8: Sensory Glove Design by (Weber, Reuckert, Calandra, Peters, & Beckerle, 2016).....	20
Figure 2-9: Sensory Glove Design by (Moreira, et al., 2014).....	21
Figure 2-10: Design of Sensory Glove by (Baldi, Scheggi, Meli, Mohammadi, & Prattichizzo, 2017) .....	22
Figure 2-11: Design of Sensory Glove by (Kortier, Sluiter, Roetenberg, & Veltink, 2018) .....	22
Figure 2-12: Levels of Interaction Framework for HRC Systems (Villani, Pini, Leali, & Secchi, 2018) .....	23
Figure 2-13: Examples of traditional and collaborative industrial robots. (Villani, Pini, Leali, & Secchi, 2018).....	25
Figure 2-14: ROBO-PARTNER production paradigm in the automotive industry (Michalos, et al., 2014).....	26
Figure 2-15: UR-5 robot on the VW factory floor (Leber, 2013).....	27
Figure 3-1: Adapted mechatronic Design Process.....	30
Figure 3-2: Configuration of Human Finger.....	40
Figure 3-3: Example of the Solidwork <sup>®</sup> 's human hand model (Rhadamanthys76, 2016).....	41
Figure 3-4: Simulink <sup>®</sup> Hand Model.....	42
Figure 3-5: Response of the FIR filter for L = 4, 8 and 16 (Gonzalez-Barajas & Montenegro, 2016).44	
Figure 3-6: Simplified Circuitry .....	45
Figure 3-7: Creality CR-10 Max 3D Printer .....	47
Figure 3-8: Sketch of the Final Mechanical Design.....	49
Figure 4-1: The Fundamental Components of a mechatronic System (Spiegel, 2017) .....	50
Figure 4-2: Initial Setup of Electronic System.....	51
Figure 4-3: Sketch of electrical & electronic architecture .....	52
Figure 4-4: Design of PCB Board: Top View (Left) & Bottom View (Right) .....	53
Figure 4-5: Design of modified PCB Board: Top View (Left) & Bottom View (Right).....	55
Figure 4-6: Design of final PCB Board: Top View (Left) & Bottom View (Right).....	56
Figure 4-7: Final Mechanical assembly of Human Hand .....	59
Figure 4-8: Simscape Multibody Model of Human Hand .....	60

Figure 4-9: Stateflow workflow of the Control System.....	61
Figure 4-10: Simplified Data Acquisition and Configuration Model .....	62
Figure 4-11: Initial (Right) and Final (Left) position of the hand model.....	64
Figure 4-12: Frequency response graph from an IFT .....	65
Figure 4-13: Sensor data before (blue line) and after (yellow line) the averaging filter was implemented. .....	66
Figure 4-14: Part 1 of the Postprocessing Model in Simulink® .....	67
Figure 4-15: Postprocessing Model (Part 2) .....	68
Figure 4-16: Entire Simulink® Model.....	68
Figure 4-17: Mac Afric Working Glove (Adendorff, 2020).....	69
Figure 4-18: Final Design of Sensor Holder.....	70
Figure 4-19: The Final Sensory Glove.....	72
Figure 5-1: 3D printed hand and Goniometer.....	74
Figure 5-2: Flat hand orientation Phase (Right) and Clench hand orientation Phase (Left).....	75
Figure 5-3: A Bland-Altman agreement graph that uses the theory from the 'Limit of Agreement' on the Index finger values.....	77
Figure 5-4: Set-up of Dynamic Range Test with a metronome, sensory glove and clay model cast....	78
Figure 5-5: Dynamic Range of the Proximal Joint (Top), Middle Joint (Middle) and Distal Joint (Bottom) on the Sensory Glove. ....	79
Figure 5-6: Flat hand Phase (Left) and Clench hand Phase (Right).....	80
Figure 5-7: Ufactory xArm 5 Lite (UFACTORY, 2020).....	82
Figure 5-8: Flowchart of the designed Algorithm.....	84
Figure 5-9: xArm 5 Lite in the waiting Phase (Left) & xArm 5 Lite in waiting Phase as Sensory glove approaches the neck of the robot (Right). ....	85
Figure 5-10: Sensory gloves unlocks the joints of the xArm robotic arm to enter the Unlock phase (Left) & the Sensory glove moves the robotic arm into its final position (Right). Once the Sensory glove releases the neck, the xArm 5 Lite will be in Operation phase.....	86
Figure 6-1: The Fundamental Components of a mechatronic System (Brown, 2011) .....	89
Figure 6-2: Final product of the sensory glove .....	93
Figure A-1: Results for Single MPU6050 from Arduino® IDE.....	108
Figure B-1: Arduino® Due Pinout Diagram (Components101, 2018).....	112
Figure D-1: Simulink® Write Function.....	117
Figure D-2: Simulink® Read Function.....	117

## LIST OF TABLES

Table 3-1: Decision Matrix for Final Mechatronic Design.....	39
Table 4-1: Mean finger lengths and palm dimensions of the hand (Chen Chen, et al., 2011).....	57
Table 4-2: Mean length of hand and phalanges of index, middle, ring, and little finger (cm) (Chen Chen, et al., 2011) .....	57
Table 4-3: Static Constraints on specific finger joints (Chen Chen, et al., 2011).....	58
Table 5-1: Measured relative angular value using the Goniometer as well as the simulated values from the sensory glove for the index finger.....	76
Table 5-2: Pearson's Co-efficient for Index Finger Joint Values .....	76
Table 5-3: Results of Repeatability Analysis.....	81
Table 5-4: Results from HRC Application Test.....	85
Table B-1: Gyroscope Specifications (TexasInstruments, 2016) .....	109
Table B-2: Accelerometer Specifications (TexasInstruments, 2016) .....	110
Table B-3: Electrical and Other Common Specifications (TexasInstruments, 2016).....	111

# 1. INTRODUCTION

The methodology of capturing, analysing and interacting with humans, such as the human hand, has been a focal point of research in several applications. (Baldi, Scheggi, Meli, Mohammadi, & Prattichizzo, 2017). These applications range from the rehabilitation of the human hand motion to human-robot collaboration. In recently years, there has been a focus placed on collaborative systems to adopt systems that can interact with humans. Different types of application are clearly stated later in the chapter. In order to achieve such systems, extensive research has been conducted on devices that could create a collaborative environment between robots and humans. Such devices that have made this possible are known as wearables.

## 1.1 Wearable Technology

Wearable technology has been the focus of achieving systems that improve the way humans interact with the surrounding environment and objects (Pacchierotti, Prattichizzo, & Kuchenbecker, 2015). Wearable technology has the advantage of being well-integrated into peoples' habits, which results in more accurate and reliable information. With this, the goal is that wearable technology will become integrated with our clothing and becoming part of our bodies. In recent years, wearable technology has seen significant improvements as there has been an increasing interest in developing solutions that can accurately track the motion of the human body (Baldi, Scheggi, Meli, Mohammadi, & Prattichizzo, 2017). Due to these reasons, wearable technology will be the focus of the research.

Wearable technology uses Micro Electro-Mechanical System (MEMS) technology. Most commonly, MARG (Magnetic, Angular Rate and Gravity) devices, which are a variant of MEMS, have been used in Wearable technology. This device consists of a MEMS triaxial gyroscope, accelerometer and magnetometer. These sensors are integrated into wearable technology and are used to track the orientation of the human body. The major drawback of these devices is that the algorithm used on these devices relies on the magnetometer. Magnetometers are sensitive to variations in magnetic fields and are not ideal in a manufacturing environment. However, these devices have been used in developing a tracking glove by (Kim, Soh, & Lee, 2005) and (Kortier, Sluiter, Roetenberg, & Veltink, 2018).

A focus of Wearable technology, in particular sensory gloves, has seen increased interest and research in the Human-Robot Collaboration (HRC) field. An HRC environment involves humans and robots working together, in a safe environment, towards a common goal. The process of collaborating with a human was defined by (De Luca & Flacco, 2012) where they outlined the broad ideology of HRC systems. The HRC systems focused on three core principles. These core principles revolved around coexistence, collaboration and safety. These principles are what make sensory gloves a promising area of research for manufacturing, production or assembly systems.



The focus of the research is specific on Flexible Manufacturing Systems (FMS). These systems are production methods that were designed to easily adapt and change to the type and quantity of a product (Hayes, 2019). This system was chosen as the focus of the research as they were designed to improve efficiency and lower production costs. Wearable technology has the potential to become a disruptive technology in this field as it enables humans to enhance the flexibility element to the system. Flexible Manufacturing Systems was one of the goals of the fourth industrial revolution as the world attempts to achieve Factories of the Future.

## 1.2 Research Question and Objectives

The purpose of the study was to find the answer to the following research question:

*'Could a low-cost mechatronic sensory glove be designed and developed to enable humans and robots to collaborate in a highly customizable environment in Advanced Manufacturing Systems (AMS)?'*

In order to achieve this, the project was divided into five objectives. These objectives ensured that the project focused on the core concepts of the project. The objectives were:

- Research technology and methodologies that enabled current sensory gloves that have the ability to provide Human-Robot Collaboration.
- Review and understand the role of humans and robots in the manufacturing environment to provide a safe environment.
- Design and develop a mechatronic sensory device for use in a Human-Robot Collaborative environment.
- Test and validate the performance of the glove versus the cost of the glove
- Conclude and discuss potential improvements of the sensory glove.

Each objective was created to highlight the potential impact that the research could have in the field of study. The first objectives focused on researching technologies associated with wearable technology and different methodologies that have been used to create sensory gloves. Sensory gloves are a form of a wearable device that was identified as a possible approach to track the orientation of a workers' hand accurately. Sensory gloves were built using different components, such as Inertial Measurement Unit (IMU) sensors and flex sensors. The research was required to determine the most efficient and cost-effective components when designing and developing a sensory glove. It was crucial as it established the formal design requirement for conventional sensory gloves.

The sensory glove was identified as a mechatronic design product. A mechatronic design was a synergistic combination of mechanical, electronic, control and computer engineering in the development of electromechanical products or systems (Silva, 2005). Therefore, extensive research

was conducted on the mechatronic design approach and the link to wearable technology. Through this research, the researcher understood that the mechatronic design approach was the best design method to create a working and effective sensory glove. Three key areas of the sensory glove were explored to determine the best and cost-effective solutions.

The first area of the research focused on the mathematical modelling of a human hand and how to capture the motion. The researcher needed to understand the structural design of a human hand and how it could be mathematically modelled. Research suggested that the hand could be modelled as a single kinematic chain with a series of links and joints that modelled the phalanges and phalange joints respectively. This was achieved by using the Denavit & Hartenberg (DH) method. The capturing of the human hands' motion required research on different mathematical approaches that model a hands' orientation. Two methods were identified as Euler angles or quaternions. Both these methods could integrate the data from the associated sensors to capture the orientation of the human hand.

The second area of research focused on the filter design of the system. The filter design was an important research area as it reduced the noise in the system and created a more accurate solution. This research area was focused on understanding the different types of filters available to develop an effective and low-cost solution. A key area was focused on achieving an accurate yet a low computationally expensive solution. This was due to the application of the project and the low-cost objective that needed to be achieved. Kalman filter and an averaging filter were both researched to determine the best solution.

The final research area included existing sensory gloves that had been designed and developed. These sensory gloves included university research as well as commercially available products. The sensory gloves all performed orientation and motion capturing of the human hand. Optitrack and Cyberglove were commercially available sensory gloves that had advanced algorithms and proprietary technology. These gloves had high performance and accuracy but at a high price. These gloves retailed for on average €3990. This was the major drawback of these products.

(Weber, Reuckert, Calandra, Peters, & Beckerle, 2016) designed and developed a sensory glove that used flex sensor technology. The project was aimed at creating a low-cost sensory glove. While it achieved this, it had poor performance as flex sensors suffered from sensor displacement errors and complex calibration procedures. (Kortier, Sluiter, Roetenberg, & Veltink, 2018) designed and developed a sensory glove that used IMU technology and an extended Kalman filter (KF). The sensory glove had a high dynamic range and small repeatability with a computational expensive Kalman filter to improve the performance of the system. Through these and many other research projects, the researcher chose (Kortier, Sluiter, Roetenberg, & Veltink, 2018) sensory glove to focus the research around while developing a low-cost solution.

In order to create an effective device for an HRC environment, the role of humans and robots in a manufacturing field was critical to understand. This was the second objective of the project as without

this understanding, a solution could not be achieved. The researcher needed to understand what collaboration meant and how it differed from a conventional human-robot operation. (De Luca & Flacco, 2012) defined the difference between coexistence and collaboration with respect to humans and robots in the same manufacturing environment. This enabled the researcher to establish a framework, that was first proposed by (Villani, Pini, Leali, & Secchi, 2018). This framework displayed the level of interaction/collaboration and the features of it. An understanding was reached that HRC systems exist when the robot and the human worker work together towards a common goal.

As the manufacturing industry evolved, a paradigm shift occurred. This shifted was towards the mass production of highly customizable products (Pedersen, et al., 2016). This promoted the growth of Flexible Manufacturing Systems (FMS) which was a production method that focused on easily adapting to the change in the type and quantity of a product. These systems could improve efficiency and lower production cost. FMS environments required higher upfront costs while this project aimed at lowering that by the introduction of the low-cost sensory glove. The sensory glove would enable companies to create FMS systems as humans could collaborate with robots when a different part or batch size was present on the production floor. With HRC environments, safety was an essential factor of the research, as it was preventing the growth and development of HRC systems. Therefore, current examples of HRC systems were researched and discussed to determine the limitations of HRC environments.

Through the research, the researcher analysed the limitations and capabilities of HRC environments, based on ROBO-PARTNER project. The main obstacle that HRC environments encountered was the lack of laws and legislations that could enable it in the production environment. These laws and legislations needed to be developed with safety as its key feature. The use of the sensory glove would provide a device that could potentially ensure the safety of humans when collaborating with robots.

The design and manufacturing of the sensory glove required extensive work to create the best possible solution. With the focus of the sensory glove being a mechatronic system, extensive research was done one each component of the sensory glove system. This was done to ensure that an effective and low-cost device could be achieved. With different components researched, three conceptual designs were created for the device. Each conceptual design featured various components in some areas of the system. These included IMU sensors compared to Flex sensors and extended Kalman filters compared to averaging filters. Each design was analysed and a decision matrix was used to determine the best design. The matrix considered factors that were centred around creating an effective, efficient and low-cost solution. With the best design chosen, the researcher began with the final design and manufacturing of the device.

The final design of the project focused on the four elements of a mechatronic system. The electrical and electronic component consisted of multiple IMU sensors, two multiplexers, an Arduino® and a PCB board. The IMU sensors presented a challenge due to the hardware operational parameters.

Serial

communication between the IMU sensors and the microcontroller presented a challenge that had to be overcome. These issues were resolved through further research and the use of an Arduino<sup>®</sup> Due to the system. A PCB board was designed and manufactured to create the electrical architecture of the system. The board created a compact and effective solution as LEDs were installed to indicate when the system was operational and where a fault may occur in the wiring if one arose.

Extensive research was conducted in order to determine the correct software package that could enable high levels of integration between the systems of the sensory glove. This was important as integration was a key feature in the development of mechatronic systems. Through research, two computer systems were chosen. They were AutoCAD<sup>®</sup> and Simulink<sup>®</sup>. These two software packages were chosen as integration tools existed between the two platforms. AutoCAD<sup>®</sup> was used to create the model of a human hand. This formed part of the computer system of the research. The dimensions and configuration of the hand was based on biological kinematic research by (Chen Chen, et al., 2011). Once built, the model was integrated into Simulink<sup>®</sup> to formulate and solve the equations of motion of the system. It was done through the Simscape multibody tool in Simulink<sup>®</sup>. This proved to be a challenge as certain complex geometric shapes were not imported correctly. Iterations of the hand were made in order to accompany these problems.

The Simulink<sup>®</sup> package was chosen as it was a robust software package. It had Arduino<sup>®</sup> hardware integration support and filter design tools. Therefore, the package provided the ability to integrate the mechanical model of the human hand with the control system of the project. The package converted the mechanical model of the hand into a single chain system that could be controlled through torque or motion inputs of each revolute joint. The model was designed to use motion data, from the sensory glove, to simulate the motion of the sensory glove while in operation. This would be used to test and validate the performance of the device.

The control system of the project required a well-built algorithm. The algorithm was divided into a data acquisition process and a post-processing process. The data acquisition process involved extracting the raw data from the IMU sensors and configuring the data into the roll and pitch values for each IMU. This was done through a series of gain blocks and mathematical equations. This process had several serial communication challenges, which included only two IMU sensors being read simultaneously. Initially, both roll and pitch values were integrated together to provide the most accurate orientation of the sensor. However, since the algorithm could only read two sensors at a time, there would be a time delay when combining the roll with the pitch value of all the sensors. This resulted in two different sets of data for the pitch and roll values from a single sensor. Therefore, only the pitch values were used to achieve the most accurate result possible for the device.

The second process of the control system involved configuring each sensor on the sensory glove to the respective phalange on the Simulink<sup>®</sup> model. This was known as the post-processing process. This

algorithm used the data values from the data acquisition process and performed mathematical calculations to integrate it with the Simulink<sup>®</sup> hand model. Two filters were researched and one was chosen to be implemented in the process. The filter was needed as it could reduce high-frequency noise and smoothen the signal from the sensors. This resulted in a more reliable and accurate system. Once designed, the filter was implemented before the configured data was sent to the Simulink<sup>®</sup> hand model. The simulated dynamic model of the hand, using these algorithms, provided a preliminary test that showed that the glove could capture the motion of a human hand.

The final component of the mechatronic design consisted of the mechanical elements. This required research into synthetic glove material that could provide high strength and durable properties. The glove needed to be easy to work with and fit on an average human size hand. The sensors and Arduino<sup>®</sup> needed to be encased in a protective holder to ensure they were safe during operation. Therefore, the researcher designed two protection holders, one for the sensors and one for the Arduino<sup>®</sup> board. The sensor holders were attached to the glove to provide a method of attachment for the sensor to the glove. The holders were 3D printed as it provided a low cost and flexible manufacturing method. It also provided a strength parameter which were needed in the project.

The fourth objective was aimed at testing the performance of the sensory glove. In order to achieve this, four tests were conducted on various parameters of the device. These tests included:

- Accuracy Test
- Dynamic Range Test
- Repeatability Test
- Application Test

Each test assisted in determining the overall performance of the sensory glove and how it compared to current devices with similar functionalities. To best analysis the results, a statistical analysis was designed and developed for the sensory glove. This data was compared to current sensory gloves to understand how well it performed in relation to other sensory gloves that were commercially available. The final test was used as a proof of concept. It was performed to verify if it was possible to implement such a device in a manufacturing environment for humans and robots to collaborate in the same space. This was an important test as it would verify if such device could be used in the desired application of the project.

The design of the sensory glove needed to be created as a mechatronic system. The components of sensory glove displayed all the components of engineering in a mechatronic system. With the major focus on integration, the designed sensory glove would be able to achieve an efficient, high performance and cost-effective solution. The focus was placed on each of the four aspects of engineering when creating the device.

### 1.3 Conclusion

This thesis will showcase the information and results that the researcher obtained when achieving the five objectives of the project. Based on the following analysis of each objective, a conclusion was made in order to answer the above-mentioned research question. Chapter Two focuses on the understanding of sensory glove technology and Human-Robot Collaboration Systems. Chapters Three and Four were centred around the design and development of the project. They displayed the transformation of the project from the initial design to the final product, outlining the limitations and difficulties experienced while developing the device. Chapter 5 was the performance section of the project. It showed the performance of the device versus similar sensory gloves that are commercially available. The sixth and final chapter summarized the successes and shortfalls of the project. It concluded on the device and improvement that could be made to improve it.

## 2. LITERATURE REVIEW

### 2.1 Introduction

In order to design and develop an innovative sensory glove, an extensive study was required to understand the state of the research. This included identifying four key aspects, where advancements could be performed in order to grow the field of study. The first aspect of the research explored the link between sensory gloves and mechatronic engineering. This laid the foundation to identify the specifications required to develop such a device. Secondly, the study needed to defined sensory gloves and the associated benefits for human motion capture. It needed to outline why sensory gloves are used over other motion capturing technology.

In order to begin the conceptual design process, an extensive study of current sensory gloves was required. These sensory gloves had made significant advances in the field, in terms of reducing orientation estimation errors and improving the kinematic hand model. This research focused on current sensory glove projects and provided fundamental advancements that progressed the state of research. While various applications of the sensory glove exist in the research work, such as rehabilitation and Advanced Manufacturing Systems (AMS), the focus of the research was to adapt it for a Human Robot Collaborative environment, for Advanced Manufacturing Systems.

This research focused on the Advanced Manufacturing sector by defining the potential application of sensory gloves with Human-Robot Collaboration Systems. The Advanced Manufacturing sector included Flexible Manufacturing Systems that were used to create highly customizable products in factories of the future. In this chapter, the literature explored the above statements and showed relevance to the master's project.

### 2.2 Mechatronics & Link to Wearable Devices

Mechatronics is a synergistic combination of mechanical, electronic, control and computer engineering in the development of electromechanical products or systems (Silva, 2005). It requires a multidisciplinary approach for the design, development and implementation of a mechatronic system. Therefore, a mechatronic solution is an integration of mechanical, electronic, computer and control components. The selection of these components must be done concurrently throughout the design stages. This improved approach differs from traditional developments of electromechanical systems, where the components of the solution were selected separately and then integrated.

The use of mechatronics in a solution allows a unique advantage as it represents an approach to the design of engineering systems that involves the integration of all the Engineering disciplines as

mentioned above at all levels of the design process (Bradley, 2000). Concurrent selection of components allow the components to be chosen, not only based on their performance, but on their integration capabilities with each other. It produces a unified system that can limit potential systematic errors due to communication errors or integration complexities.

A mechatronic system typically consists of a mechanical model, sensors, controllers, interface devices, power sources, computer hardware and software. The sensors and controllers allow for data acquisition, while the interface devices allow for the transfer of information. This makes up the fundamental electronic components of the design. The mechanical model of the system is the fundamental mechanical component of the project. The control aspect of the design is built with the use of an algorithm. The algorithm is implemented onto the desired hardware of the project. It ensures that the hardware and software of the project are integrated. The computer hardware and software make up the computer components of the system.

In order to create a mechatronic system, a simultaneous design process of a multi-component system is required to ensure that the design of all the components have the ability to be efficiently integrated. Figure 2-1 below shows the concurrent design process in order to achieve a complete mechatronic system.

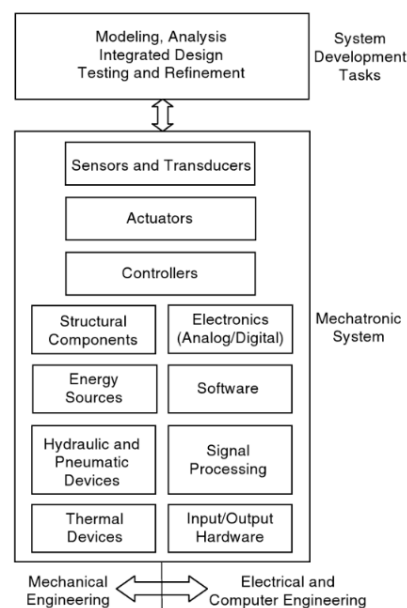


Figure 2-1: Concept of a mechatronic System (Silva, 2005)

This design approach ensures that the development of a mechatronic system is efficient and economical. It provides a solution that is of higher quality, improved operational performance and more reliable. Therefore, a mechatronic design should be defined as an optimal system that has produced a synergistic and integrated relationship between components.



In order to create a sensory glove, the process of tracking the human hand motion was important. Extraction, capturing and analysis of the human hand motion is a fundamental component in human motion tracking. This allows for the collection and prediction of a human's motion, with the use of various methods and processes. The process of extraction and analysis of the human motion data is modelled in four stages (Liu & Wang, 2018). The model allows for the data to be extracted from the system; the system analyzes the information, makes a decision based on the information and reacts to the changing environment. The four-stage process can be seen in Figure 2-2 below.



Figure 2-2: A four-stage model of human information processing (Liu & Wang, 2018)

There are multiple methods of motion tracking, from the use of three-dimensional Time of Flight (TOF) depth cameras to wearable technology. These methods are based on two fundamental sensory technologies. It included image-based data acquisition and non-image-based data acquisition (as seen in Figure 2-3 below). Image-based data acquisition is an approach that was inspired by nature and is the creation of a visual image of objects, which are digitally encoded (Liu & Wang, 2018). This includes the use of AR camera and 3D Time of Flight (TOF) depth cameras. These methods of motion tracking are mainly used for gesture/pattern recognition. The benefits of this technology is the ability to capture the human's motion, as well as the changing environment. The drawback is that it requires expensive computational power while providing a low resolution of the human's movement.

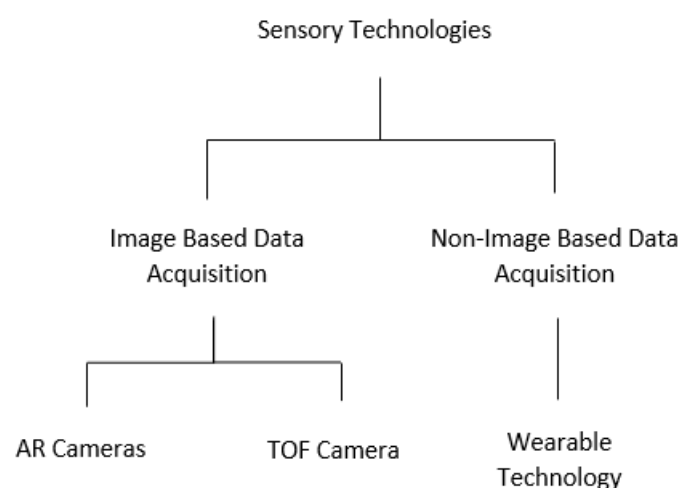


Figure 2-3: Different types of Sensory Technology

Non-image-based data acquisition includes the use of wearable devices such as wrist bands and gloves. Wearable technology improves human motion tracking as it is more precise and accurate due to recent capability developments in Micro Electro Mechanical System (MEMS) devices and sensors (Liu & Wang, 2018). This approach was focused on in this research project, as it had the potential to effectively and accurately track human motion. Furthermore, it encompassed all aspects of what was needed to achieve a mechatronic system.

The above research suggested that wearable technology require all four key multidisciplinary approaches in order to achieve a robust and economic system. Wearable devices require Inertial Measurement Units (IMU), in order to track a human's motion, which forms the electronic components of the system. They required the computational power offered by a computer to process and analyse the data. The microprocessor that controls all the sensors and components on the sensory glove offer the control aspect of the system. The kinematic hand model makes up the mechanical component of the project. All these components need extensive integration to create a synergistic relationship between them. This would create a mechatronic wearable device that is efficient and economical.

### 2.3 Sensory Glove

Due to recent advancements, MEMS technology has reduced the size of gyroscopes and accelerometers, where is it now possible to design and construct an IMU to the size of a fingernail (Moreira, et al., 2014). IMUs are the fundamental electronic components that are used in the design and construction process of most sensory gloves. They have the capability of extracting and processing the motion of an object. This includes monitoring the orientation of the object, which is captured from the device's linear acceleration and angular velocity. IMUs are a broad category of devices that include gyroscopes, accelerometers and magnetometers. There are unique configurations of IMUs that have integrated two or three of the above devices into a single chip in order to reduce size and complexity while improving functionality.

Research suggests that sensory gloves are developed as a motion tracking system that consists of kinematic hand modelling and IMU sensors. Sensory gloves are an integration of human kinematic modelling, IMU sensors, a microprocessor, computer software and hardware. They require these components to control the IMUs while extracting and producing relevant data about the motion of the human hand for the end-user. Sensory gloves are classified as a mechatronics system, due to the complex integration required between the fundamental components which are outlined above.

Extensive research has been conducted on sensory gloves that use various technologies to capture the motion of a body. Some sensory gloves used resistive bend sensors and optical fibre sensors. These types of glove had been used in human hand rehabilitation and gesture recognition. Results showed that

these sensory gloves were advantageous as they could capture the orientation of the hand to a considerable degree of accuracy. The drawbacks were the lack of rotational capability, cumbersome calibration methods and lack of hand motion tracking. These drawbacks would result in an inefficient and unsafe device for a Human Robot Collaboration environment application.

With the goal of the project being a low-cost sensory device, a key component revolved around the cost of these gloves. Flex sensors were relatively expensive components, in comparison to IMU sensors. The sensitivity of flex sensors was also an issue, as it reduced the reliability of their operation. Some devices used resistive bend sensors in conjunction with an IMU sensor. This was done to improve the performance of the device. The results of such designs are outlined in the sensory glove examples in the following subsection.

The Degree of Freedoms (DOF) of the human hand made it a challenging task to accurately model (Nanayakkara, et al., 2017). Extensive research had been performed on the kinematic modelling of the human hand. This research had provided the foundation to create accurate motion tracking models. To develop the hand models, the structure of a human hand needed to be outlined and analysed. Therefore, research was conducted to explore the human hand configuration.

The hand was made of up of four prominent bones, which are known as the distal phalanges, middle phalanges, proximal phalange and metacarpal bones. These bones form the structure of the hand from the wrist to the fingertip of each finger. Research showed that the best way to model the human hand was as a straight chain link between the wrist and fingertips (Knez, Slavic, & Boltezar, 2017). These bones are linked together with the Distal Interphalangeal (DIP) joint, Proximal Interphalangeal (PIP) joint, Metacarpophalangeal (MCP) joint, Interphalangeal (IP) joint and Carpometacarpal (CMC) joint (Nanayakkara, et al., 2017).

In order to model the human hand, each finger was modelled as a planar kinematic chain with four hinge joints at the DIP, PIP, IP and MCP joints while and CMC joint was a universal joint. These hinge joints had one degree of freedom which included the single rotation motion of the DIP, PIP and MCP joint. The universal joint offers three degrees of freedom due to its roll, pitch and yaw motion capabilities. The skeleton structure of the human hand can be seen in Figure 2-4 overleaf.

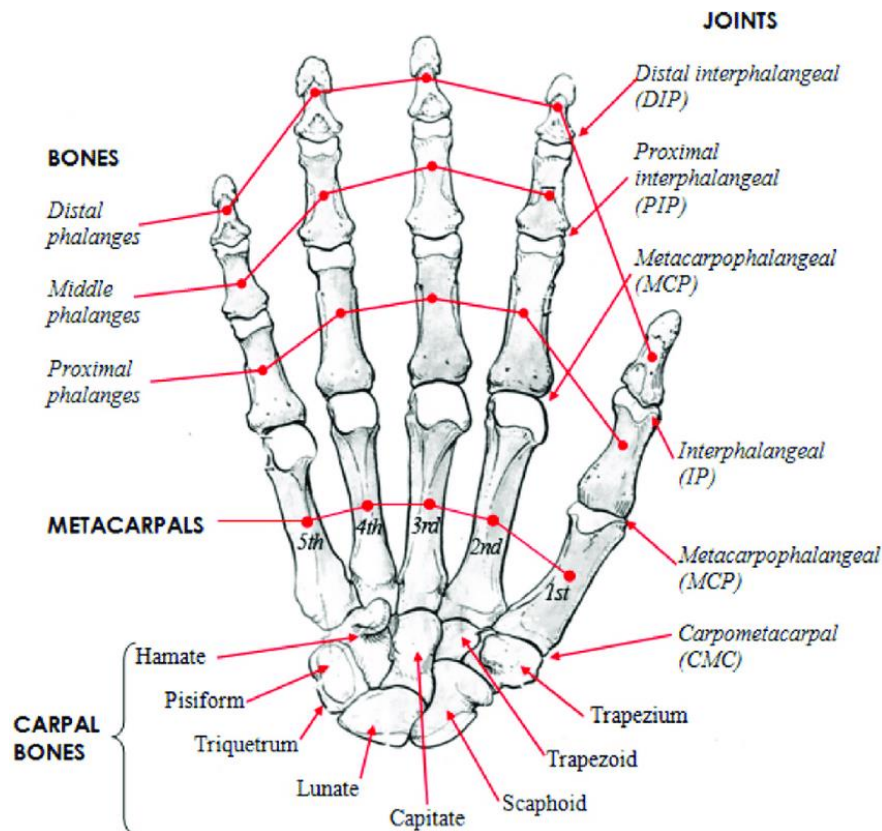


Figure 2-4: Skeleton Structure of the Human Hand (Nanayakkara, et al., 2017)

Sensory gloves make up one of the various methods to conduct human motion tracking. In terms of human body tracking, techniques such as optical trackers, depth sensors and camera-based tracking algorithms have been used to track the position and movement of the human body accurately. Vicon and Optitrack have used passive optical markers to estimate a human body configuration. While these companies have been able to achieve human body tracking with great precision and accuracy, there are drawbacks in these ventures. The main drawback is that it requires a structured environment (Baldi, Scheggi, Meli, Mohammadi, & Prattichizzo, 2017). The use of optimal markers requires a rigid structure of the device and high-quality sensors. This drives the cost and the size of the solution to increase beyond what is feasible. Furthermore, the aforementioned solutions are nonwearable nor usable in a dynamic environment, such as Flexible Manufacturing System environments, which eliminates it as a possible solution for the research.

Other Camera-based systems like depth sensor, use TOF technology in order to track the motion of the human body. The fundamental principle of TOF technology is that it identifies the light travel time (Hansard, Lee, Choi, & Horaud, 2013). Depth sensors provide a relatively straight forward solution for motion tracking but the camera resolution limitations and cost, make it a nonviable solution.

Research suggests that sensory gloves provide a viable, cost-effective and dynamic solution for human hand motion tracking. Sensory gloves have the advantage of being portable and well-integrated with people's habit, which can provide invaluable information to the end-user (Baldi, Scheggi, Meli,

Mohammadi, & Prattichizzo, 2017). The relatively small size and reduced setup time make it a relevant research topic in order to determine the possibilities and limitations in an Advanced Manufacturing environment.

## 2.4 Mathematical Modelling

In order to simplify the kinematic model of the human hand, feed-forward kinematics was outlined in this section. With reference to the previous section, based on the human hand structure, the research uses the methodology of modelling the finger as a planar kinematic chain. The distal phalanges, middle phalanges, proximal phalange and metacarpal, are modelled as rigid bodies and the joints were modelled as revolute joints and a universal joint respectively. This simplified human hand structure was presented in Figure 2-5 below.

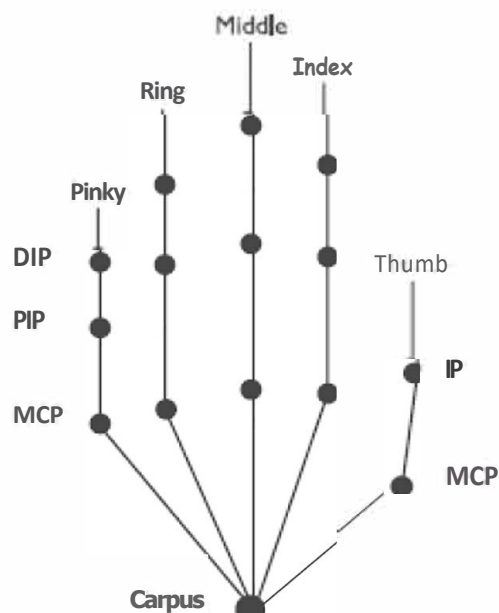


Figure 2-5: Simplified kinematic structure of the human hand

Kinematics studies the motion of a body without any moments or forces, causing motion (Kucuk & Bingul, 2006). Kinematics is widely used in robotics to analytically determine the motion and position of an end-effector on a robot. This is done by performing kinematic models of the robot. There are two different modelling conventions used in kinematic modelling. The modelling conventions used either the Cartesian co-ordinate system or the quaternion co-ordinate system (Kucuk & Bingul, 2006). When performing the transformation between the two Cartesian co-ordinate systems, it is represented as a translation and a rotation with the use of Euler angles. The standard way of achieving this was by using the Denavit & Hartenberg method. It has become a standard for describing robot kinematics and the parameters were known as the Denavit & Hartenberg Parameters.

When performing the transformation between two quaternion co-ordinate systems, one represented it as a dual quaternion, as it represented rotation and translation in a single vector. It reduced the number of elements in the homogenous transformations, which resulted in added computational robustness and storage efficiency when dealing with kinematic of robot chains (Kucuk & Bingul, 2006). The research focused on the quaternion space due to the above-mentioned advantages. The kinematic hand modelling focused on feed-forward kinematics as it was less computationally expensive and simpler to solve.

#### 2.4.1 Quaternions

Quaternions are an extension of a complex number in which it includes three imaginary units ( $\hat{i}$ ,  $\hat{j}$ ,  $\hat{k}$ ) and one real unit. Quaternions are four-dimensional and are used extensively in determining the orientation of an object. The standard form of a quaternion can be seen in equation below (Adorno, 2017):

$$\mathbf{h} = h_1 + h_2\hat{i} + h_3\hat{j} + h_4\hat{k}$$

Where  $h_1$ ,  $h_2$ ,  $h_3$ , and  $h_4$  are real numbers and  $\hat{i}$ ,  $\hat{j}$ , and  $\hat{k}$  are unit vectors directed along the  $x$ ,  $y$ , and  $z$  axis respectively. Quaternions have the capability of defining the rotation of object by a rotation axis and the magnitude of the rotation.  $h_1$  represents the magnitude of the rotation while the remainder of the equation represents the axis of rotation. There are multiple different approaches in order to define the rotation of an object from one frame to another. Commonly used methods are rotation matrices and Euler angles.

The limitation that these methods have is that gimbal lock can occur while the object is in rotation. Gimbal lock is when an object loses a degree of freedom during rotation. This results in a three-dimensional rotating object to only rotate in 2 dimensions, as one rotational axis is locked within another. This is a common drawback that occurs when calculating rotational motion with Euler angles and rotational matrices. Quaternions are immune to this type of error and are less computational expensive.

With the use of quaternions, one can determine the relative orientation between two bodies by the solving the differential equation (Kortier, Sluiter, Roetenberg, & Veltink, 2018):

$$\dot{q}^{ij} = q^{ij} * \frac{1}{2}\omega_{ij}^j$$

Where  $q^{ij}$  is the unit quaternion describing the orientation of the frame,  $*$  is the quaternion multiplication operator, and  $\omega_{ij}^j$  is the angular velocity of the body  $j$  with respect to the body frame  $i$  expressed in the body frame  $j$ .

In order to determine the angular relative velocity, the absolute angular velocity is subtracted from the two moving bodies. This research uses IMU sensors in order to determine the absolute velocity of each moving part of the hand. The output of the IMU sensor can be modelled as:

$$\mathbf{y}_S^b = \mathbf{W}^b \omega + \mathbf{b}_S^b + \mathbf{E}_S^b$$

Where  $\omega$  is the angular velocity of the sensor with respect to the world frame expressed in the body frame,  $\mathbf{b}_S^b$  is the slow varying sensor bias and  $\mathbf{E}_S^b$  is the independent identically distributed white Gaussian noise. Therefore, in order to calculate the relative angular velocity ( $\omega_{ij}^j$ ) between the two bodies, it is modelled as:

$$\omega_{ij}^j = (\mathbf{y}_S^j - \mathbf{b}_S^j - \mathbf{g}_S^j) - \mathbf{R}^{ji}(\mathbf{y}_S^i - \mathbf{b}_S^i - \mathbf{g}_S^i)$$

Where  $\mathbf{R}^{ji}$  is used to reflect the angular velocity from the body frame  $i$  to the body frame  $j$ .

#### 2.4.2 Euler Rotation Theorem

In terms of Euler rotation theorem, a rotation can be described using rotation angles. If the rotations are written in terms of rotational matrices (eg A, B and C), then the general rotation, R, is written as:

$$\mathbf{R} = \mathbf{A} \mathbf{x} \mathbf{B} \mathbf{x} \mathbf{C}$$

Euler angles are the three angles ( $\phi$ ,  $\theta$ ,  $\psi$ ) that make up the three rotational matrices. The convention of Euler angles depends on the axes around which the rotations occur. In terms of the x-axis convention, this can be seen in the Figure 2-6 below. In this convention, the Euler angles which define the rotations are given as:

- $\phi$  - the first rotation about the z-axis in A
- $\theta$  - the second rotation about the former x-axis ( $x'$ ) in B
- $\psi$  - the third rotation about the former z-axis ( $z'$ ) in C

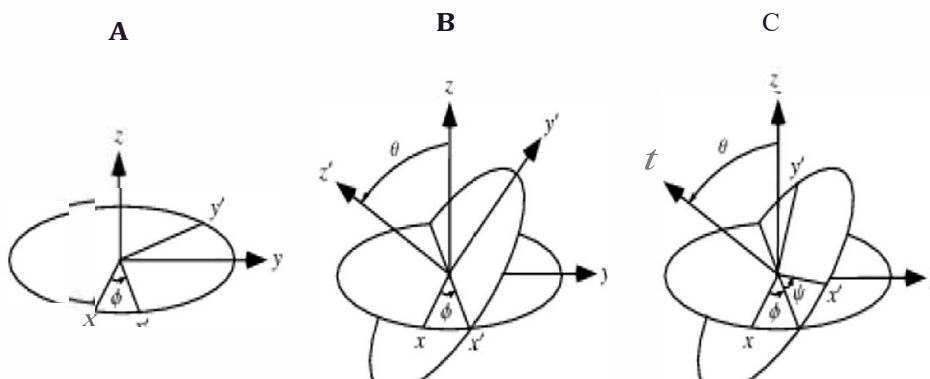


Figure 2-6: Euler Angle Rotation Diagram A, Band C (Weisstein, 2020)

The rotational matrices A, B and C, which would be used in the x-axis convention, can be seen below:

$$A = \begin{bmatrix} \cos \varphi & \sin \varphi & 0 \\ -\sin \varphi & \cos \varphi & 0 \\ 0 & 0 & 1 \end{bmatrix}$$

$$B = \begin{bmatrix} 1 & 0 & 0 \\ 0 & \cos \theta & \sin \theta \\ 0 & -\sin \theta & \cos \theta \end{bmatrix}$$

$$C = \begin{bmatrix} \cos \varphi & \sin \varphi & 0 \\ -\sin \varphi & \cos \varphi & 0 \\ 0 & 0 & 1 \end{bmatrix}$$

Where the simplified matrix R would be,

$$R = \begin{bmatrix} \alpha_{11} & \alpha_{12} & \alpha_{13} \\ \alpha_{21} & \alpha_{22} & \alpha_{23} \\ \alpha_{31} & \alpha_{32} & \alpha_{33} \end{bmatrix}$$

And,

$$\alpha_{11} = \cos \varphi \cos \theta - \cos \theta \sin \theta \sin \varphi$$

$$\alpha_{12} = \cos \varphi \sin \theta + \cos \theta \cos \theta \sin \varphi$$

$$\alpha_{13} = \sin \varphi \sin \theta$$

$$\alpha_{21} = -\sin \varphi \cos \theta - \cos \theta \sin \theta \cos \varphi$$

$$\alpha_{22} = -\sin \varphi \sin \theta + \cos \theta \cos \theta \cos \varphi$$

$$\alpha_{23} = \cos \varphi \sin \theta$$

$$\alpha_{31} = \sin \theta \sin \theta$$

$$\alpha_{32} = -\sin \theta \cos \theta$$

$$\alpha_{33} = \cos \theta$$

## 2.5 Filters

Filtering is an important component of this research as it improves the accuracy and efficiency of the system. Extensive research was done on the different types of filtering methods that could be integrated into this system. Two types of filtering were highlighted as potential solutions for the project. These solutions centred around creating an accurate, yet optimised process, of filtering the system. This was important as it ensured a safe and efficient device was developed for the use in Human Robot Collaborative environments. The first filtering solution was a Kalman filter and it was an optimal state



observer (Mehrabi & McPhee, 2019). The second included an averaging filter that was a Finite Impulse Responses (FIR) filter within the digital filtering category. Both of these filters are explored below.

### 2.5.1 Kalman Filters

Kalman filters are an algorithm that provides an estimate of unknown variables given the measurement observed over time (Kim & Bang, 2018). The filter can be used to calculate the errors introduced in the actual relative angular velocity reading of a body due to the sensor. This was required to eliminate the slow varying sensor bias and the independent identically distributed white Gaussian noise. The filter ensures that the optimal estimate of the actual angular velocity is calculated accurately, while keeping the error to a minimum.

Kalman filters are not only a way to eliminate error but serve as a method for sensor fusion. This allows multiple connected sensors to be fused together to extract relevant information. The drawback of the Kalman filter is that they require robust hardware to operate. This results in Kalman filters being computationally more expensive compared to averaging filters. The Kalman filter sensor fusion tool enables the orientation of the user's hand to be calculated.

Kalman filters are used to solve linear systems. They assume a Gaussian distribution. If the state transition function is linear, then after undergoing linear transformation, the state distribution maintains its Gaussian properties. However, if the state transition functions are non-linear, the state distribution will not be Gaussian. This results in the Kalman filter not converging to an optimal estimation.

When IMUs are used in sensory gloves, they create a non-linear system as the output of the IMUs are non-linear. Therefore, Extended Kalman Filters (EKF) was explored for the project. Extended Kalman filters linearize the non-linear functions around the mean of the current state estimate. Therefore, they are a suitable option for state estimation of non-linear systems. Extended Kalman filters have a feature that allows them to deal with systems that have differential models. In order to calculate the orientation of an object, one uses a differential model, as seen in the quaternion section above. All of these features make the filter more complex and more computationally expensive.

### 2.5.2 Averaging Filter

An Averaging filter is a low-pass digital filter that calculates the outputs samples using the average from a finite number of input samples. This filter forms part of digital filtering that uses algorithms based on differential equations of a system. This filter uses a straightforward algorithm known as Finite Impulse Response (FIR) (Gonzalez-Barajas & Montenegro, 2016). Finite Impulse Response filters consist of a '1' sample followed by a large number of '0' samples. Therefore, the output of the filter

would consist of a set of co-efficients that have 1 valued sample move past each coefficient in turn to form the output (Oshana, 2006). The FIR filter treats each input sample as an independent impulse and the net output is the sum of the impulse responses to every previous input. The shape of the waveform determines how all the individual impulses add up. The filter also has no feedback loop.

Averaging filters are found in real-time applications. It was an important characteristic as the goal of the research was to lay the foundation for the development of a Human Robot Collaboration environment, which required a real-time response system. This filter smoothens the data that carries high-frequency distortions. The filter was ideal for reducing noise, as the noise present inside IMU sensors and flex sensors was higher frequency. Researchers (Gonzalez-Barajas & Montenegro, 2016) found that due to their simplicity, averaging filters were easy to implement and design. They suggested that averaging filters were ideal for real-time applications. Due to the simplicity of the filter, they required low computational cost.

## 2.6 Current Sensory Gloves

Currently, there are a wide range of sensory gloves that have been researched, tested and built for research and commercial use. Sensory gloves have grown in industries that focus on the rehabilitation of hand movement, gesture to text recognition for the deaf and hand motion tracking for computer games. This section focused on the research that has been done in this field and the contributions which it makes to the research project.

Optitrack and CyberGlove are examples of datagloves that have been developed for commercial use. They have advanced algorithms and priority technology that have been used in the development of the gloves. This has made them a high-cost sensory glove for the use of hand motion tracking. Cyber Glove III is the latest sensory glove that has been created by CyberGlove Systems. It features 22 sensors, with a sensor resolution of one degree and sensor repeatability of three degrees (CyberGlove Systems Inc, 2020). The Cyber Glove has a high degree of accuracy and precision for motion capturing and it originally retailed for \$17 000. Prime Xsens is a motion capture glove that has twelve motion tracking sensors in order to track hand orientation, thumb orientation and flexion of knuckles, as well as the top joints of the user's fingers (Manus VR, 2020). It offers high precision and accuracy with easy calibration. It is used for motion capture. The major drawback of the glove is the €3990 price tag. All commercial sensory gloves follow the same trend of a high price for advanced performance. Therefore, commercial gloves are not feasible in this research. An example of the Prime Xsens can be seen in Figure 2-7 overleaf.



Figure 2-7: Prime Xsens Glove (Manus VR, 2020)

According to (Patel, Nayak, & Venkatkrishna, 2018), people from the age of 60 and above face hand motion disorder. In order to create an early detection method for this, a group of students researched and designed a wearable sensory glove. The main principle of the glove involved using voltage signals to measure the deflection of flex sensors in order to determine the user's hand orientation. The glove was designed with five flex sensors with one for each finger. An IMU was positioned on the palm of the glove and it acted as a sensor fusion tool for the motion tracking device. The research focused on the overall performance of the device but offered no comparison to existing sensory glove. The project was only able to register the orientation of the hand. The research provided low accuracy and precision due to signal drift and sensor saturation from the flex sensors.

(Weber, Reuckert, Calandra, Peters, & Beckerle, 2016) looked at the individual motion measurement for the proximal and distal finger joints for hand orientation detection. The research aimed to develop a low-cost solution to establish Human-Robot Interaction. The glove was designed with the use of ten flex sensors and an MPU-9150. The device had 19- degrees of freedom. This was relevant as a Hand's dexterity contributes to around 20 degrees of freedom (Nanayakkara, et al., 2017). However, flex sensors are prone to sensor displacement errors and complex calibration procedures. The sensor data quality was ignored and no filter was implemented. Through research, it was identified that filters were essential in these systems as it reduced noise and smoothed the signal from the device. These noises included IMU sensor drift and independent identically distributed (i.i.d) white gaussian noise. The sensory glove design can be seen in Figure 2-8 below.

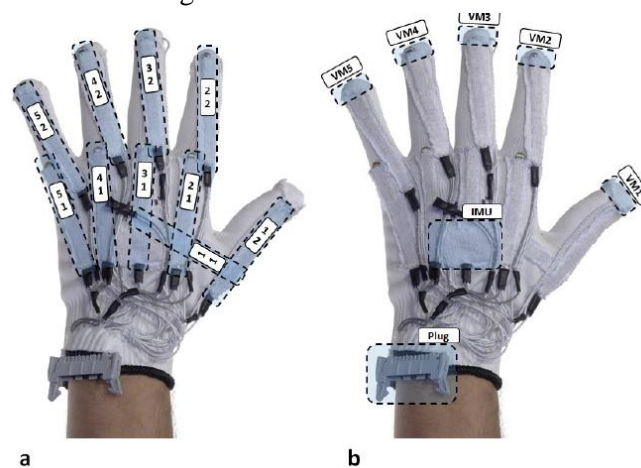


Figure 2-8: Sensory Glove Design by (Weber, Reuckert, Calandra, Peters, & Beckerle, 2016)

According to (Moreira, et al., 2014), hand and finger tracking was of major importance in the healthcare and animation industries. The aim of the research was to provide a low-cost sensory glove with precision, stability and feasibility with the combinations of IMU sensors. The sensory glove was designed with eleven IMUs with a capability of nine DOF. Two IMUs were placed on each finger, one on the distal phalange and one on the proximal phalange, while one IMU was positioned at the back of the palm. The research introduced a soft and hard iron correction algorithm alongside a temperature compensation method which was able to provide increased precision and accuracy to the sensory glove. Furthermore, the glove was able to achieve a high average Intra-Class Correlation (ICC) values. The main drawback was that during some orientations, the thumb presented a mismatch in terms of the yaw values when compared to the real orientation. The design of the glove can be seen in the Figure 2-9 below.

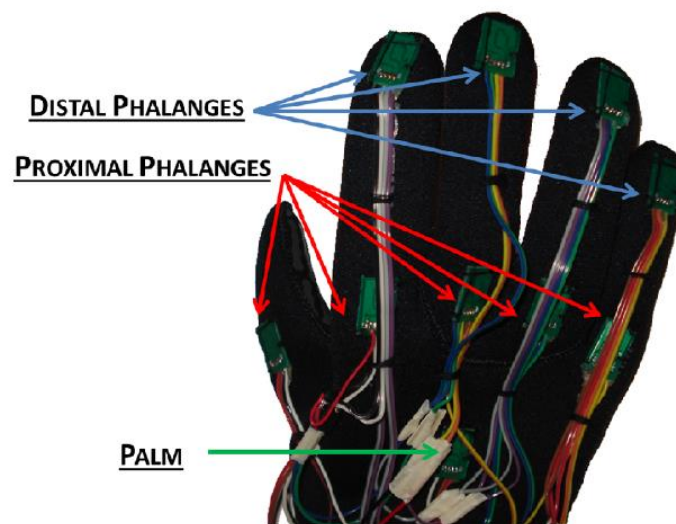


Figure 2-9: Sensory Glove Design by (Moreira, et al., 2014)

Researchers (Baldi, Scheggi, Meli, Mohammadi, & Prattichizzo, 2017) designed and developed a wearable sensory glove for enhanced sensing and touching purposes. It was based on IMU sensors for hand tracking and introduced components for cutaneous force feedback. The glove was designed with eleven magnetic, angular rate and gravity (MARG) sensors. Sensors were positioned on the proximal phalanges and middle phalanges on each finger with one sensor positioned on the palm of the hand. The glove was able to achieve a 95% confidence interval and an orientation estimation error of  $3.06^{\circ} \pm 0.12^{\circ}$ . These results showed the capability of providing an accurate hand tracking device with the integrated use of IMU sensors. The researcher identified that further work could be done by adding accelerometer and gyroscopic sensors on the distal phalanges to improve performance of the device. The sensory glove can be seen in Figure 2-10 overleaf.

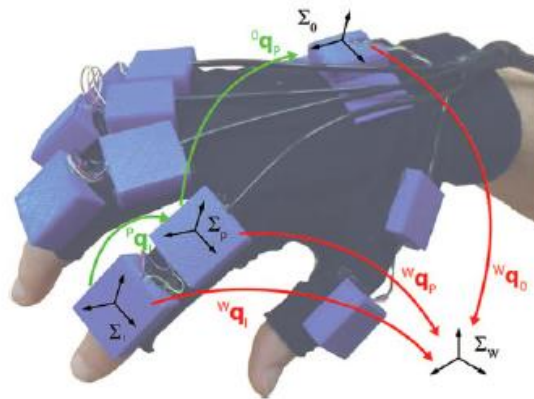


Figure 2-10: Design of Sensory Glove by (Baldi, Scheggi, Meli, Mohammadi, & Prattichizzo, 2017)

(Kortier, Sluiter, Roetenberg, & Veltink, 2018) looked at the development of a sensory glove system that could be used as an ambulatory system using inertial sensors to track the motion for a user's hand. The glove was designed with sixteen IMU sensors and an atmel XMEGA microprocessor for the data acquisition and processing algorithms. An extensive extended Kalman filter and a comprehensive hand kinematic model was developed to minimize the orientation estimation error. This resulted in a high dynamic range (116-degree full range finger movements a second) and small repeatability (approximately 2 degrees). The device displayed high performance while achieving a compact and efficient design. The researcher noted that due to the lack of protection around the device, it would not be viable in a manufacturing environment. The sensory glove can be seen in Figure 2-11 below.



Figure 2-11: Design of Sensory Glove by (Kortier, Sluiter, Roetenberg, & Veltink, 2018)

While most of the researched sensory gloves are not related to the application of the project, the improvements and advancements made in the tracking methods of human hand motion was vital. These devices all display similar methods to what is required to tracking the motion of the human hand in a Human Robot Collaborative environment. Therefore, the research project focused on using the fundamental principles achieved by (Kortier, Sluiter, Roetenberg, & Veltink, 2018) and (Baldi, Scheggi,

Meli, Mohammadi, & Prattichizzo, 2017) as it presented the best motion tracking solutions while reducing the cost of the glove and achieving a high performance from the device.

## 2.7 Human-Robot Collaboration Environments

The definition of Human-Robot Collaboration systems is a broad ideology that focuses on three main principles, according to (De Luca & Flacco, 2012). These principles focused on the distinction between safety, coexistence and collaboration. It suggested that HRC systems included not only the sharing of a physical workspace but also the task. HRC systems can be achieved if the absolute safety of the worker can be guaranteed and accomplished. A proposed framework was developed, which consists of three levels of interaction between the robot and the human worker. This can be seen in Figure 2-12 below.

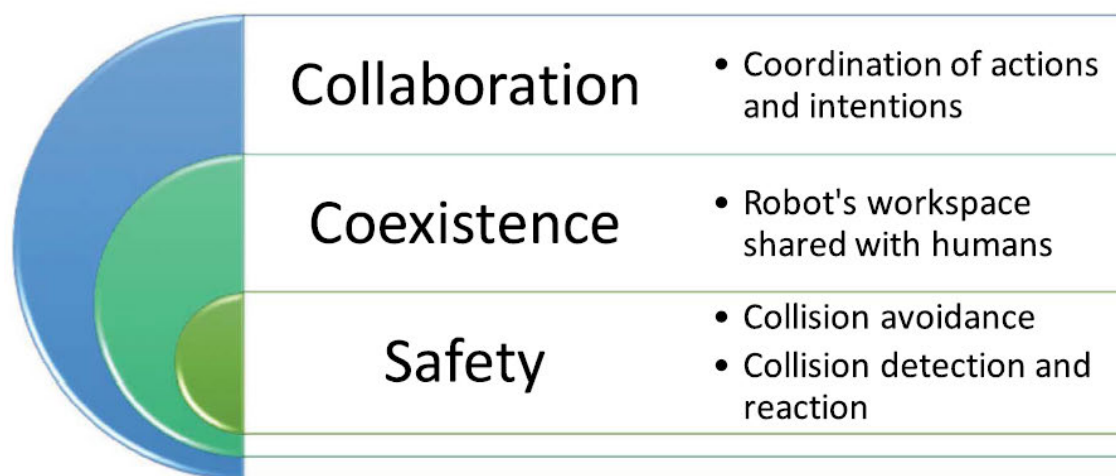


Figure 2-12: Levels of Interaction Framework for HRC Systems (Villani, Pini, Leali, & Secchi, 2018)

The framework proposed that any level of interaction must include the features associated with it as well as the features of previous level interaction. This Framework explained that if there was an HRC system where collaboration existed, it was essential that safety was a critical feature to achieve. This would be done by integrating external mechanics, sensory equipment and path avoidance algorithms. With regard to HRC systems, the safety of the workers was the main goal, as it is the limiting factor that prevented laws and legislations from being created and passed. Without legislation being established to enable HRC systems to operate in manufacturing sectors, the research field will not develop. This is the fundamental goal for researchers and companies that are exploring this initiative.

Coexistence defines when a robot and a human worker share a workspace and could work on the same object but have no physical interaction or mutual contact. Therefore, collaboration allows for a worker and a robot to perform a complex task together through direct co-ordination and interaction (De Luca & Flacco, 2012). This requires a control architecture that includes collision avoidance systems, detection system and reaction capabilities, which was proposed in (De Luca & Flacco, 2012). (Bauer, Wollherr, & Buss , 2008) defined the distinction between Human-Robot Interaction (HRI) System and

HRC systems based on the principle that in HRC systems, the robot and the human worker work together towards a common goal. HRI systems exist where robots and humans interact but not towards a common goal.

Robots are automated manufacturing equipment that can perform operations, usually carried out by a worker, with a higher degree of accuracy, precision and repeatability. However, robots don't have the flexibility and the problem-solving capability that humans have. Robots have been developed with greater DOF and with smart technology such as optical cameras and sensors. While robots primary use is to perform operations in advanced manufacturing systems, they can also be used to recognize defects but at a substantial cost. HRC systems allow for the integration of the human and the robot to create a synergy effect with high levels of accuracy, precision and performance. Humans add flexibility and problem-solving capabilities to HRC systems, which tend to limit most industrial robots from becoming multifunctional.

Through technological advancements, a paradigm shift has occurred in the production industry. This shift has been from the mass production of generic products to the mass production of customizable products (Pedersen, et al., 2016). This type of mass production requires industries to be highly reconfigurable and flexible. While manufacturing companies have been able to achieve improved efficiency and production of products through automation, this has mainly been geared towards the manufacturing of generic products. Manufacturing systems have traditionally been automated to a large degree and reconfiguration has become a labour-intensive task. Manual labour has allowed for flexibility but it is not sustainable for large scale production.

There have been significant research advancements in a production method known as Flexible Manufacturing System (FMS). These systems have been designed to allow for easy adaptation to changes in the type and quantity of a product being manufactured (Hayes, 2019). The concept of FMS was first developed by Jerome Lemelson, who filed multiple patents on a robot-based system that could weld, rivet and inspect manufactured goods. The ideology of an FMS environment was that a system could be programmed to run a batch of a certain product and automatically switch to producing another set of products. As the research progressed, the focus was changed towards creating a make-to-order production process that would allow customers to customize their product before it was manufactured. The advantages of an FMS environment were that it would increase the production efficiency and reduce downtime of a production line. The drawback of these environments was the high upfront cost and greater development time. Therefore, the research was focused on developing a low-cost sensory glove that could promote the development of FMS environments economically.

In order to achieve mass customization, (Pedersen, et al., 2016) suggests that it will be necessary to combine high reconfigurability with larger degrees of automation. This goal can be achieved through the development and establishment of HRC systems, as they act as an enabler.

Cobots are robots that collaborate with human workers in Advanced Manufacturing assembly lines. They were the first type of collaborative robot which were developed for the manufacturing sector. They were used to reduce the ergonomic concerns with workers while providing a safe, high quality and highly productive environment (Cherubini, Passama, Crosnier, Lasnier, & Fraise, 2016). These robots were activated by the worker and assisted the worker with simple linear and repetitive operations. The Cobots were required to perform one task in one motion. They required no interaction with the human. An Example of traditional and collaborative industrial robots can be seen on Figure 2-13 below.



(a) Non-collaborative robot: safety fences are required to prevent harming human operators.



(b) Collaborative robot allowing the human worker to stand in its proximity and work together at the same task.

*Figure 2-13: Examples of traditional and collaborative industrial robots. (Villani, Pini, Leali, & Secchi, 2018)*

A recent EU project known as ROBO-PARTNER, aimed at creating a seamless HRC system for safe operations in Advanced Assembly Factories of the Future. The project used the foundation of Cobots and the principles laid out by (Pedersen, et al., 2016) in order to create the Framework of the project. The project revealed that human skill was the main driver towards high added-value products and the integration of a robot's strength, precision and repeatability would improve it. This integration involved safe cooperation with autonomous adapting robots through a user-friendly interaction (Michalos, et al., 2014). This research focused on four aspects. The project aimed at creating intuitive interfaces for HRC during the assembly process. The project needed to develop advanced safety strategies to ensure a safe



environment between the worker and the robot (Michalos, et al., 2014). This was achieved through the development of safe interactions between a robot and a worker. The creation of a communication architecture between the robot and the human was also established.

The communication architecture was based on enhanced sensor-based interaction. The study defined the levels of human-robot interaction with the ROBO-PARTNER Architecture that could lead to advancements in the field of HRC environments. This sensor-based interaction allowed for collision avoidance and detection. The sensor-based interaction could be achieved with the use of a device such as a sensory glove. It would provide the hardware for data acquisition and data processing of the hand motion. The three human-robot interaction levels and the description of the ROBO-PARTNER project can be seen in Figure 2-14 below.

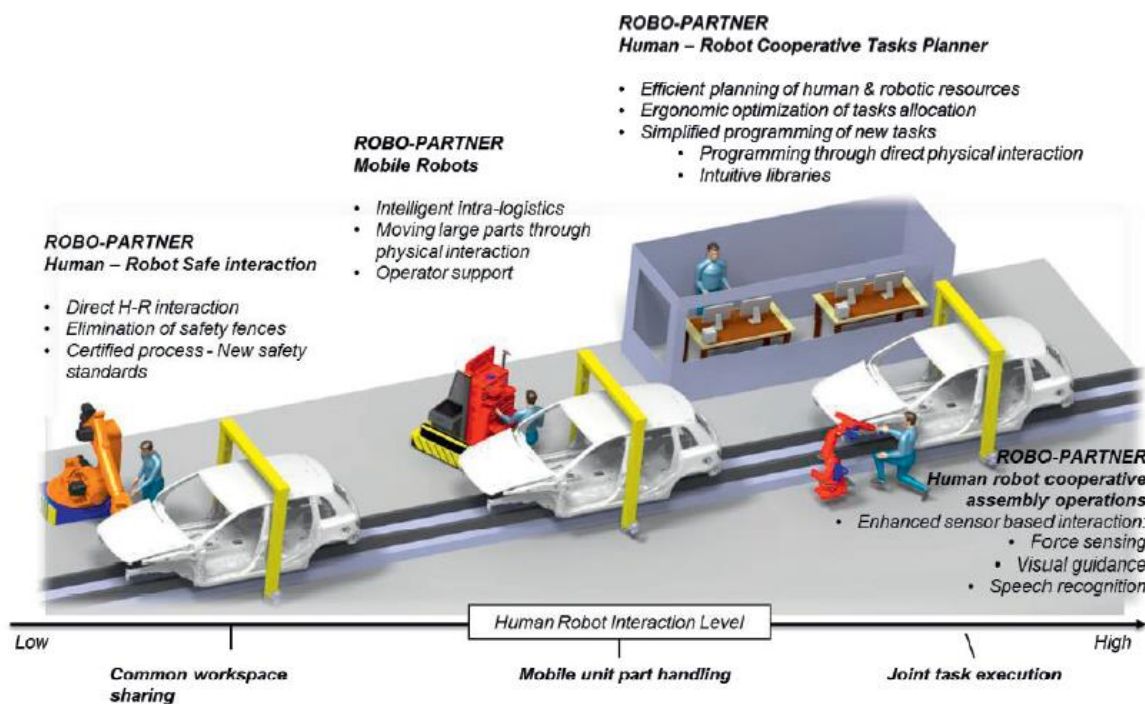


Figure 2-14: ROBO-PARTNER production paradigm in the automotive industry (Michalos, et al., 2014)

Currently, various manufacturing companies have researched and introduced HRC systems where humans and robots collaborate at a limited level. In the following examples, the robots act more as an assistant to the human than a partner, when performing a task. In a BMW automotive plants, Universal Robots UR10 had been implemented onto the manufacturing floor to assist human workers with the sealing of car doors. The robots had no fences and assisted in the transportation and position of the car doors to be sealed onto BMW vehicles. The goal of the initiative was to introduce collaborative robots that would assist the worker by handing them tools and parts during the assembly processes (Michalos, et al., 2015).

A VW automotive plant in Germany integrated an UR-5 robot into the cylinder head assembly section to insert glow plugs into the cylinder heads of various VW engines. The robot picked the glow plug and placed the plugs into hard-to-reach drill holes. The human worker was responsible for fixing the glow plugs and insulating the cylinder heads (McCall, 2020). The robot acted as an assistant to the human worker and allowed the worker to monitor the process continually and intervene where necessary. The UR-5 robot can be seen on the VW factory floor in Figure 2-15 below. Audi AG introduced a collaborative KUKA robot in its automotive plant. The robot worked in close cooperation with workers and acted as an assistant in the assembly process. These robots were designed for a collaborative process as they were lightweight and had a low payload. Therefore, the robots were limited in their functionality but at a high cost.



Figure 2-15: UR-5 robot on the VW factory floor (Leber, 2013)

Safety was an important factor of HRC systems as they needed to ensure a safe environment for workers to work in. Over the years, different strategies have been introduced in order to improve and perfect the safety aspect. According to (Michalos, et al., 2015), these strategies are aimed at different types of safety:

- Crash safety, which ensured that controlled collisions only occur between human, robots and obstacles. This was achieved by limiting the power/force that a robot can produce.
- Active safety, which ensured that timely detection of collisions between humans, robots and obstacles occurred. This was achieved through proximity sensors, vision systems and sensory glove/devices.

- Adaptive safety, which ensured the prevention of future collisions. This was achieved through the design and development of collision avoidance algorithms.

These strategies, among others, had been used to pave the way to establish new laws and legislation that would promote the use of HRC systems in the manufacturing and assembly sector. These laws and legislations are important as they are a fundamental component in ensuring the introduction of HRC systems. Without them, HRC systems can not develop and be integrated into manufacturing plants and assembly factories. Research by (Zanchettin, Ceriani, Rocco, Ding, & Matthias, 2016) showed that according to available standard, there are several restrictions that restrict the motion of the robot's motion during collaboration with a human. These restrictions limit the speed of the robot or driving torque dependent on the separation distance from the human worker. This restriction, with reference to the robot's motion vs separation distance, can be seen in the following equation below:

$$distance \geq velocity \times t_b$$

Where  $t_b$  is the braking time and depends on the robot's payload (Zanchettin, Ceriani, Rocco, Ding, & Matthias, 2016). This relationship was developed to ensure that all tasks between robots and humans were performed safely. This resulted in a compromise between production and safety. The research conducted in this study was aimed at preventing the compromise of production for safety. It focused on showing alternate ways that companies could ensure the safety of the workers when collaborating with robots. This would allow robots to operate at operation parameters while collaborating with workers. Therefore, the system could increase the productivity and efficiency of the manufacturing/assembly plant.

This research explained how sensory gloves could be used as a tool to enable HRC systems. Furthermore, sensory gloves could be an opportunity for Small, Medium and Micro Enterprises (SMME) to establish HRC systems as research shows that most robots that have HRC capabilities come at a substantial cost. Other industries, such as the automotive industry, also benefit from this research as it will significantly improve productivity and lower the setup cost of FMS within the advanced manufacturing sector.

## 2.8 Conclusion

In summary, this chapter covered an extensive study that identified four key aspects related to the field of research. A link between sensory gloves and mechatronic Engineering was established through the literature. The design and development process for a sensory glove encompassed all aspects of a mechatronic system. It highlighted that a sensory glove must be developed as a mechatronic system in order to achieve a functional solution. Research into sensory gloves showed that they were a preferred solution for human motion tracking due to it being cost effective and adaptable. While solutions, such

as optical sensors and depth sensors with TOF technology, might provide more information of a person with reference to their environment, it lacked the accuracy and precision required for the projects application.

Kinematic human hand modelling had been researched by multiple researchers and a common approach was the Denavit & Hartenberg Parameters. In recent years, the use of quaternions has been investigated as an improved and more effective method over the use of Euler angles. This research compared and analysed the best approach to model the human hand through these above methods. Two filtering methods were explored for the system. While the extended Kalman filter showed greater accuracy and a substantial reduction in the orientation estimation error, averaging filters were less computationally expensive and could achieve comparable accurate results. The application of the project required a real time response system, the best filtering solution was the averaging filter.

Current sensory gloves laid the foundations of the research in this study. This study took the advancements made by (Kortier, Sluiter, Roetenberg, & Veltink, 2018) glove design and (Baldi, Scheggi, Meli, Mohammadi, & Prattichizzo, 2017) kinematic hand modelling algorithm, and merges them to create a more robust and cost-effective device. With safety being a primary concern for HRC systems in an advanced manufacturing environment, the sensory glove could aid in the creation of a safe environment where workers have the ability to closely collaborating with robots in an FMS environment. This would result in new laws and legislations being established, which would promote FMS in the Advanced Manufacturing sector.

### 3. MECHATRONIC DESIGN APPROACH

#### 3.1 Introduction

In order to establish design concepts for a sensory glove, a mechatronic design approach was the most appropriate. The mechatronic design approach, as described in the literature review, focused on the concurrent creation and selection of mechanical, electrical, electronic computer and control components. This ensured that the components not only operated at high performance but had an effective integration capability to create a synergic combination of mechanical, electronic, computer and control engineering.

#### 3.2 Proposed Mechatronic Design Approach

(Silva, 2005) proposed a mechatronic design process in order to achieve a complete mechatronic system. This approach had been adapted for the research project and can be seen in the Figure 3-1 below. The design approach demonstrates how the four types of engineering were used in order to achieve the mechatronic system.

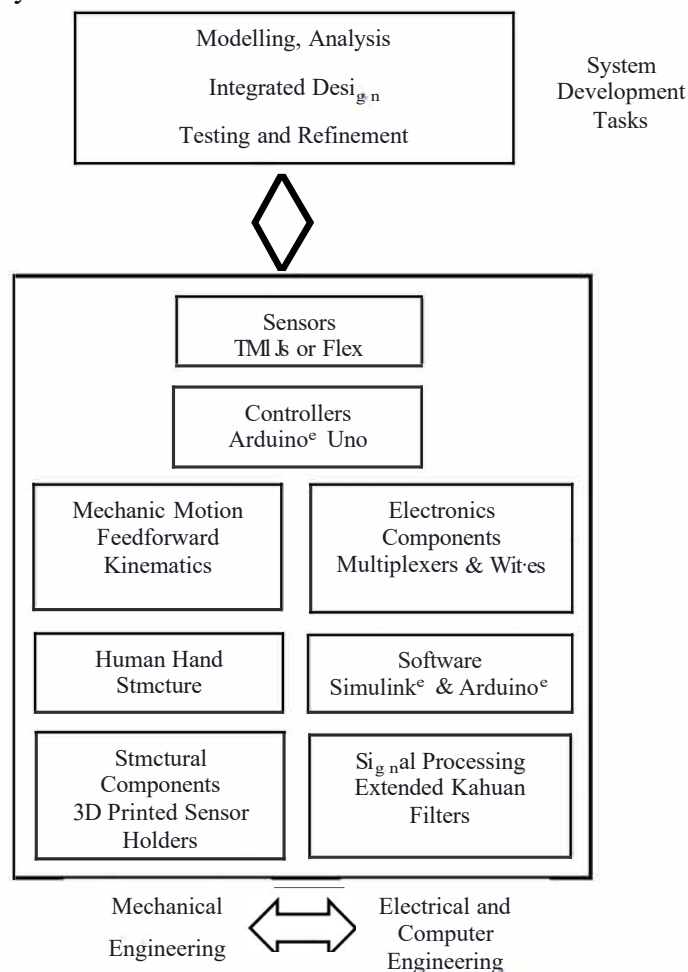


Figure 3-1: Adapted mechatronic Design Process

The design of the sensory glove involved components from different engineering fields. The model of the hand involved feed forward kinematics as the bone structure of each finger was modelled as a kinematic chain with revolute joints between each bone segment. This was the fundamental kinematic approach that was used to describe the position and orientation of an end effector in robotics. The suitable kinematic model was the Denavit-Hartenberg method and it was the mechanical engineering approach used in this research.

IMUs were used in this research to measure and determine the motion and the orientation of a human hand. Recent developments in the capabilities of IMU sensors had provided significant improvements to the precise and accuracy of these sensors. IMUs are a collection of sensors which include accelerators, gyroscope and magnetometers. They are all used to accurately track and predict the motion and orientation of an object. An MPU6050, which is a fusion of an accelerator and gyroscope, is such an IMU device and has 6 degrees of freedom. Flex sensors are devices that have been used to measure and estimate the orientation of the human hand in sensory gloves. Flex sensors have been used in a sensory glove that have gesture recognition systems as seen in (Moreira, et al., 2014). They have proven to be advantageous due to the degree of accuracy when estimating orientation but do possess potential drawbacks, as mentioned in the literature review. The IMUs or flex sensors are the electronic engineering aspect of the system.

These sensors are used in conjunction with a microcontroller, such as an Arduino<sup>®</sup> micro-controller, which captures and processes data. This data can be translated into accurate and reliable information of a human hand to the end-user. The microcontroller was used as an input/output device to allow for the acquisition and analysis of sensor data. The microcontroller has the capability to control the information received from the sensors. The data was used to calculate and estimate the motion and orientation of the human hand. In order to connect all the IMU or flex sensors to the microcontroller, a multiplexer chip will be used. This allowed the microcontroller to select and control the data acquisition from the sensors. The multiplexer used logic gate technology in order to control the input and output of data. The microcontroller and the multiplexer are the electrical engineering aspects of the system while providing the foundation of the computer engineering aspect.

The control engineering aspect of the research was explored with the use of a filter. Two filtering options were considered in the research. The first filtering solution included an Extended Kalman filter. Kalman filter is an algorithm that provides an estimate of unknown variables given measurements observed over time. The filter is used to reduce the process noise of the system and the sensor bias drift of the sensor. Since the system was non-linear, an Extended Kalman filter (EKF) needed to be used. Extended Kalman filters have the capability of fusing the accelerator and gyroscopic readings from the IMU sensors to estimate the motion and orientation of the human hand. These features come at a high computational cost.

The second filtering solution included an Averaging filter. An Averaging filter is a low-pass digital filter that calculates the output samples using the average from a finite number of input samples. These filters sample the signal over a certain number of steps and average the data to create a smooth signal. Through this process, they reduce the high-frequency distortions that are present in the signal. Averaging filters require little computational power due to the simplicity of the design.

The final aspect of the mechatronic design approach was the computer component. This was addressed with the use of a Solidworks<sup>®</sup> and Simulink<sup>®</sup> software. The Solidworks<sup>®</sup> software was used as a three-dimensional modeling package to create the human hand model. Simulink<sup>®</sup> is a block diagram software for multidomain simulation and Model-Based Design (MathworksInc, 2020). It was used to create the project's control system and integrate the human hand model with the control system. Simulink<sup>®</sup> had the tools necessary to create the single kinematic chain structure for the human hand from the CAD model of it. The software provided an integration platform between the hardware, software and the human hand model. This enabled an effective and efficient path to ensure accurate and precise estimations of the hand's position and orientation.

Simulink<sup>®</sup> was also used to create a filtering solution for the project. It had Arduino<sup>®</sup> integration capabilities so that it could deploy a filter onto the microcontroller. Simulink<sup>®</sup> had a variety of filtering tools. It was able to deploy a filtering solution on the hardware as it had a C++ code compiler tool. Simulink<sup>®</sup> provided a real-time observation tool for algorithms that are deployed onto hardware to be modified during operation.

### 3.3 Design and Performance Specifications

In order to design the sensory glove, design specifications need to be determined. These specifications guided the research towards a product that would create a contribution to the field of research. These specifications are defined through the analysis of current sensory gloves, within the research and commercial fields. The market research of current sensory gloves can be seen and referred to in the literature review. The list of specifications for the sensory glove are represented below.

#### 3.3.1 Sensors

The sensors that are used on the sensory glove need to adhere to the following specifications. The sensors are required to have small repeatability (approximately 2 degrees), highly sensitive (approximately 60 to 80-degree full range finger movements a second) and can provide the reliability for the type of applications. These requirements are benchmarked off current sensory glove's specifications. The sensors needed to be cost-effective while having the capability of accurately tracking the motion and orientation of the human hand. To accurately track the human hand, the sensors

need to provide high degrees of freedom (Approximately 6 degrees of freedom). The sensors do not require a magnetometer as the application of the device consists of robotic machinery. Robotic machinery had built-in magnets, which would affect the magnetometer within the sensors. This would result in more significant sensor bias drift on the sensors and an inaccurate system.

### 3.3.2 Microcontroller

Microcontroller is a fundamental electrical and electronic component of this research project. The microcontroller needed to be open-source, robust and cost-effective. The open source requirement allows for easy operation and integration with the control system software, such as Simulink<sup>®</sup>. To control multiple motion tracking and orientation sensors, it needed to be robust and reliable. Reliability was a key feature as the potential HRC application requires strict safety guidelines. The microcontroller needed to handle multiple digital inputs to ensure multiple sensors can be controlled and monitored. The size and weight were important as it will be mounted onto a human's hand. WiFi/Bluetooth capabilities would enhance the microcontroller as it allows the sensory glove to be potentially portable and cordless but it was not a focal point of the research. A clock speed of approximately 16 MHz to ensure adequate communication between components and an operating voltage of 5 V would make the microcontroller practical and energy efficient.

### 3.3.3 Software

The Software component was the building blocks of the computer engineering aspect of the mechatronic design approach. The software was required to have extensive kinematic and hardware capabilities. It needed to contain tools to create dynamic models and perform filter design. The software needed integration capabilities to enable multiple components to function in an efficient process. Due to the complex feed-forward kinematic model that was required with the research, a software package that can perform such modelling and analysis was needed. A software that can provide real-time observation and modification of Algorithm would enhance the efficiency and performance of the sensory glove as it allowed for a simplified troubleshooting process.

### 3.3.4 Filter Design

The filter design included either a Kalman filter or an Averaging filter. A Kalman filter is advantageous as it is an error estimation algorithm as well as a sensor fusion tool. These requirements are necessary to allow for the fusion of data from the motion tracking and orientation sensors. Due to the system being non-linear, the system can be linearized with the use of an EKF. This allowed the error estimation algorithm to run optimally and effectively; however, it increased the computational costs.

The



Averaging filter is advantageous as it required little computational power compared to a Kalman filter, and it had real-time application use. An Averaging filter did not have the degree of accuracy and filtering efficiency as the Kalman filter due to the computational cost. The type of filter will be determined by the design of the sensory glove along with the hardware that is used.

### 3.3.5 Glove and Structural Components

The glove was required to be made from a light and durable material. It needed to be comfortable for the user to wear. The glove needed to be malleable as the researcher needed to integrate the hardware components onto the glove. The glove needed to be able to house all the sensors. This requirement was fundamental as the glove needed the hardware in the correct positions to accurately and efficiently estimate the motion and orientation of the human hand. If the data from the sensor were sent to an external Microprocessor to be recorded and analyzed, it would lead to increased process noise and greater time delay. Component holders needed to be designed for the glove to allow for precise location and alignment of the sensors. The holders needed to be light to keep the weight the glove at a minimum, and compact to improve the ergonomics of the sensory glove. A cost-effective manufacturing process was required to keep the cost to a minimum while providing a workable solution for the housing of the sensors on the sensory glove.

### 3.3.6 System Integration

The primary objective of the research was to create an integrated system that had the capability to be collectively optimized. Each component of the system needed be optimized for its specified objective. However, each component needed to be integrated effectively together so the system could achieve a collective optimal point. In terms of the research, the mechanical, electrical, electronic, computer and control aspects of the system needed to operate optimally as individual components, as well as in unison with each other.

The kinematic human hand model was modelled using feed-forward kinematics. The feed-forward kinematics needed to be modelled on software that had microcontroller support. The software was required to perform complex and computationally expensive models to verify the model's accuracy and efficiency for the mechatronic system. The software was used to develop the filter for the sensory glove. The software needed to have the ability to integrate the human hand model with the filter. The software also needed the ability to deploy the human kinematic model and the filter onto existing hardware. Real-time monitoring and algorithm modification were key to a robust and efficient system. The software was the core computer engineering component of the sensory glove.

The sensors were required to be open source and have the capability to be compatible to a Microcontroller. This ensured that the sensors could integrate effectively with existing components of the sensory glove. The size and optimal performance was a crucial factor in creating a compact system that efficiently works on a single power source.

### 3.4 Concept Design

The design of the sensory glove involved a complex process of creating unique, compact, effective and low-cost concepts. The design process began with rough ideas that laid the foundations for the final design. This included investigating multiple different components that could achieve the required objective of the project. Each design component included multiple options to choose from when developing the conceptual designs. Each conceptual design that was created had the design and performance requirements in mind that were stated at the beginning of the chapter. The conceptual designs were developed using the proposed model of a mechatronic system to ensure the systems were well integrated.

#### 3.4.1 Design Concept 1

The first conceptual design used the Denavit-Hartenberg method to create a feed-forward single kinematic chain model of the human hand. The Denavit-Hartenberg approach, was coupled with Euler angles, to create a suitable model for tracking the motion and orientation of the human hand. Denavit-Hartenberg method was a popular kinematic method for robotics and was used to model the human hand by other research groups. This was the mechanical and computer Engineering aspect of the design.

The control engineering aspect of the concept design detailed the algorithm and Kalman filter design. The algorithm would extract, process and analysis the information from the sensory glove. It was created with the Arduino<sup>®</sup> IDE software. It was an open-source software that provided the control capabilities and coding language to write code on the sensory glove's hardware. The Kalman filter was designed on the Simulink<sup>®</sup> software due to its computational capabilities and extensive filter design tools. A complementary Kalman filter was used to reduce the estimation orientation error of the model. The Kalman filter also acted as sensor fusion tool to fuse the sensor data to produce the most accurate results.

The ATmega328P Microcontroller, five flex sensors and single IMU sensor formed the electronic and electrical engineering aspect of the design. The ATmega328P Microcontroller allowed the system to run at board rate of 8 MHz while provided with a 5V power supply to the system. This enabled the design to be effective and energy efficient. The five flex sensors, which ran on the same 5V power

supply, used the technology of resistor bands and voltage to detect motion of each finger. One flex sensor was fitted onto each finger of the glove to estimate the orientation of the human hand.

The change in the voltage from each flex sensor produced an analogue signal that was interpreted by the microcontroller. These analogue signals were calibrated to determine the flexion of the finger. The voltage values vs flex angles were recorded and used to determine the orientation of the human hand. The flex sensors only had one degree of freedom and measured the flex movement of the fingers. A single IMU, such as a MPU6050, was attached to the palm of the glove to calculate the hand's general motion in free space. The limitation of one IMU sensor on the glove was that the general motion of the hand could only be estimated. The exact motion or position of each finger was difficult to calculate accurately. The IMU was power by the same 5V power source.

Design Concept 1 provided a foundation for the sensory glove design. It provided a compact, integrated and power efficient system but lacked the accuracy and precision required for such applications. While the system showed aspects of mechatronic design, it did not provide high-performance at a low-cost as required for the research.

### 3.4.2 Design Concept 2

The second concept design approach used the same Denavit-Hartenberg method to create a feed-forward single kinematic chain model of the human hand. It used quaternion vectors to drive the DH method in determining a suitable model for tracking the motion and orientation of the human hand. The quaternion vectors defined the axis of rotation for each bone segment of the hand and the magnitude of rotation. Using quaternion vectors provided a compact formulation for the kinematic equations while reducing the number of the equations compared to Euler angles. This made the quaternion vectors less computationally expensive and more efficient. This was the mechanical and computer engineering foundation of the design.

Arduino<sup>®</sup> IDE software was used to create the algorithms for this design to extract, process and analysis the information from the sensory glove. This software remained the same form the first design due to the robust and open-source environment that was established. An Extended Kalman filter was designed on the Simulink<sup>®</sup> software. The Extended Kalman filter was developed as the system was non-linear.

Since measurement vectors were produced from the IMU sensors, the measurement equations were non-linear and resulted in the Kalman filter becoming complex. An extended Kalman filter had the capability to convert a non-linear system into a linear system through the process of linearization. This increased the computational cost whilst reducing the process noise of the sensor. This formed the foundation of control engineering aspect of the conceptual design.

The Arduino<sup>®</sup> Uno microcontroller with fifteen IMU sensors formed the electronic and electrical engineering aspect of the design. The Arduino<sup>®</sup> Uno operated at the same board rate as the ATmega328P. The Arduino<sup>®</sup> had multiple analogue and digital input/output pins with a dedicated SCL and SDA lines. These were essential as they provided a methodology to extract and control data from multiple IMU sensors. MPU6050 sensors were used in order to track the motion and orientation of the human hand. The sensors fused the accelerometer and gyroscopic values to compute the orientation of each sensor. The sensor offered six DOF. Fifteen MPU6050 sensors were positioned on the glove. Three were placed on the distal phalanges, middle phalanges and proximal phalange for each finger. The MPU6050 provided more accurate and reliable data of the human hand while in operation. The sensors were powered by the same power source as the microcontroller. This created a compact and energy efficient system. In order to control all IMU sensors, one multiplexer was used. This ensured that the microcontroller could extract and control multiple sensors simultaneously.

This concept design took the learnings from the first conceptual design and improved on them. Improvements were made with the use of quaternion vectors which drove the Denavit-Hartenberg approach. This ensured that the human hand model was more accurate and efficient. The Extended Kalman filter provided further improvement by reducing the orientation estimation error of the hand model. The multiple IMU sensors allowed for better performance of the sensory glove. It significantly increased the accuracy and precision of the motion and orientation tracking system with the higher degree of freedom. It provided an energy efficient and well-integrated system. The system displayed all the aspects of mechatronic design. The main drawback of the system was the computational expense of the design.

### 3.4.3 Design Concept 3

The final concept design used the Solidworks<sup>®</sup> package to create a three-dimensional hand model of a human hand. Once it was designed, it was imported into Simulink<sup>®</sup> using the Simscape multibody tool that created a suitable model for the human hand based on techniques such as DH method. The model would be less computational expensive as the software package would optimize the dynamic equations of the model for the target hardware. This was the computer engineering foundation of the design.

The foundation of the control engineering aspect of the conceptual design involved the use of Simulink<sup>®</sup>. Simulink<sup>®</sup> was used to create an Averaging filter for the system and had the capability to deploy the code directly onto the hardware. An Averaging filter was used as it was less computationally expensive while providing a possible solution for real-time application. Simulink<sup>®</sup> had robust filtering tools which allowed for an effective and efficient filtering solution. Simulink<sup>®</sup> had Arduino<sup>®</sup>

compatibilities, which allowed the computer and control engineering aspect to be integrated with the electrical and electronic elements of the project.

The electrical and electronic engineering aspects of the design were based on Arduino<sup>®</sup> Uno Microcontroller with fifteen IMU sensors. The Arduino<sup>®</sup> Uno's operational performance was outlined in the previous design with the board rate of 8 MHz and 5V power supply. The Uno had the capability to extract and control data from multiple IMU sensors due to its robust design. Multiple MPU6050 sensors were used in order to track the motion and orientation of the human hand. Fifteen MPU6050 sensors were positioned on the glove. Three were used on each finger, along the distal phalanges, middle phalanges and proximal phalange.

The MPU6050 data was captured using a data acquisition process. Once captured, it was configured to the orientation and motion data of the sensors through the dynamic mathematical equations. The fusion of the accelerometer and gyroscopic values allowed the system to validate the information calculated from the accelerometer using the gyroscopic data. It provided accurate and reliable data of the finger's motion and orientation. This allowed for significant improvements in the performance of the hand motion and orientation tracking ability of the system. All the sensors were powered by the same power source as the microcontroller. This created a compact and energy efficient system. All the IMUs, were connected with two multiplexers to enable the microcontroller to extract and control the sensor data simultaneously.

The final concept design focused on improvements that were made on the previous two designs. With the use of Solidworks<sup>®</sup> and Simulink<sup>®</sup>, the human hand model was a more effective and integrated system as it had the tools and capabilities to combine all the aspects of the design effectively. The Averaging filter allowed for greater efficiency and less computational cost while reducing the high-frequency noise and smoothing the signal. The use of dynamic mathematical equations for the accelerometer data of the sensors and fusing the gyroscopic values to that information enabled a more accurate system. The overall system was more compact, effective and integrated. The system displayed all the aspects of a mechatronic system and created a solid foundation for the final design of the sensory glove.

#### 3.4.4 Decision Matrix

In order to determine the best possible concept design, a decision matrix chart was used. The decision matrix chart allowed the research to systematically identify, analyse and rate the strength of the relationship between all the components of the system. The chart used various decision factors that were based on the aims and objectives of the research. Some of the elements were based on design specification, while others were based on design performance. The key factor in the decision matrix was integration. Each factor was weighted, depending on its significance to the research's objectives.

The total score for each design was calculated, and the greatest score determined the best suitable conceptual design for the research. The decision matrix can be seen in the Table 3-1 below.

Table 3-1: Decision Matrix for Final mechatronic Design

Factors	Weight	Design Concept 1	Design Concept 2	Design Concept 3
Energy Efficiency	1	3(X1) =3	3(X1) =3	3(X1) =3
Degree Repeatability	2	1(X2) =2	3(X2) =10	3(X2) =6
Degree of Accuracy & Precision	2	1(X2) =2	5(X2) =10	3(X2) =6
Compact Design	1	3(X1) =3	3(X1) =3	5(X1) =5
System Integration	3	3(X3) =9	3(X3) =9	5(X3) =15
Potential Motion Tracking	2	1(X2) =2	5(X2) =10	3(X2) =6
Potential Orientation Tracking	2	3(X2) =6	5(X2) =10	5(X2) =10
Cost Effectiveness	2	3(X2) =6	3(X2) =6	5(X2) =10
Ease of Use	1	1(X1) =1	3(X1) =3	3(X1) =3
Potential Applications	1	1(X1) =1	3(X1) =3	5(X1) =5
Total Rating		35	67	69

The Decision matrix showed that Design Concept 3 was the most suitable and efficient solution for the sensory glove system. With its use of an Averaging filter, a hand kinematic model driven by Simulink® Simscape Multibody tool and multiple IMU sensors, it provided a solution for the sensory glove design.

### 3.5 Final Mechatronic Design

The final mechatronic design that is proposed below was based on multiple key factors to ensure that it achieved the objectives of the research project. The decision matrix, from the above subsection, highlighted the essential features that were considered when determining the most efficient, integrated and cost-effective solution for a sensory glove. The main goal of the design was to ensure an energy efficient and low-cost integrated system between all the components was achieved. From the

mechanical feed-forward kinematic model to the averaging filter, all aspects of engineering involved in the creation of system needed to work in unison to create the ideal mechatronic design.

### 3.5.1 The Mechanical Hand Model

In order to model the kinematics of the human hand, each finger and thumb was modelled using solutions such as feed-forward kinematics. This was done by using the Simulink<sup>e</sup> Simscape Multibody tools. The tool also solved the equations of motion for the human hand model. This approach was outlined in the literature review, while the mathematics of the model is presented in this section.

The finger configuration was modelled as a single kinematic chain, orientated with the hand co-ordinate system. The finger configuration can be seen in the Figure 3-2 below. The finger configuration was for the index finger on the user's left hand. The co-ordinate axis was orientated such that, the y-axis was pointed to the MCP joint, the x-axis was pointed outwards with respect to the back of the palm and the z-axis was the axis that the joints rotated about. The distal, middle, proximal and metacarpal phalanges were modelled as rigid bodies. The local co-ordinate frame of each phalange was modelled at the midpoint of each bone segment. The z-axis of the local frame was aligned with the flexion-extension axis of the joint frame. These configurations are based on (Lortier, Sluiter, Roetenberg, & Veltink, 2018) due to ISB recommendations.

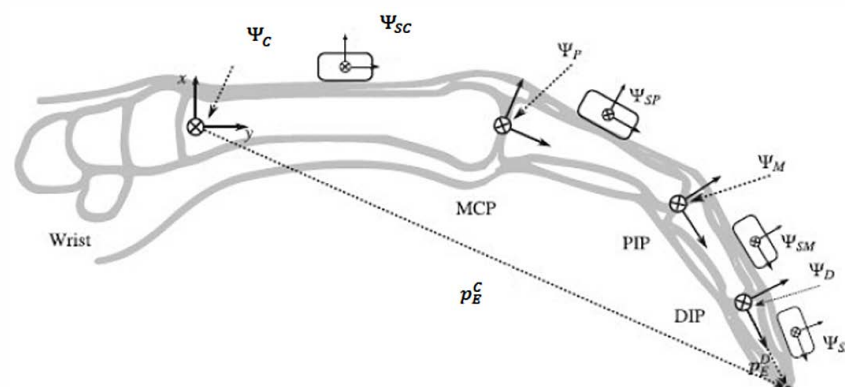


Figure 3-2: Configuration of Human Finger

In order to calculate the endpoint of the finger  $p$  (ie. Fingertip), the following expression was derived using forward kinematics with the Denavit-Hartenberg approach.

$$\begin{bmatrix} p_E^C \\ 1 \end{bmatrix} = H^{CD} \begin{bmatrix} p_E^D \\ 1 \end{bmatrix}$$

The expression is expressed in the carpal co-ordinate frame. The  $H$  notation represents the transformation between two bodies. The subscript represents the end of the finger (E). The superscript represents the Carpal body frame (C) and the Distal body frame (D). The  $H^{CV}$  was the transformation

matrix from the carpal phalange frame to the distal phalange frame. This transformation is derived below.

$$H^{CD} = \begin{bmatrix} R(q^{CD}) & p_D^C \\ 0_3^T & 1 \end{bmatrix}$$

Where the  $R(q^{CD})$  was the orientation of the distal phalanx with respect to the carpal frame, and  $p_D^C$  was the position of the distal frame with respect to the carpal frame.  $R$  represents the rotational matrix, which is defined by a unit quaternion and is expressed below.

$$R(q) = qq^T + q_0^2 I_3 + 2q_0[q]_{\times} + [q]_{\times}^2$$

Where  $q$  and  $q_0$  are the vector and scalar quaternion part. The above-mentioned mathematical models are used to determine the phalangeal joint angles and fingertip position. These calculations are similar what the Simulink<sup>®</sup> Multibody tool uses when creating the hand model for the project.

In order to import the model into Simulink<sup>®</sup>, a CAD model of the human hand needed to be designed. A CAD model of a human hand was created in Solidworks<sup>®</sup>. An example of a Solidwork's human hand model can be seen in Figure 3-3 below. The purpose of this model was to validate and verify the performance of the sensory glove system. The human hand was created in Solidworks<sup>®</sup> and then exported into Simulink<sup>®</sup>, using a toolbox known as Simscape Multibody tool. The tool allowed for three-dimensional models to be exported into a simulation environment within Simulink<sup>®</sup>. The tool formulates and solves the equations of motion of the human hand.

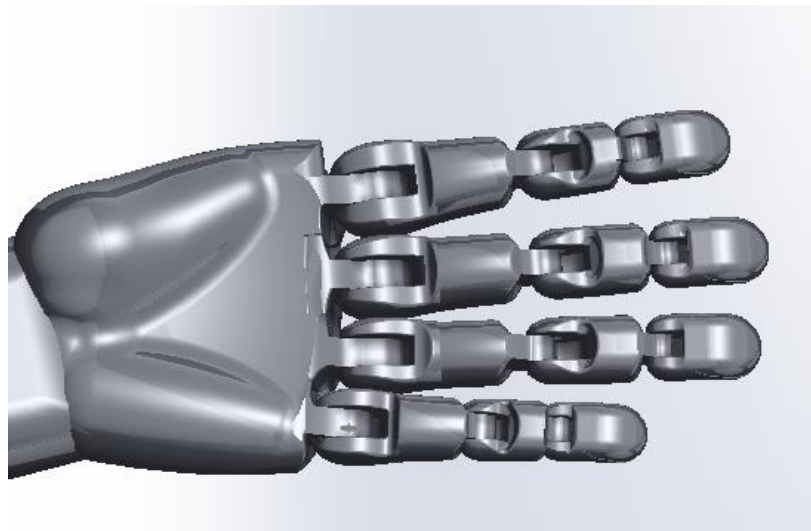


Figure 3-3: Example of the Solidwork<sup>®</sup>'s human hand model (Rhadamanthys76, 2016)

The Simulink<sup>®</sup> model of the hand was imported as a kinematic chain model with links representing the phalanges of the finger and revolute joints representing the finger joints. The tool eliminated the inefficiencies of the model and optimized the mathematical equations for the system. Once imported, it allowed the model to be integrated with the control, electrical and electronic systems of the project. The tools supported C++ Code generation which allowed the model to be exported onto external hardware.



This enabled the system to operate without the use of Simulink<sup>®</sup>. This model can be seen in Figure 3-4 below. The model allowed the user to simulate the motion of the hand as it provided a visual representation of the hand's orientation. In order to simulate the motion, actuators were used. Actuators were fitted to each joint of the Simulink<sup>®</sup> hand model to simulate the sensory glove's motion. The data from each sensor drove the respective joints on the Simulink<sup>®</sup> model. This was the method used by the researcher to verify and validate the performance of the sensory glove.

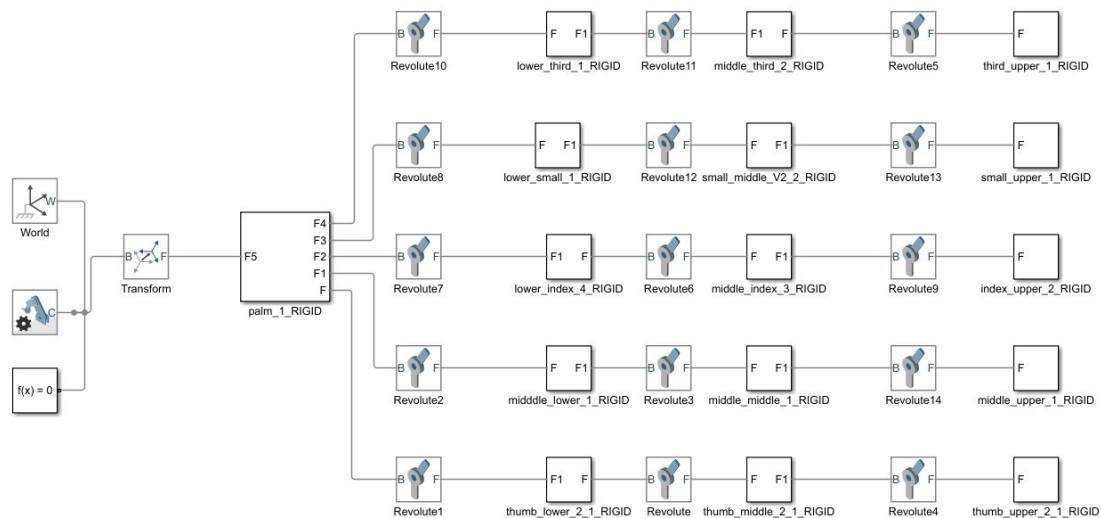


Figure 3-4: Simulink<sup>®</sup> Hand Model

The built-in actuators in the revolute joints of the model were controlled by the sensors on the sensory glove. These sensors were the MPU6050 as ADXL335 sensors consisted of a magnetometer. These sensors allowed for each phalange to have 6 DOF. The MPU6050 provided both accelerometer and gyroscopic data. This provided a more accurate sensor measurements at a low-price. The output of the sensors was the linear acceleration and angular velocity of each phalange on the hand structure. High-frequency noise was present in the data that was received from the sensors. To reduce the noise and smoothen the signal, an averaging filter was implemented.

### 3.5.2 An Averaging Filter Design

In this section, the development and implementation of the Averaging filter was explained. The use of an Averaging filter was essential for the system of the sensory glove as it provided a cost-effective method to reduce the noise from the sensor data. The filter was cost-effective as it required low computation power compared to the Extended Kalman filter, which was researched in the literature review. The main objective was to provide a cleaning stage for the data that was received from the MPU6050 sensors. This involved reducing the high-frequency noise that was present in the sensor data.

This increased the performance of the system. The averaging filter had the ability to smoothen the data, which provided a more stable and accurate system.

Digital filtering is a set of algorithms that are based on differential equations (Gonzalez-Barajas & Montenegro, 2016). Within the set of algorithms is a filtering solution known as Finite Impulse Response (FIR). They require only input samples to generate a filtered output. These filters are created for real-time application and have low computational cost. An Averaging filter is an example of a low-pass FIR filter that calculates the outputs samples using the average from a finite number of input samples. This type of filtering solution best fit the project as it had low computational cost. The filter smoothen the data by reducing the high-frequency distortions. Researchers (Gonzalez-Barajas & Montenegro, 2016) found that due to their simplicity, averaging filters were easy to implement and design for systems that required real-time applications.

The Averaging filter was based on the mathematical differential equations of a Digital filter. A Digital filter is a discrete system designed for processing data that has been stored in an array (Gonzalez-Barajas & Montenegro, 2016). The mathematical equations that modelled a digital filter are shown below:

$$\sum_{k=0}^{L-1} V_k y(n-k) = \sum_{k=0}^{L-1} W_k x(n-k)$$

The type of digital filter used was known as a Finite Impulse Response (FIR) filter. This filter used actual and previous inputs to perform a filtering process. It allowed previous outputs to be avoided and required less computational power. The mathematical equation for a FIR filter, when calculating the output, is shown below:

$$y[n] = \sum_{k=0}^{L-1} W_k x(n-k)$$

An averaging filter was a particular function of the digital FIR structure. The filter smoothen the signal and attenuates at higher frequencies. The mathematical equations for the averaging filter, when calculating the output, can be seen below:

$$y[n] = \frac{1}{L} \sum_{k=0}^{L-1} W_k x(n-k)$$

Where  $L$  is the order of the average filter and the filter has only one constant term in the transfer function. The poles were in the origin of the Z plane, which guaranteed the stability of the filter as the impulse response counts the finite number of terms. To obtain the parameters of the filter, the data can be passed through an Inverse Fourier Transform (IFT).

When designing an Averaging filter, the frequency response of the filter depends on the  $L$  values according to (2) and (3). With the relevant code and program, such as MATLAB®, the researcher can

estimate the frequency response. Once the code is run, the response of the filter in the frequency domain can be calculated for different values of  $L$ . This is further explained in Chapter 4 and an example of the frequency response of a system can be seen in Figure 3-5 below.

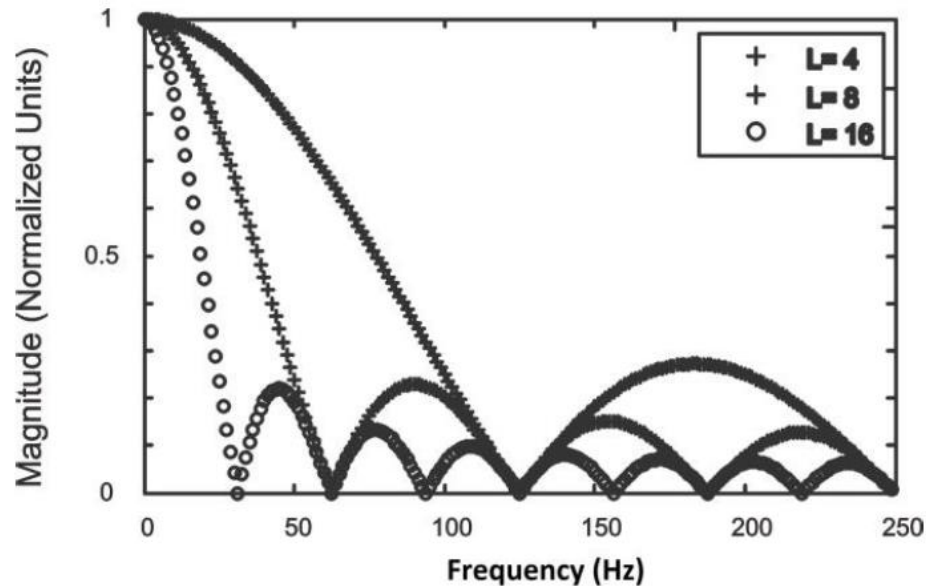


Figure 3-5: Response of the FIR filter for  $L = 4, 8$  and  $16$  (Gonzalez-Barajas & Montenegro, 2016)

### 3.5.3 Data Acquisition and Post-processing Algorithm

To extract the data from the IMU sensors, a data acquisition algorithm was developed. This process formed part of the control aspect of the project. The algorithm would extract the raw data from each sensor and configure the data to represent the linear acceleration and angular velocity of the sensor. The algorithm was created on Simulink<sup>®</sup> with the use of the Stateflow toolbox. The Stateflow toolbox is a graphical language tool that uses state transition diagrams and flow charts to build MATLAB<sup>®</sup> algorithms. It was used to build the algorithm as it allowed for Simulink<sup>®</sup> model integration. This enabled the algorithm to be integrated to the Arduino<sup>®</sup> hardware, which controlled the data from the IMUs. The algorithm used multiplexers to cycle through all the sensors to extract the data from each sensor. Once the data was extracted, the data needed to be post-processed and configured to the human hand model in Simulink<sup>®</sup>.

Since the Stateflow toolbox was integrated into Simulink<sup>®</sup>, it enabled the researcher to transfer the data to the Simulink<sup>®</sup> model to verify and validate the performance of the sensory glove. Before the data could be transferred to the model, the data needed to be passed through a post-processing algorithm. The goal of the algorithm was to reduce the noise in the sensor data and configure the data to the Simulink<sup>®</sup> hand model. To achieve this, the data was passed through an averaging filter as it reduces the high-frequency noise and smoothens the data. Once the noise was reduced, the data was be

configured to the respective phalanges on the human hand. This process considered the relative angles of each sensor between adjacent phalanges to achieve an accurate system. Once the relative angles of each sensor were configured to the associated phalange on the human hand, the data was fed to the Simulink<sup>®</sup> hand model. With the data fed to the Simulink<sup>®</sup> hand, the validation and verification process of the performance of the sensory glove began. This process is outlined in Chapter 6 of the thesis.

### 3.5.4 Circuitry

The circuitry for the sensory glove consisted of the electrical and electronic aspect of the project. The circuitry included fifteen MPU6050 sensors, two multiplexers and an Arduino<sup>®</sup> microprocessor. The fifteen MPU6050s were not all able to be connected to a single Arduino<sup>®</sup> without a multiplexer device. Therefore, two multiplexers were used as it was a three-line to an eight-line decoder was used. This enabled eight MPU6050s to be connected to one multiplexer while the remaining seven connected to the other multiplexer. The multiplexers had three controller pins, which allowed the Microcontroller to control the data from each sensor as it cycled through the sensors. The multiplexers had three enabler pins. This allowed the Arduino<sup>®</sup> to switch between them. The multiplexers were powered by the same a 3.3V supplier.

The fifteen IMUs had their voltage and ground line mning in parallel as they all required the same 3.3V supply. The researcher identified an effective method to read the data of all the IMUs. This involved mning all the SCL and SDA lines in parallel with each other into the Inicrocontr-oller. In order to differentiate the sensor data, the contr-oller would allow only one data line to be activated at a time. This was achieved by connecting each ADO line to one of the sixteen multiplexer input ports. The Arduino<sup>®</sup> would controller the multiplexers, which would contr-ol the data flow from each MPU6050 sensor into the Inicrocontr-oller. Once all the sensors were read, the cycle would continuously repeat itself. A more in-depth process is explained in Chapter 4 of the thesis. Figure 3-6 below showed a simplified example of the circuitry with only one multiplexer, one IMUs and an Arduino<sup>®</sup> UNO

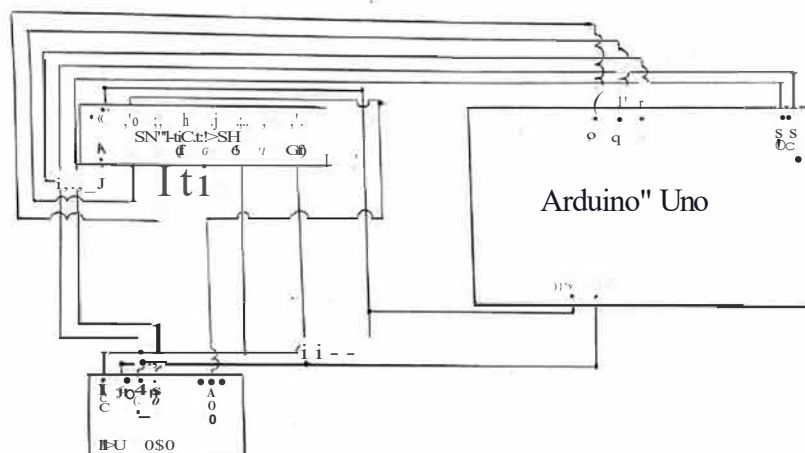


Figure 3-6: Simplified Circuitry

An Arduino<sup>®</sup> Uno was used as the microcontroller for this system (as seen in Figure 3.6). The Arduino<sup>®</sup> Uno performed the data acquisition of the system. It controlled all the data from the IMU sensors and performed the necessary calculations to determine the motion and orientation of the sensory glove. The device's board rate and operational power supply was the same as the IMU sensors. This allowed all the electronic components of the system to be operated by a single power supply and eliminated power complexities. The Microcontroller acted as the interface between the sensory glove and the Simulink<sup>®</sup> model of the human hand. It sent all the relevant data to the model to simulate the hand model and test the performance of the system. The Arduino<sup>®</sup> Uno is an open-source microcontroller that had Simulink<sup>®</sup> integration capabilities. The microcontroller was wired through the circuitry to the IMU sensors. The wiring that connected the IMU sensors to the Arduino<sup>®</sup> Uno was fed on the outside of the glove.

### 3.5.5 Glove Structure

The structure of the sensory glove outlined below was based on the design decisions that were made in order to develop and build a compact, integrated and energy efficient device. The glove needed to be made from a synthetic material that had elastic properties. This was important as it allowed the glove to be durable and malleable. The glove needed to be easy to work with as the hardware for the motion capturing needed to be sewed onto the glove. The glove was primarily made for a medium-size male hands with the parameters of the hand estimated by (Chen Chen, et al., 2011) . In order to ensure a cost-effective and ergonomic approach, a glove from the local hardware store was bought. The generic glove provided the requirements to meet the research objectives. The cost of designing and manufacturing a glove for the application was not feasible. The glove was initially intended for garden and home improvements work, which added a greater reliable and strength feature to the solution.

The IMUs sensors that were used on the final design included MPU6050 sensors. Fifteen MPU6050 sensors was used in order to track the motion and orientation of the human hand. The fifteen MPU6050 sensors were positioned across the hand on the glove. Three MPU6050 sensors were dedicated to each finger, with a sensor positioned on the distal phalange, middle phalange and proximal phalange.

In order to position the sensors on each phalange, a sensor holder was designed and developed on Solidworks<sup>®</sup>. The requirements of the design were to ensure that the holders could easily be attached to the glove while providing a compact yet cost-effective solution. The sensor holders needed to ensure that they would not compromise the ability of the MPU6050 when capturing data of the phalanges when in motion. The goal was to ensure that it was a well-integrated solution to minimize the errors in the motion and orientation captured by the device. The holders were manufactured with the use of a 3D printer. An example of the 3D printing machine that was used can be seen in Figure 3-7 overleaf. This manufacturing process allowed the holders to be designed to the specified size and shape of the

hardware. The material used was Polylactic Acid (PLA). PLA is a thermoplastic material that has high strength and easy to manufacture properties. With PLA having high strength properties, it allowed the sensor holders to add a layer of protection around the sensors while in operation. Therefore, this manufacturing method provided a light, cost-effective and compact solution. Therefore, 3D printing the components was the best method to manufacture the holders.



Figure 3-7: Creality CR-10 Max 3D Printer

### 3.6 Conclusion

In order to achieve an effective mechatronic design for a sensory glove, a detailed analysis of each component of the system was explored. The components included the fundamental aspects of a mechatronic system. These were the electronic and electrical, mechanical, control and computer engineering components of the system. The Solidworks<sup>®</sup> and Simulink<sup>®</sup> model of the human hand provided the computer component. The IMU sensors, Arduino<sup>®</sup> Microcontroller and circuitry provided the electrical and electronic part of the system. The control components were incorporated into the data acquisition and post-processing algorithm. The Averaging filter design contributed to the control component as it was integrated into the post-processing algorithm for the system. The synthetic glove and hardware holders were the focus of the mechanical element of the project.

To establish a cost-effective and robust design, the design process began by creating conceptual designs. Different sensor technologies and filtering solutions were explored. The three conceptual designs had to ensure that the core objectives of the research were achieved. The objectives were to ensure that a low-cost sensory glove apparatus was to be built with high performance and reliability while providing

an integrated solution. The main goal was to create a system that was effectively and efficiently integrated. That task included motion capturing and orientation estimation of a human hand while stationary or in motion. Through the above parameters, the best conceptual design was chosen and used as a foundation for the creation of the final mechatronic design of the sensory glove.

The final mechatronic design of the sensory glove was built with different components that were introduced in the conceptual design process. In terms of the computer engineering aspect, the feed-forward kinematics with the Denavit-Hartenberg approach was used as it effectively modelled the human hand as a single kinematic chain. This reduced the complexity of the model while decreased the computational resources required. This was achieved by developing a human hand model on Solidworks<sup>®</sup> and importing the model in Simulink<sup>®</sup> using the Simscape Multibody tool. The software also formulated and solved the equations of motion for the human hand. It enabled the model to be easily integrated with the control, electrical and electronic systems of the project. The Simulink<sup>®</sup> model allowed the researcher to verify and test the performance of the sensory glove as it had Arduino<sup>®</sup> integration capabilities.

The control engineering aspect of the system was divided into two sections. The first involved the development and implementation of an Averaging filter. The objective of the filter was to reduce the noise and smoothen the data from the sensors. This type of filtering solution best fit the project as it had low computational cost and real-time application. In order to design the filter, the data was passed through an Inverse Fourier Transform (IFT). This was done to determine the frequency response of the system and the parameters of the filtering solution. The second section involved the development of data acquisition and post-processing algorithm. The data acquisition process was created to extract the data from the sensors and configure it to represent the motion and orientation of the device. Once the data was extracted, it was passed through a post-processed algorithm to configure it to the human hand model in Simulink<sup>®</sup>. The algorithm involved reducing the noise in the sensor data by passing it through an averaging filter. Once complete, the data was configured to respective phalanges on the human hand. With the data configured to the Simulink<sup>®</sup> model, the testing of the sensory glove's performance could be performed.

In terms of the electrical and electronic component of the system, the MPU6050 sensors were the ideal solution in order to track the motion and orientation of the human hand. With the use of two multiplexers, all the MPU605s were integrated with the Arduino<sup>®</sup>. The sensors provided the required information about the phalanges. The sensors were a compact and power-efficient solution. The sensors, multiplexers and Arduino<sup>®</sup> were powered with the same voltage supply. The Arduino<sup>®</sup> Uno was used as the microcontroller for the system. It was able to perform all the data acquisition for the project. Since Simulink<sup>®</sup> had Arduino<sup>®</sup> capabilities, the Arduino<sup>®</sup> Uno was the ideal solution to integrate all the aspects of the project.

The Mechanical engineering aspects of the system involved the synthetic glove and the hardware holders. A synthetic glove was required to be durable and cost-effective. The sensors needed to be attached to the glove and a synthetic material allowed for this. Three MPU6050 sensors were positioned across each finger on the glove. The sensors were placed on the distal phalange, middle phalange and proximal phalange respectively. Hardware holders were designed and manufactured to achieve this. The holders also served as protection layer for the hardware during operation. The holders were manufactured using a 3D printer. This was to ensure that a compact, lightweight and low-cost solution was achieved.

For the reasons stated in this section, the final mechatronic design that was developed provided an adequate solution for the research. The design encompassed all the requirements that were needed for the solution to achieve the objectives of the research. A sketch of the final mechanical design can be seen in Figure 3-8 below.

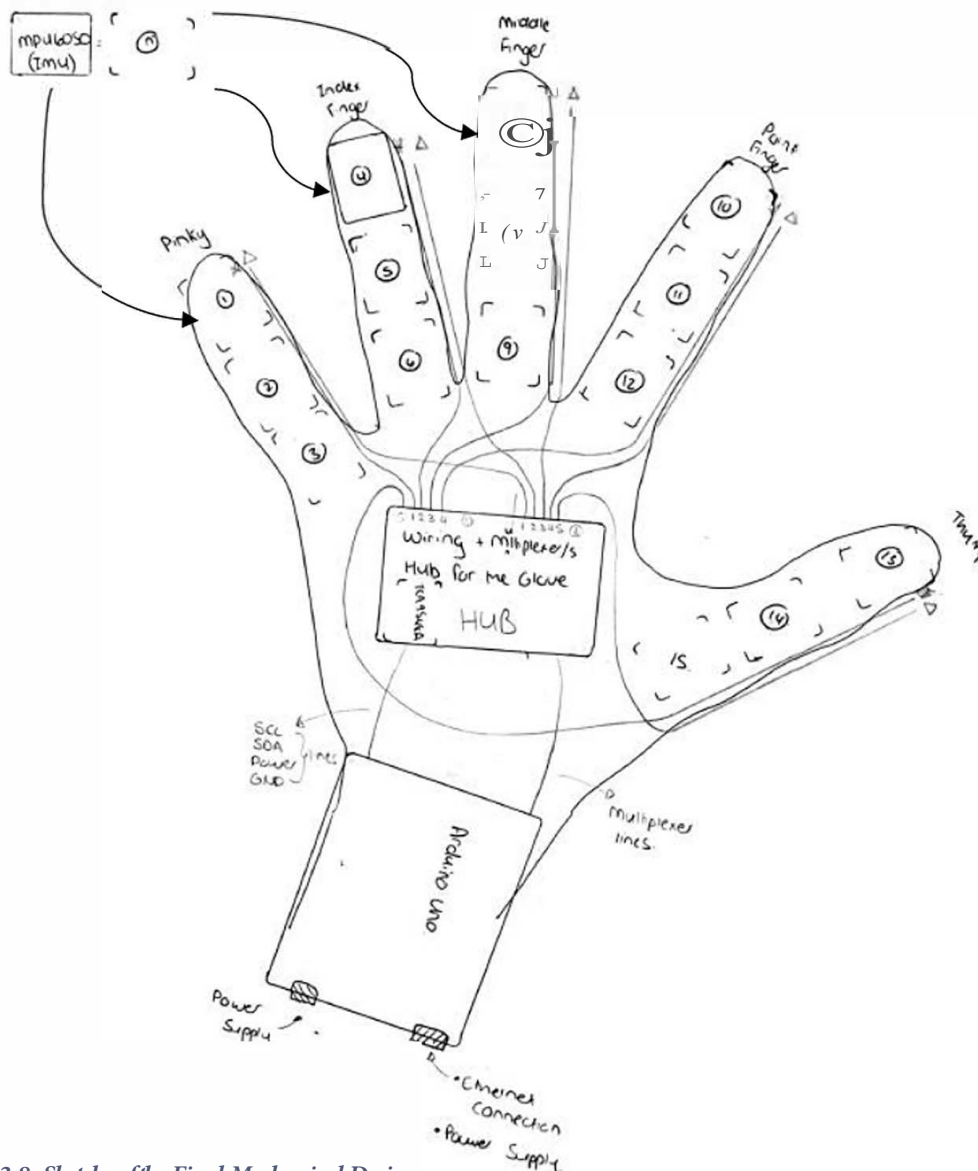


Figure 3-8: Sketch of the Final Mechanical Design



## 4. MANUFACTURING & ASSEMBLY OF SENSORY GLOVE

### 4.1 Introduction

Through the design process, different approaches were developed to create the sensory glove system. These ideas and techniques theoretically showed the ideal solution to the problem. Through the manufacturing and assembly process, engineering challenges arose. These problems were a result of multiple factors, which included hardware limitations, integration configurations, and random errors. These all contributed to the process of manufacturing as well as validating the effectiveness of the device. The manufacturing and assembly process were divided into four subsections. These subsections dealt with the mechatronic fundamentals of the project. Figure 4-1 below represents the four key aspects of a mechatronic system.

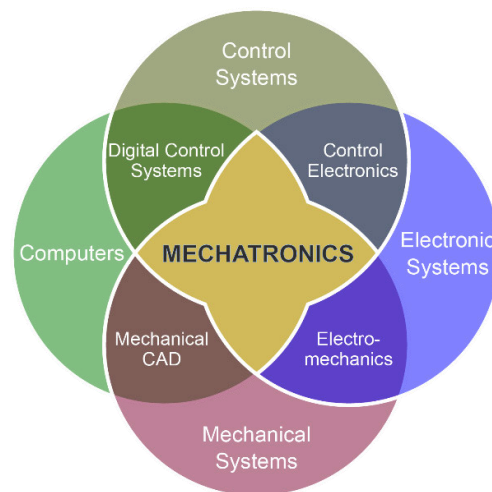


Figure 4-1: The Fundamental Components of a mechatronic System (Spiegel, 2017)

This diagram illustrates the thought process when dividing the project into the following four elements of a mechatronic system. These elements include:

- Electrical and Electronic System
- Control System
- Computer System
- Mechanical System

The subsections of the system were used to identify and create the most efficient and cost-effective solution. Each element of the system was manufactured and integrated into the mechatronic system. The components needed to work efficiently as an integrated system to ensure a high-power efficiency and performance.

Each component presented unique challenges. This is outlined in the chapter to follow. The subsections described the problems that arose due to hardware limitations or integration configurations. It is

followed by a detailed approach of how the problems were resolved. Each challenge required a troubleshooting process, which led to the creation of alternate solutions. This allowed the components to work efficiently, as well as effectively, within the mechatronic system. Once the systems were created, the final product was assembled, and testing began. The final product can be seen at the end of the chapter (See Figure 4-19).

## 4.2 Manufacturing and Assembly Process of the Sensory glove

### 4.2.1 The Electrical & Electronic System

During the manufacturing process of the electrical and electronic system of the project, multiple modifications were conducted. The modifications were based on the limitations of the hardware and system integration configurations. The hardware limitations were due to the operational parameters of components in the system. The integration configuration challenges arose during the implementation of the electrical and electronic system, with the control and computer system. The electronic system's initial design, outlined in the final mechanical design section, presented significant issues due to the type of system that the project required. The initial setup of the electronic system is displayed in Figure 4-2 below. The image represented the initial system development to reduce potential electrical problems that would arise.

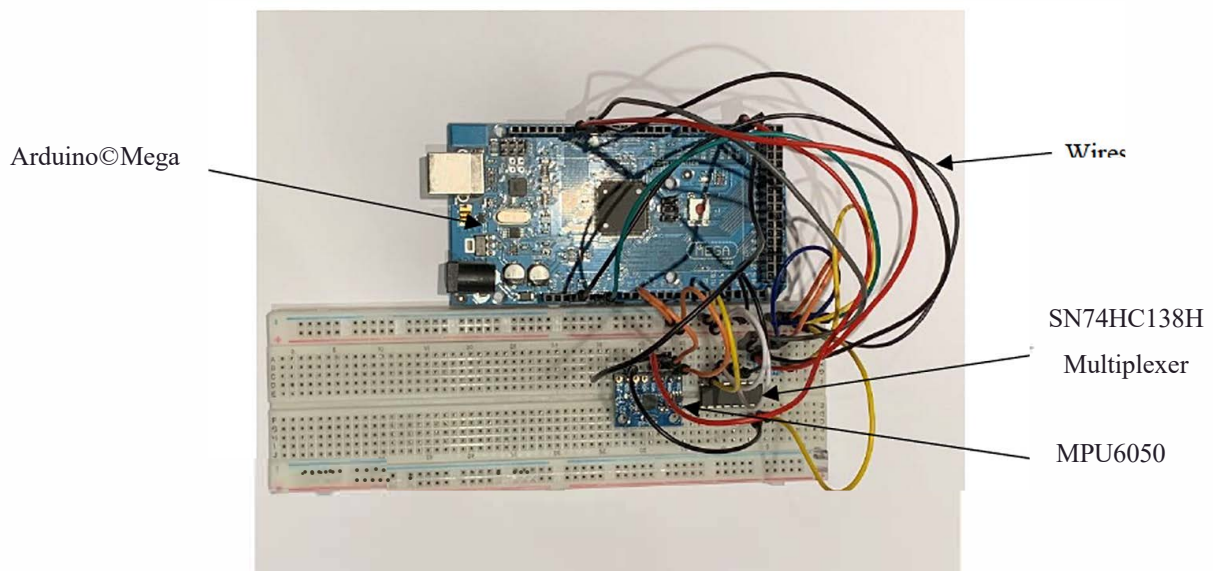


Figure 4-2: Initial Setup of Electronic System

Figure 4-2 illustrated the system architecture that was used to extract the data from a single MPU6050 sensor. It was developed by creating a circuit that included an Arduino<sup>®</sup> Mega, an SN74HC138H multiplexer, and an MPU6050. The Arduino<sup>®</sup> Uno was replaced with an Arduino<sup>®</sup> Mega due to its higher computational capacity. The SN74HC138H multiplexer was a three-line to an eight-line decoder. It allowed the microprocessor to connect and communicate with eight different I2C devices

by activating eight selected outputs. The multiplexer was implemented in the initial development stage to validate the performance and reliability of the device.

The Arduino® controlled the multiplexer with three selector pins. The selector pins, based on the combination of high and low signals sent to the multiplexer, managed the data received by the Arduino® when in operation. The multiplexer voltage input was connected to the 3.3V port on the Arduino®. The three enabler pins G2A, G2B, and G1, were connected to ground port (1), ground port (2), and 3.3 V port, respectively (See Figure 4-3 below). The MPU6050 voltage input was connected to the 3.3 V port on the Arduino®, as that was the sensor's operational voltage. The SDA and SCL ports on the sensor were connected to the same associated pins on the Arduino®.

There were no pull-up resistors implemented between the sensor and Arduino® as the I2C communication lines had built-in pull-up resistors. These resistors are present as I2C bus standard requires pull-up resistors on the line to drive an open collector or drain device (like the MPU6050 sensor). The built-in pull-up resistors were sufficient for the application of the system architecture. The sketch of the electrical & electronic architecture can be seen in Figure 4-3 below.

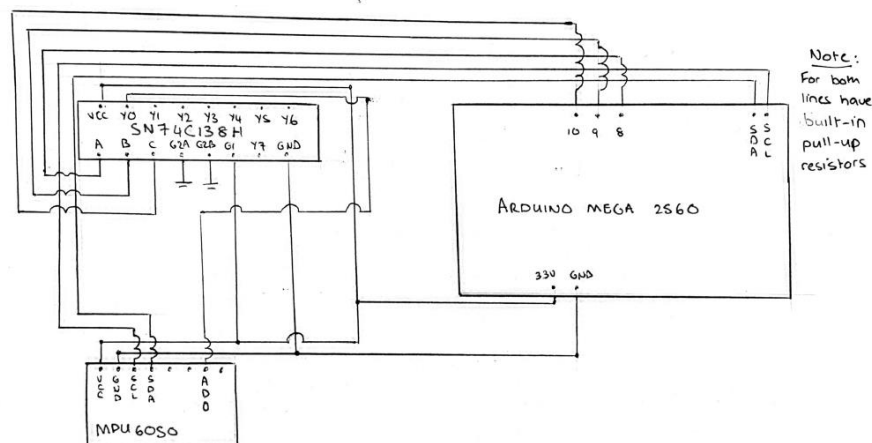


Figure 4-3: Sketch of electrical & electronic architecture

The Arduino® code, which is present in Appendix A1, was used to perform the data acquisition process to obtain the accelerometer and gyroscopic data of one MPU6050. This was done using the Arduino® IDE software package. This package was only used in the initial development stages. It was a success, as the values obtained by the MPU6050, when rotated into three predetermined orientations, represented accurate values. An example of the results can be seen in Appendix A2. Therefore, additional sensors were connected in parallel.

To connect multiple sensors, the SDA and SCL lines of all sensors were connected in parallel. Each sensor's ADO line was connected to the next available output pin on the multiplexer. The Arduino® code was duplicated and configured to control the selection of data using the multiplexer during every loop. Once the data from all the sensors were read to the Arduino®, the code repeated the process. With

each sensor added, the orientation test was performed to ensure that the sensors were operational in parallel. This was a preliminary test to ensure that the system architecture was operating as intended.

With the sixth MPU6050 sensors installed in the circuit, a problem arose. The configuration shorted the board during the initialization stage of the code. To troubleshoot the problem, multiple checks were carried out to determine the fault. Firstly, the wiring configuration of the system was investigated. This was stage I of the check process as most of the problems that could arise were from a mismanagement of wires. Secondly, an oscilloscope was connected to the SDA and SCL lines. The oscilloscope was used to validate the voltage signals that were sent from the sensors into the Arduino<sup>®</sup>. With five sensors connected, the oscilloscope voltage readings from the SDA and SCL signals showed that they were adequate and sufficient to allow for communication between the devices.

However, when the sixth sensor was added, the code would terminate during the initialization process, and the sensors would send no data. It was noted that the code would terminate only when the sixth SDA line was connected. It was anticipated that it was a bus overloading problem that was causing the code to stop during the initialization process. Therefore, to test this theory, the researcher altered the Arduino<sup>®</sup>'s I2C bus board rate. This was done by decreasing the I2C bus board rates to check if it was an overload problem. The board rate was adjusted between 10 Hz and 100 kHz speeds, with increases in the order of ten. This approach had no success in solving the problem.

Through further research and development, a more compact and efficient circuit arrangement was designed and implemented to troubleshoot the problem further. This resulted in the designing and manufacturing of a single Printed Circuit Board (PCB) board. The PCB board simplified the circuit architecture and created a more compact solution. A PCB board is an operational circuit that has electronic components and conductive line traces that connects the electronic components to form a working assembly (Integrated, 2020). The board was made from a non-conductive material such as fiber-glass. The PCB board can be seen in Figure 4.4 below.

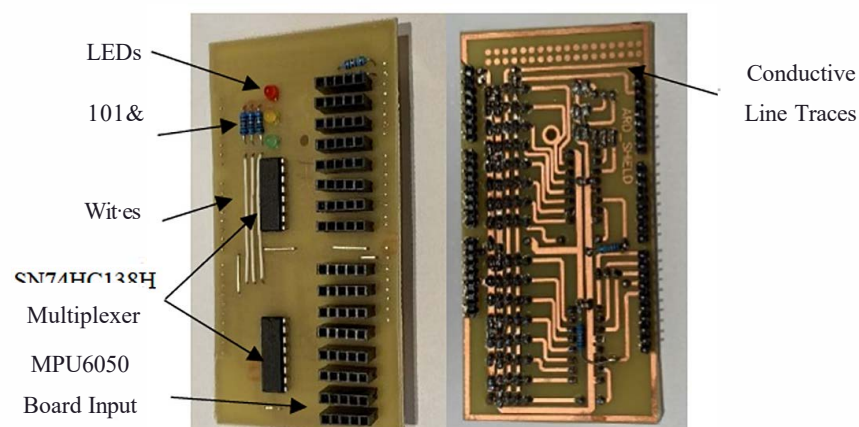


Figure 4-4: Design of PCB Board: Top View (Left) & Bottom View (Right)

The PCB board was designed for the footprint of the Arduino® Mega to ensure easy connection and implementation. The board's configuration copied the designed circuit, which had been created on the breadboard for the system. An additional multiplexer was added to allow for future implementation of MPU6050 sensors to be connected to an Arduino® Mega. Three LEDs were also installed to validate the programming code visually. The code logic enabled the selection and deselection of the output lines on the multiplexers.

Once the PCB was implemented on the Arduino® Mega, any internal connection issues were resolved. It was thought that it could be a connection issue that was causing the communication problem; however, it was not the case. The next stage of troubleshooting the system was initiated. It involved the use of a multimeter and oscilloscope to check the current and voltage across the sensors. The VCC port of the pin was 3.3 V, which is the operational voltage of the device (see data sheet in Appendix B1). The current through the device was approximately 2 mA, which was the desired current of the device (see data sheet in Appendix B1). The voltage across the SDA and SCL lines of the sensor was 5 V. It showed the voltage received through the AD0 line of the sensor, during operation, was above the operational value of the MPU6050. This occurred as the operating voltage of the Arduino® Mega board was 5 V. The Arduino® Mega operated at 5V due to the configuration and onboard components. It resulted in a higher current to flow into the sensor via the SDA and SCL lines. Therefore, the circuit shorted when the sixth sensor was attached to the system.

To correct this, an Arduino® chip that operated at 3.3 V and had the same footprint of the Arduino® Mega had to be used. The new Arduino®'s footprint needed to be a replica of the Arduino® Mega as the PCB board was built to fit on the Arduino® Mega. Through research, based on operational performance and capabilities, an Arduino® Due was chosen as it met the above requirements. Once the Arduino® Due was acquired, it was implemented in the system, and it resolved the circuit issue. With the new Arduino® Due installed into the system, the sixth sensor (MPU6050) was installed. With this success, more sensors were added to the system one at a time. When the tenth sensor was installed into the system, a second problem arose. The code terminated during the initialization when the tenth sensors were connected. Troubleshoot steps were repeated, as mentioned above, to find a potential solution.

With the new system architecture (PCB board), the error was not caused by wiring management. The oscilloscope was connected to the SDA and SCL lines to examine the voltage readings. Through investigation, the voltage signals did not raise any potential concerns. A multimeter was used to validate the operational current flowing through the sensors (MPU6050). These values were verified to be correct for the system based on the data sheet's operational values.

After careful analysis, it was determined there could be a problem with I2C communication. An alternate approach was researched to fix the problem. When nine sensors were connected in parallel, the system could cope with the I2C communication with all the devices. When the tenth sensor was

added, the system I2C communication failed. Since Arduino<sup>®</sup> Due had two I2C communication ports, which included two SDA and two SCL lines, it provided a potential solution. The solution was to split all the sensor's communication in half. It was done by connecting eight sensors to SDA and SCL line one, while the remaining seven sensors were connected to SDA and SCL line 2. With the maximum number of sensors being nine before causing an error in the system, it had the potential to solve the problem.

With this as a solution, the process of using the second I2C communication port was tested. The pinout diagram of the Arduino<sup>®</sup> Due (See Appendix B2) revealed that pull-up resistors did not exist on the second SDA and SCL lines. Two pull-up resistors were implemented on the two lines between the Arduino<sup>®</sup> and sensors to enable the I2C communication. The PCB board had to be modified to adjust for the new configuration. With this adjustment, it was noted that two sensors could be read simultaneously with two separate I2C communication lines. It presented two significant benefits to the system. Firstly, the system was able to read all the values of the sensors at half the sampling time. Secondly, the system allowed more movement to be tracked in the same space of time while providing a more accurate system to track the human hand's motion and orientation. With safety being a driving factor in the potential application of the system, it made the solution more attractive and realistic. The design of the modified PCB board system can be seen in Figure 4-5 below.

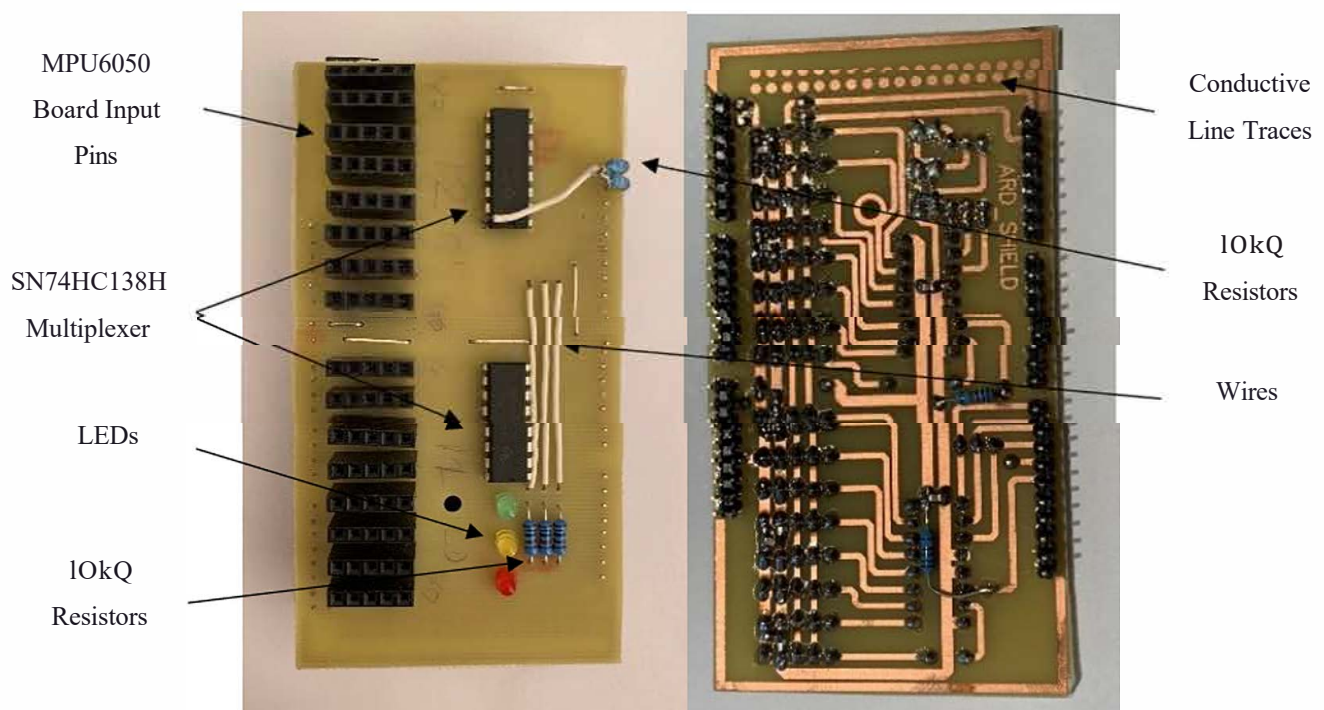


Figure 4-5: Design of modified PCB Board: Top View (Left) & Bottom View (Right)

The electronic system was further modified to reduce configuration complexity. Both multiplexers were activated at the same time and selected the same output data pins on their respective device. The multiplexer enabler pins were set up to ensure that they were operational once a power supply was

connected. The selector pins were wired in parallel with each other to ensure that both multiplexers were reading the same output data pin on their respective devices simultaneously. LED lights were connected in series with the ADO lines of the sensors to verify the programming code. It provided another method of troubleshooting if errors occurred as one could observe what sensor the code crashed on due to the illumination of the respective LEDs. A programming code was created for this system. It required less computational power, given the more straightforward circuit setup. It had higher efficiency as more sensors were read in a shorter period, with a decrease in sample time. All these benefits enabled a more effective and efficient system for the sensory glove. The redesigned PCB board and the system architecture can be seen in Figure 4-6 below.

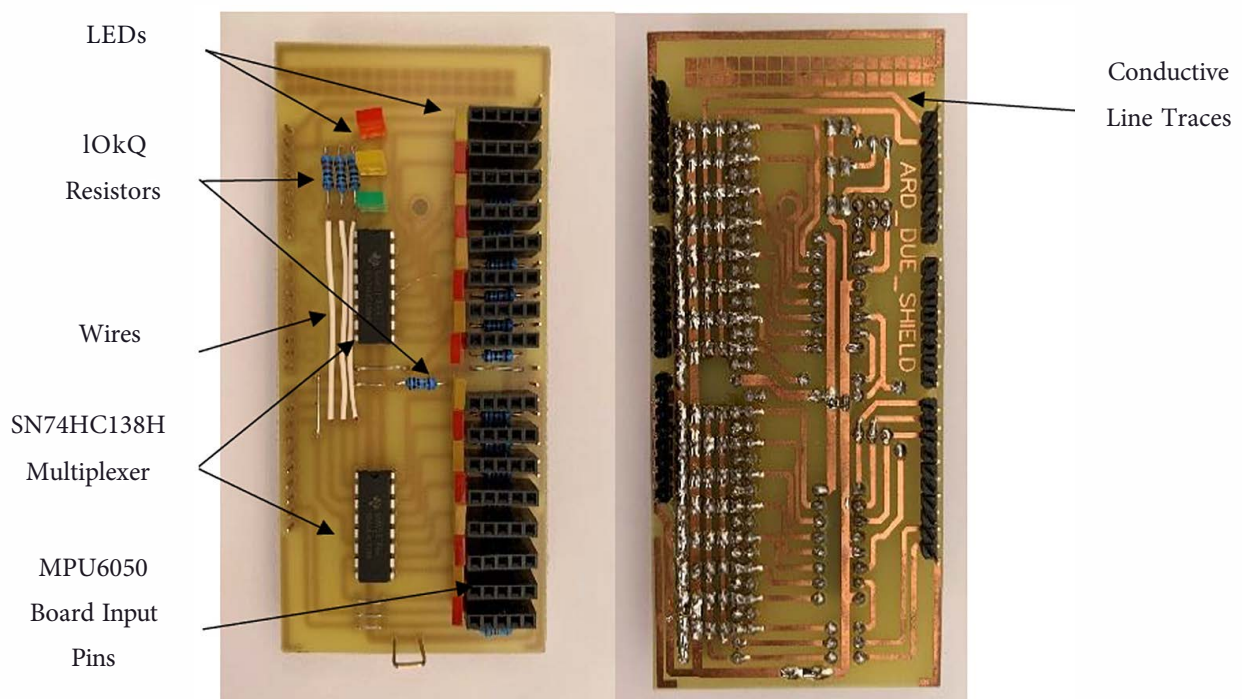


Figure 4-6: Design of final PCB Board: Top View (Left) & Bottom View (Right)

#### 4.2.2 The Computer System

The design of the computer system for the project involved two different software packages. AutoCAD<sup>®</sup>, a three-dimensional modelling computer-aided design program, was used to create the human hand's three-dimensional model. The hand model was designed in two parts. This included the palm and the fingers. The model's dimensions were based on studies that were conducted to measure the average human hand dimensions in (Chen Chen, et al., 2011). The study focused on the static, dynamic and kinematic characteristics of the human hand. The mean finger lengths and palm dimensions of the hand can be seen in Table 4-1 overleaf.

Table 4-1: Mean finger lengths and palm dimensions of the hand (Chen Chen, et al., 2011)

M	Finger length (crotch to tip)				Finger length (wrist crease to tip <sup>1</sup> )			
	mean	s.d.	5%<	95%<	mean	s.d.	5%<	95%<
Thumb	5.87	0.45	5.07	6.57	12.70	1.13	11.05	14.68
Index	7.53	0.46	6.83	8.19	18.52	0.88	17.33	20.06
Middle	8.57	0.51	7.82	9.74	19.52	0.92	18.10	21.04
Ring	8.0	0.47	7.44	8.93	18.72	0.91	17.52	20.28
Little	6.14	0.47	5.44	6.99	16.61	0.91	15.11	18.10

The crotch to tip length was measured along the axis of the finger. It was the distance from the tip of the finger to the level of the same numbered webbed crotch between the fingers. The wrist crease to tip was measured along the axis of the digit (Chen Chen, et al., 2011). It was the distance from the midpoint of the fingertip to the wrist crease baseline.

Table 4-2 below shows each phalange dimension in the finger structure with I1, I2 and I3 being the distal phalanx, middle phalanx and proximal phalanx of the index finger respectively. A similar notation was used for the remaining phalanges on each finger.

Table 4-2: Mean length of hand and phalanges of index, middle, ring, and little finger (cm) (Chen Chen, et al., 2011)

	Hand	I 1	I 2	I 3	M 1	M 2	M 3	R 1	R 2	R 3	L 1	L 2	L 3
Male Right hand	19.29	2.32	2.37	2.65	2.60	2.78	2.80	2.29	2.56	2.76	1.96	1.92	2.51
Male Left hand	19.36	2.32	2.39	2.61	2.60	2.82	2.75	2.30	2.59	2.78	1.95	1.98	2.49
Female Right hand	17.60	2.23	2.24	2.45	2.44	2.55	2.56	2.12	2.34	2.52	1.79	1.74	2.26
Female Left hand	17.62	2.20	2.24	2.35	2.24	2.43	2.53	2.13	2.36	2.49	1.77	1.77	2.26

Table 4-3 represents the limits of movement of specific joints. These static constraints were collected by (Cobos, Ferre, Sanchez, Ortegom, & Pena, 2008). The constraints on finger flexion, extension and abduction/adduction can be seen in Table 4-3 overleaf.



Table 4-3: Static Constraints on specific finger joints (Chen Chen, et al., 2011)

Finger	Flexion	Extension	Abduction/ adduction
<b>Thumb</b>			
TMC	50° - 90°	15°	45° - 60°
MCP	75° - 80°	0°	5°
IP	75° - 80°	5° - 10°	5°
<b>Index</b>			
CMC	5°	0°	0°
MCP	90°	30° - 40°	60°
PIP	110°	0°	0°
DIP	80° - 90°	5°	0°
<b>Middle</b>			
CMC	5°	0°	0°
MCP	90°	30° - 40°	45°
PIP	110°	0°	0°
DIP	80° - 90°	5°	0°
<b>Ring</b>			
CMC	10°	0°	0°
MCP	90°	30° - 40°	45°
PIP	120°	0°	0°
DIP	80° - 90°	5°	0°
<b>Little</b>			
CMC	15°	0°	0°
MCP	90°	30° - 40°	50°
PIP	135°	0°	0°
DIP	90°	5°	0°

The first part of the hand-design was the palm. The palm was created as a semi-spherical shape with a rectangular footprint. It was modelled as the palm, as it best captured the centre of gravity and moment of inertia. The hand's dimensions can be seen in Table 4.1 above and an exploded CAD drawing of the hand model in Appendix C1. The palm was designed with five-link connectors so that the fingers could be easily attached to the palm. The link connectors resembled a one dimensional joint between the palm and the finger. It is known as the metacarpophalangeal (MCP) joint. This can be seen in Appendix C2.

After the design of the palm, the finger structure design began. Each phalange in the finger, which included the proximal, middle and distal phalanges, were designed as rectangular blocks with link connectors on either side. The link connectors were used to model the one DOF joints between adjacent phalanges. The phalanges were developed in this configuration to represent the first and second moments of inertia accurately. The second moment of inertia was a critical part of phalanges parameters, as it determined how the bones would move when in motion due to an applied torque. The muscles in a finger provided a force that allowed the phalanges to rotate. To accurately capture the hand's movement and form, the bone structure needed to be modelled effectively. The final dimensions of the phalanges were taken from Table 4.2 above and an assembly of the index finger can be seen in Appendix C3.

When all the parts of the hand model were developed, the parts were integrated into a hand assembly. The palm was fixed to the world frame. Each phalange was imported and joined to the palm, one section at a time. All the phalanges were designed with joint connectors to allow for easy assembly. The link connectors were used to mate the phalanges together. The phalanges were coupled together to ensure that all the joints between the bone segments had one degree of freedom. The final assembly of the human hand model can be seen in Figure 4-7 below.

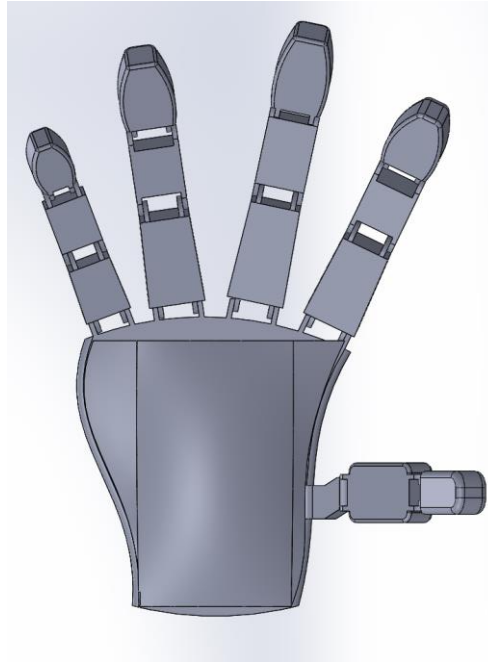


*Figure 4-7: Final Mechanical assembly of Human Hand*

With the hand model designed and developed, the next stage involved importing the model into a software package to build the control system. The software package, known as Simulink<sup>®</sup>, was chosen for the research project. Simulink<sup>®</sup> is MATLAB<sup>®</sup>-based programming software for modelling, simulating, and analysing data. Simulink<sup>®</sup> was the preferred software package as it had the Simscape multibody tool and Arduino<sup>®</sup> Integration capabilities. The Simscape multibody tool is an add-on package that allows users to model and simulate three dimensional mechanical systems. It allowed the researcher to import the CAD models of human hand. Once imported, the tool formulated and solved the equations of motion and dynamics of the system. The package provided the ability to integrate the mechanical model of the hand with the control system.

It also enabled the researcher to perform tests on the system's performance. The goal of the model was to validate and analyse the performance of the sensory glove. The Simscape multibody tool modelled the phalanges in the bone structure of the hand as links. The joints between adjacent phalanges were modelled as one DOF revolute joints. The package created a single kinematic chain system controlled through torque or motion inputs of each revolute joint. The model was designed to use motion inputs to simulate the motion of the sensory glove. Figure 4-8 below shows the model of the human hand created using the Simscape multibody tool in Simulink®.

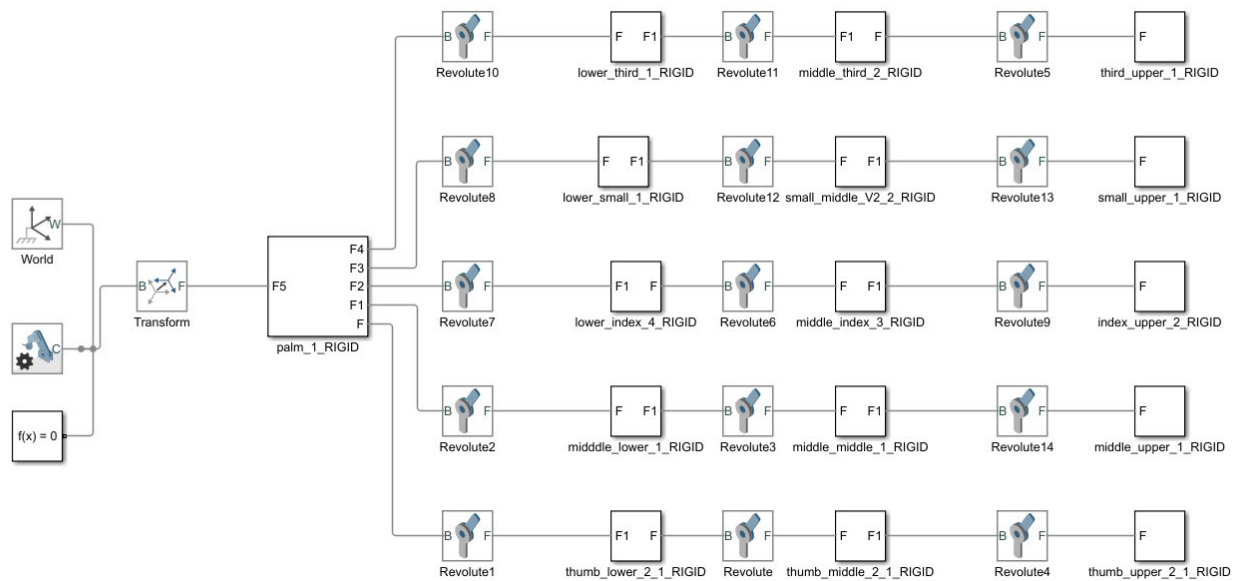


Figure 4-8: Simscape Multibody Model of Human Hand

With the hand model in Simulink®, it enabled the researcher to integrate the hand model into the control system for validation and data analysis.

### 4.2.3 The Control System

The design of the control system for the project involved the use of a software package known as Simulink®. The control system design began with the data acquisition process. The data acquisition process involved a control algorithm to perform multiple operations on sensor data from respective MPU6050 sensors. The process started by writing a Simulink® function to read the sensors' data (i2cRd) and write the data (i2cWr) to the hardware. It was created in the Simulink® workspace as there was no function available in the software package that could achieve this. The functions can be seen in Appendix D1 and D2

Once the functions were established, a Stateflow workflow was created (see Figure 4-9 below). The Stateflow began by initializing the sensors, setting the sensors to predefined sensitivity, and configuring the data before reading it. It included setting the gyroscope sensor's full-scale range to  $\pm 1000^\circ/s$  with a sensitivity scale factor of  $32.8 \text{ LSB}/(^\circ/s)$ . The accelerometer was set to a full range scale of  $\pm 8g$ , with a sensitivity scale factor of  $4096 \text{ LSB}/g$ . This allowed the sensors to detect fast rotation and abrupt motion. The abrupt motion would occur when a worker needed to change or stop the robot.

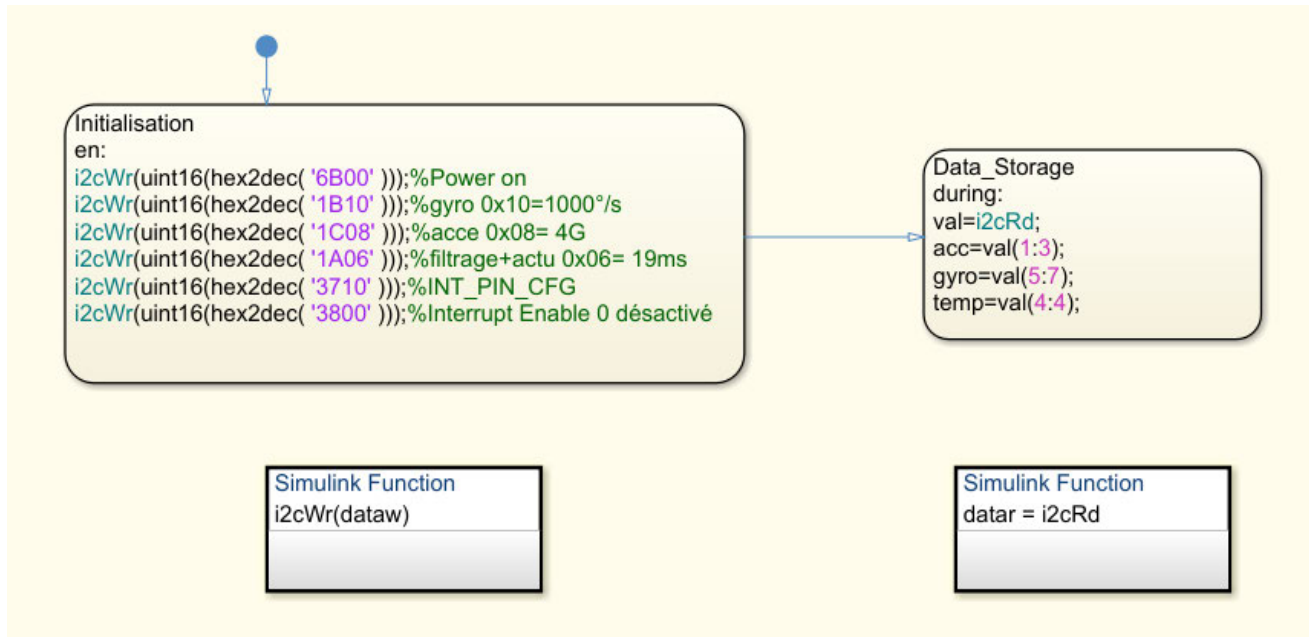


Figure 4-9: Stateflow workflow of the Control System

Once the sensor was initialized, the Stateflow commanded the sensor to read and write the data to the computer. The data was stored to a variable known as `acc` and `gyro` (See Figure 4-9 above). These variables captured the accelerometer and gyroscopic values, respectively, from the sensor. Both sets of data needed to pass through a gain device to configure the sensor's data. It included the angular velocity of the phalanges as well as the linear acceleration. The gain device was implemented in the model and depended on two operational parameters of the sensor. The first parameter included the full-scale range of the sensor, as shown above. The second parameter was the size of the information in bits that were read from the sensor. This allowed the raw byte data from the accelerometer to be converted into the gravitation vectors of the sensor (ie  $1 g = 9.81 \text{ m} \cdot \text{s}^{-2}$ ). The gyroscope's raw byte data was converted into an angular velocity vector (radians per second). The gain calculation for the accelerometer and gyroscope gain device can be seen below.

Accelerometer Gain ( $K_A$ )

$$K_A = \frac{\text{Full Scale Range}}{\text{Bit size of received information}}$$

$$K_A = \frac{4}{2 \times 10^{15}}$$

Gyroscopic Gain ( $K_G$ )

$$K_G = \frac{\text{Full Scale Range}}{\text{Bit size of received information}}$$

$$K_G = \frac{1000}{2 \times 101s}$$

Once the data from the sensors had been converted, the data was split up into its individual gravitation vectors, with respect to the x-coordinate frame, y-coordinate frame and z-coordinate frame (See Figure 4-10 below). A demultiplexer device was used to achieve this as it takes a single input data line and divided it into three digital output data lines. The gravitation vector with respect to the x, y, and z-axis frame was recorded over a period of time. This data was inputted into a user-built MATLAB<sup>®</sup> function to determine the roll ( $\theta$ ) and pitch ( $\theta$ ) estimation of the sensors (See Appendix D1 for custom MATLAB<sup>®</sup> code). The equation used to determine the above parameters (roll and pitch) can be seen below:

$$\theta = \arctan\left(\frac{Bby}{\sqrt{Blx + Blz}}\right)$$

$$\theta = \arctan\left(\frac{Bbx}{Bbz}\right)$$

After the data was inputted into the MATLAB<sup>®</sup> functions, the data was recorded and stored as a variable. These variables are known as Roll and Pitch (See Figure 4-10 below). The data was then required to undergo postprocessing. Due to the configuration of the hand model, only the pitch of the hand was important. Since the joints were modelled as one-dimensional revolute joints, it only required the pitch data values. No abduction was considered in this research. The goal was to establish a proof of concept within the field of Human-Robot Collaboration. A simplified version of the model can be seen in Figure 4-10, which illustrates the data acquisition and configuration process of the sensor's data.

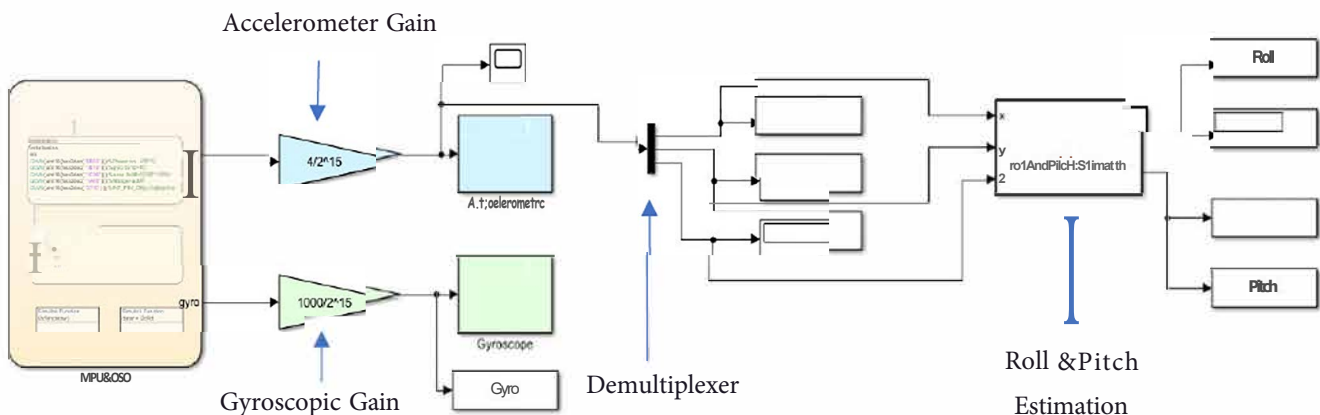


Figure 4-10: Simplified Data Acquisition and Configuration Model

Initially, the calculated roll and gyro values of the sensor were to be integrated to provide further accuracy for the orientation of the sensors. During the initial stage, it was discovered that while this process could work when dealing with a single sensor, it would not work with multiple sensors due to the time delay. The algorithm read all the sensors, one at a time. There was a time delay of ten milliseconds when cycling from one sensor to the next. The gyroscopic value was integrated with respect to time elapsed. This introduced significant errors in the angle of the sensor being measured. Furthermore, the gyroscopic values, within that time delay, would be in a different position or motion. Therefore, the sensory glove would be unable to detect the motion of the hand accurately.

Unlike the gyroscopic values, the accelerometer values were not integrated with respect to time to calculate its orientation. A trigonometric function was used to calculate the angle of roll ( $\phi$ ) and pitch ( $\theta$ ) of the sensor with respect to the direction of gravity. These equations are presented above in the text.

Once the data acquisition process was completed, the values were imported into a post-process model. The postprocessing model configured the data for the human hand model. The process began by importing the data into a MATLAB<sup>®</sup> function called Cleaning Function. The code assigned all the pitch values to the associated phalange and finger structure. Each finger was dealt with independently to compute its orientation accurately. With three phalanges that make up the finger, known as the proximal, middle, and distal phalange, the three signals from the sensors were assigned to their corresponding finger structure. This can be seen in Appendix D5. With the finger structure assigned, the values from each sensor were converted into a matrix. This allowed calculations to be performed using data from the sensors. A limit was imposed on the data values to ensure that values below negative ten degrees were ignored. That represented the smallest pitch that a finger could experience. A maximum pitch limit of the sensor was set at one hundred and twenty degrees. This is done with the DataPrep Function and is present in Appendix D6. This value was chosen based on research done by (Chen Chen, et al., 2011). The dynamic range of the finger joints rotation ranged between ninety degrees and one hundred and ten degrees. Therefore, each finger joint's dynamic range was set accordingly, with a safety factor of ten degrees.

With limits imposed, the configuration of the bone structure was established. To configure the sensors to represent the orientation of each phalange on the finger accurately, the structure of the finger was important. The proximal phalange was the base phalange of the finger. The sensor reading of that phalange represented the absolute angle. The sensor reading on the middle phalange, which is the second phalange in the finger structure, would represent the absolute angle of the sensor. However, as the finger was modelled as a single chain mechanism, the relative angle was required. This was the angle of the middle phalange relative to the proximal phalange. The middle phalanges reading needed to be an angular value based on the measurement from the proximal phalange. Therefore, the following

calculation was performed to calculate the angular value of the middle phalange about the proximal phalange,

$$PitchMidData = PitchMidData - PitchProxData$$

The same approach was applied to calculate the Relative Angle of the distal phalange, as it was relative to the middle phalange. The following calculation were performed to calculate the angular value of the distal phalange about the middle phalange,

$$PitchDistData = PitchDistData - PitchMidData$$

With these equations, the data from sensors enabled the Simulink<sup>®</sup> hand model to take form. The Simulink<sup>®</sup> model represented the form and orientation of the glove if it met the following criteria:

- The hand was in a horizontal position.
- The hand was performing a flat or flexion action.
- At least one finger was involved in the action.

If the following criteria were not met while the hand was in motion, the form and the orientation of the hand would not be determined by the system. It was to ensure that only the designated orientation was captured due to the application of the system. The application of this system was complex and required high safety protocols. When the glove was operational, the initial and final position of the hand can be seen in Figure 4-11 below.

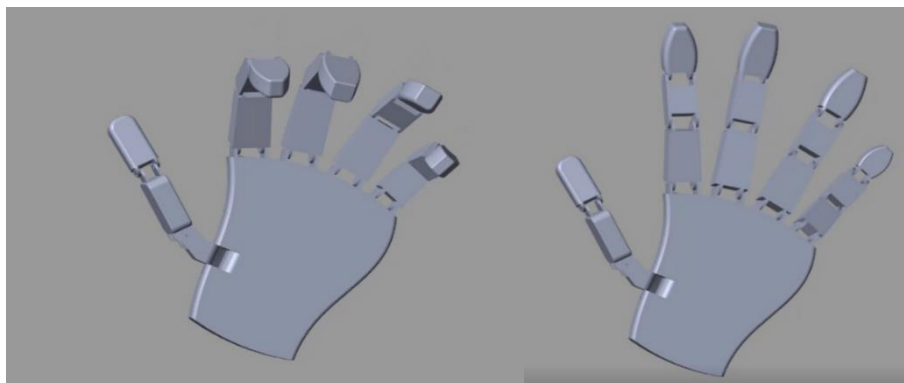


Figure 4-11: Initial (Right) and Final (Left) position of the hand model

Once these configurations had been complete, the final stage of the data processing began. It involved integrating the data from three sensors (three sensors per finger) into the Simulink<sup>®</sup> hand model. The integration into the hand model was complex as it involved second-order Simulink<sup>®</sup> functions, as well as a filtering process.

To integrate the configured data, the data was imported into the Simulink<sup>®</sup> workspace. It was imported via the MATLAB<sup>®</sup> workspace tool. This tool allowed the data to be stored in MATLAB<sup>®</sup>. Once imported into Simulink<sup>®</sup>, the data was initially passed through a windowed Chebyshev filter. The

window Chebyshev presented was an ideal filter as it had fast and robust characteristics (Smith, 1999). In order to design the filter, the sensor data was passed through an Inverse Fourier Transform (IFT).

The IFT produced a frequency spectrum of the configured sensor data. This spectrum was used as it showed the nature of the noise present in the measured signal. The IFT graphs the frequency spectrum signal verse frequency. The main signal components were located in the 0 and 10 Hz range (green block), while the remaining frequency spectrum represented the noise in the signal (red block). The filter was designed to filter out this noise. The above frequency spectrum was obtained by running the *FrequencySpectrumAnalysis* function (See in Appendix D2). The frequency spectrum of the system can be seen in Figure 4-12 below.

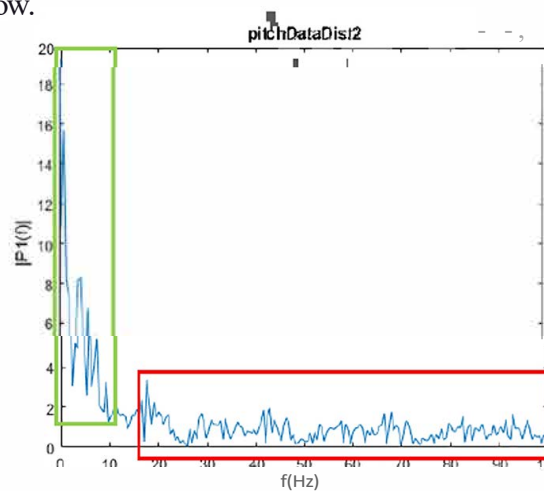


Figure 4-12: Frequency response graph from an IFT

The spectrum of the IFT in the diagram above indicated the cut-off frequency. It was a fundamental parameter in designing the Chebyshev filter. In order to design the filter, a Digital Filter design block was used within Simulink<sup>e</sup>. The block allowed the researcher to build a filter with the predetermined requirements. These requirements included:

- Response Type: Lowpass
- Design Method: FIR Window
- Filter Order: 10
- Sidelobe Attenuation: 100 dBs
- Cut-off Frequency: 10 Hz

The 10<sup>th</sup>-order provided better cut-off points for the filter. The sampling frequency of the filter was based on the sampling time of the system. The sampling time of the system was 0.005 seconds. The following equations were used to determine the sampling frequency.

$$F_s = \frac{1}{\text{Sampling Time}}$$

$$F_s = \frac{1}{0.005}$$



$$F_s = 200 \text{ Hz}$$

The cut-off frequency of the system was taken from the IFT spectrum and used in the filter design. Once the parameters were calculated, the filter was designed in Simulink<sup>®</sup> software and implemented into the system. Through initial verification of the filter, the efficiency of the filter was not adequate. Therefore, an alternate approach was taken by designing an Averaging filter.

The design parameters required for the Averaging filter was taken from the IFT spectrum that was used during the Chebyshev filter design. This filter only required an additional design parameter and it was the window length. The value of the window length varies greatly from application to application. The window length must not be large enough to contain noise in your signal while being too small that it diminishes the signal's properties.

With the average filter designed, the filter was implemented into the system. Figure 4-13 below shows the data from the sensors before and after the averaging filter was implemented.

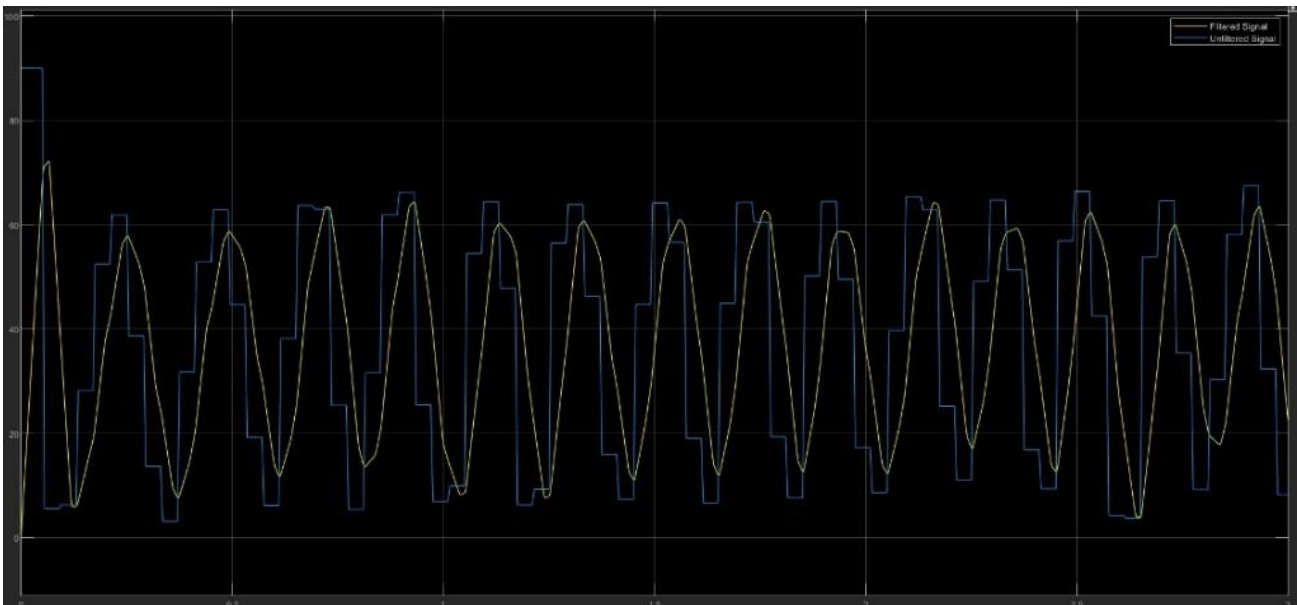


Figure 4-13: Sensor data before (blue line) and after (yellow line) the averaging filter was implemented.

It was noted that it eliminated the high frequencies that were present in data, which was due to noise in the system. It also provided more realistic angular values when a sudden motion occurred. It demonstrated the efficiency and speed of the filter when in operation. This was due to the small-time delay of the filter.

With the filtered implemented, the data was passed through two gain blocks. The first gain block converted the angular displacement of the rotation from degree to radians. The second gain block was the correction orientation block. It was performed to ensure the data sent to the joints resulted in the correct direction of motion. The block would either multiple the data by a positive or negative one to correct the object's rotation. With the filtered implemented, the data was fed through a PS-Simulink converter. It converted the physical input signal into a Simulink<sup>®</sup> output signal. It enabled the data to be integrated into the Human hand Simulink<sup>®</sup> model. The converter had a built-in second-order filter, which further refined the data for the hand model. This system model can be seen in Figure 4-14 below, which represents Part 1 of the postprocessing model in Simulink<sup>®</sup>.

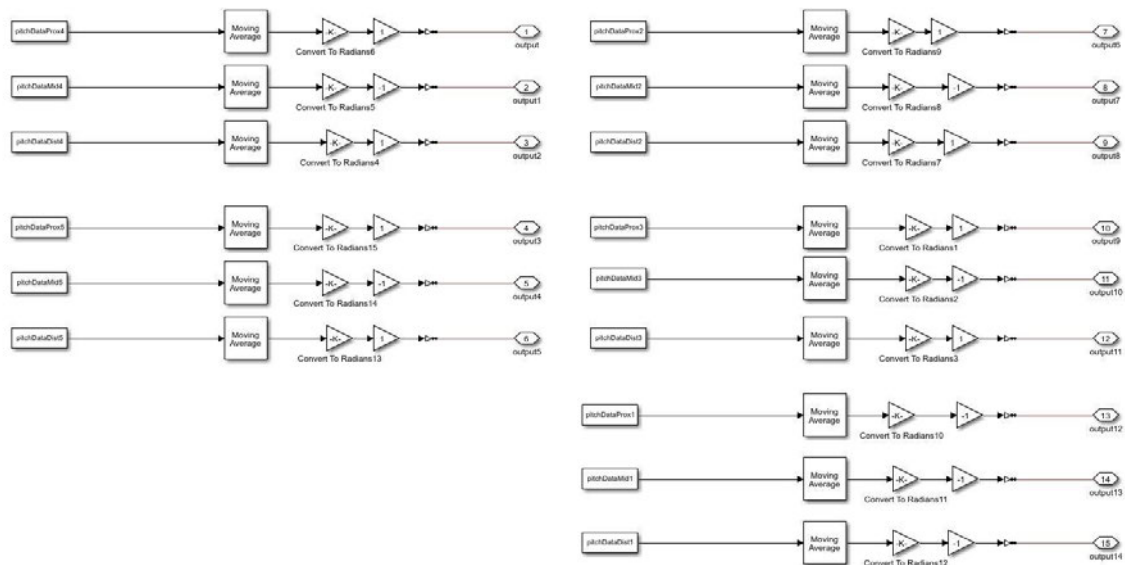


Figure 4-14: Part 1 of the Postprocessing Model in Simulink<sup>®</sup>

With the data converted, the data was inputted into their respective joints to control the phalanges on the hand. The phalanges were controlled by the input sensor data of the joints. The pitch data was fed into the respective joint as they had one degree of freedom. This can be seen in Figure 4-15 overleaf, which shows the Part 2 of the postprocessing model in Simulink<sup>®</sup>. With the data inputted, the simulation brought the hand model to 'life'. The motion and orientation of a human hand could be tracked as the sensory glove was in operation. The hand model mimics the movement and orientation of the sensory glove.

The final design of the Simulink<sup>®</sup> hand model can be seen in Figure 4-16 overleaf. It displays the entire Simulink<sup>®</sup> hand model and how the postprocessing model in Simulink<sup>®</sup> were integrated together.

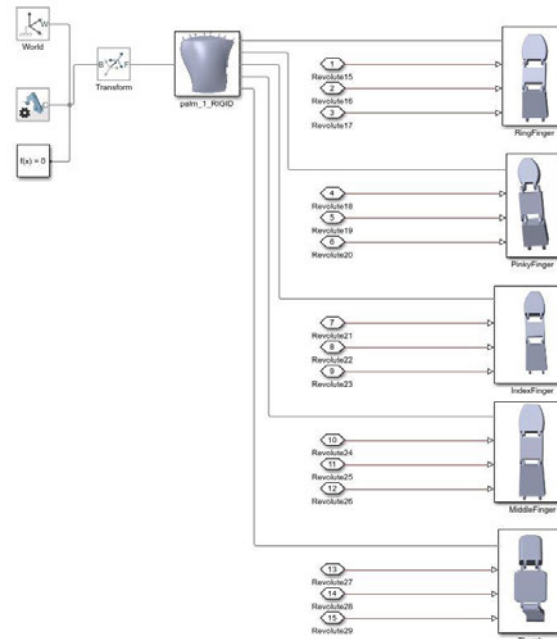


Figure 4-15: Postprocessing Model (Part 2)

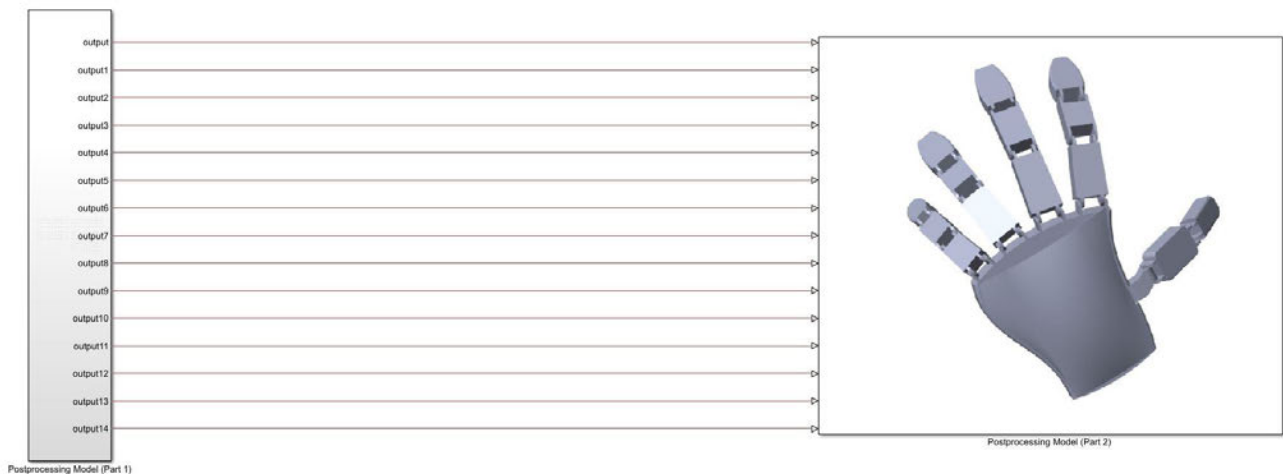


Figure 4-16: Entire Simulink® Model

#### 4.2.4 Mechanical System

The Mechanical system of the project included the design and manufacture of the architecture of the glove. The glove needed to be made of a low-cost material to ensure that the budget constraints were met. The project aimed to design and build a low-cost solution for this type of application. The glove needed to be durable to ensure high reliability when working in a dynamic environment. Since alterations were required on the glove, the glove needed to be malleable. Based on the requirements mentioned above for the glove, a Mac Afric working glove was acquired. The glove was made from a fleeced cotton and latex coating, which provided the lightweight and malleable properties required.

The

glove's size was chosen based on the requirements laid out in the human hand modelling section of the thesis. The glove can be seen in Figure 4-17 below.



*Figure 4-17: Mac Afric Working Glove (Adendorff, 2020)*

To attach the sensors to the glove, alterations needed to be made on the glove. The alterations included sewing Velcro patches to the glove. The hook side of the Velcro was sewed onto the glove. The velvet side was attached to the sensors. The sewing of the Velcro proved to be a challenging task due to the material of the glove. However, it provided a secure and robust base for the sensors to be attached on.

To attach the sensors to the glove, sensor holders needed to be designed and manufactured. These sensor holders were customized to the dimensions of the sensors and the dimensions of the fingers. The holders provided support for the sensors to operate while protecting them in operation. The holders needed to be light and cost-effective to meet the budget requirements of the project. Through the investigation of multiple different manufacturing techniques to produce the holders, it was chosen to 3D print them. 3D printing provided the ideal solution to manufacture the holder. It allowed the holders to be explicitly designed for the sensors while providing a cheap manufacturing process. The holders were designed using the Solidworks® package. When designing the holders, three criteria were considered:

- Stability
- Cost-effective
- Protection

Stability was an important parameter that had to be met to ensure that sensor was always in the correct orientation while stable during operation. If the sensors moved around the finger while in operation, it would affect the sensory glove's accuracy and precision. The sensors also needed to remain secure in the sensor holder while the glove was tracking the user's hand motion and orientation. Therefore, pins were designed in the holder to prevent lateral movement. The sensor holder not only needed to be made from a cost-effective material, but it was also required to be manufactured with a cost-effective method. The material which was used to print the holders was known as Polylactic Acid (PLA). It is a thermoplastic material that has high strength, lightweight and easy to manufacture properties. PLA was derived from renewable resources and is biodegradable. It makes the material eco-friendly and versatile. With PLA having high strength properties, it provided greater protection for the sensors while in operation. It was the final criteria that was considered when designing the holders.

The sensors holders were designed to hold the sensors and fit around a person's finger to ensure a secure and stable position. The base of the sensor holders was designed to the curvature of the phalanges. The top of the holders was designed to hold and protect the sensors. All of the above requirements went into the design and development process of the sensor holders. The Solidworks<sup>®</sup> design of the sensor holders can be seen in Figure 4-18 below. The Solidworks<sup>®</sup> drawing can be seen in Appendix C4.

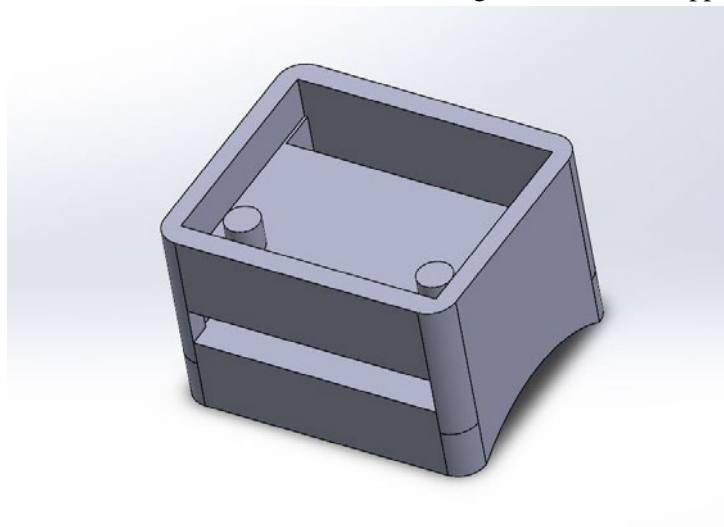


Figure 4-18: Final Design of Sensor Holder

Once it was created on Solidworks<sup>®</sup>, it was imported into a program known as Ultimaker Cura to perform the manufacturing process. The design was spliced into multiple layers, and the parameter of the print was set to produce the desired product. The printer printed layer by layer until the whole part was created.

### 4.3 Conclusion

A mechatronic design approach was fundamental in the design and development of the Sensory glove.

The theory of a mechatronic system allowed the researcher to divide the project up into four key

components. The design stage enabled the researcher to design a system that was inclusive of all the key components that existed in the sensory glove system. The manufacturing stage enabled the researcher to develop a mechatronic system that was well integrated with high performance. The performance of the system is tested in the following chapter.

Integration was a significant factor in the development of the system, as it was the glue that creates a well-developed mechatronic system. During the development of the system, a balance between integration and performance had to be reached. This approach was the focus area when developing each subsystem of the design while providing a low-cost solution. For the software and control aspect of the project, Simulink<sup>®</sup> and Solidworks<sup>®</sup> were the ideal software packages. Simulink<sup>®</sup> was used to create the project's control system, as it integrates all the components of the project together. Simulink<sup>®</sup> provided extensive filtering design capabilities and robust libraries for mathematic equations, which enabled the creation of a control system. The Solidworks<sup>®</sup> package was used to design and develop the system's human hand model, as it was linked to Simulink<sup>®</sup>. The Simscape multibody tool provided an effective way to integrate the Solidworks<sup>®</sup> hand model with the Simulink<sup>®</sup> Control model.

For the electronic and electrical aspect of the system, the Arduino<sup>®</sup> Due microprocessor provided a robust solution for the data acquisition process. The dual I2C communication lines allowed the researcher to solve the I2C communication problem and reduce the data acquisition process's sampling time by half. Simulink<sup>®</sup>'s Arduino<sup>®</sup> support enabled an effective integration of the electronic system with the control component of the mechatronic system. Compared to similar devices, the MPU6050 sensors were an effective solution for motion capturing due to its low-cost, size, and performance capabilities. The mechanical system ensured that all the hardware components of the system were protected. The glove provided a cost-effective and flexible device to integrate the sensors and Arduino<sup>®</sup> hardware. The sensor holders enabled the MPU6050s to be woven into the glove. It ensured that all movement of the human hand was captured.

With the above design and development of the Sensory system, the project was clearly positioned in the mechatronic domain (See Figure 4-1) as it encompassed the four key components of a mechatronic system. The sensory glove can be seen in Figure 4-19 overleaf.

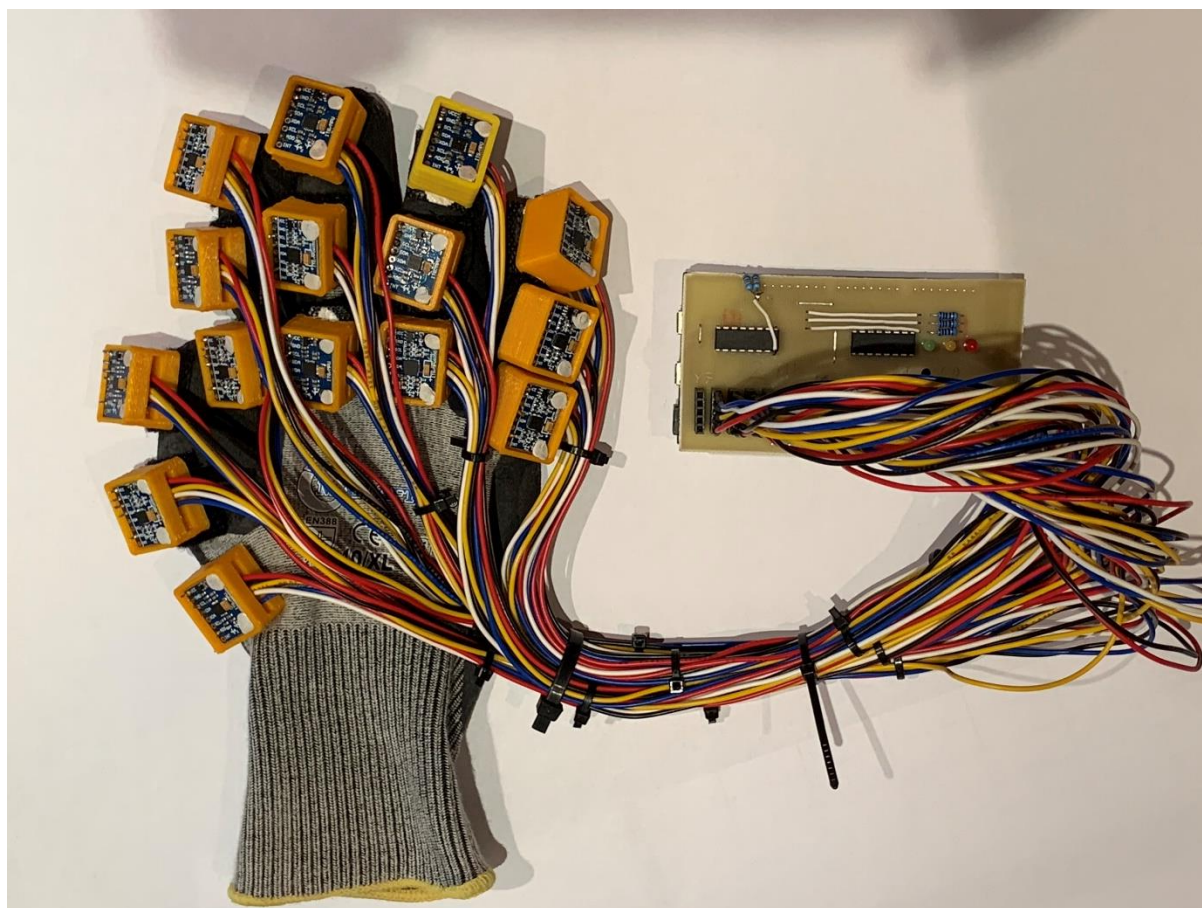


Figure 4-19: The Final Sensory Glove

## 5. TESTING & RESULTS OF SENSORY GLOVE

### 5.1 Introduction

In order to determine the effectiveness and reliability of the sensory glove, validation tests were developed and performed on the device. The validation tests covered key aspects of the glove to ensure the project's aims and objectives were met. The first three tests were used to measure the performance of the sensory glove. The results of the tests were benchmarked with similar gloves that have been researched and developed at other institutions around the world. These tests included the accuracy, the dynamic range and the repeatability of the sensory glove.

To determine relevant and comparable data from each test, a statistical analysis of the results was needed. The analysis needed to show that there was a strong linear statistical relationship or association present between two variables. Based on this, the Pearson's Correlation coefficient was used. The Pearson's correlation coefficient was used to give information about the magnitude of association as well as the direction of the relationship (StatisticsSolution, 2020). When comparing measurements of new measurement techniques with an established one, there needed to be sufficient information to agree that the new method was more effective. The use of only the correlation coefficient of a measure of effectiveness can be misleading. Pearson's correlation coefficient only shows a relationship between two sets of values and how strong the relationship is. It does not indicate if the values obtained are comparable.

Therefore, in order to overcome this problem, the use of the 'Limit of Agreement' technique was used by (Bland & Altman, 1986). This technique analyzed if the two techniques of taking measurements agree and the extent to which the techniques are compatible. This method was based on a graphical approach, with results from mathematical calculations. These results are used to quantify the differences between the two methods of measurement. This included the mean difference and the limits within which the differences lie (Williams, et al., 2000). These statistical techniques were used for the accuracy test. (See Section 5.2)

With Human-Robot Collaboration being the primary objective of the project, an application test was developed. An application test was created to validate the effectiveness of the device in a Human-Robot Collaborative environment. With these critical factors outlined, the chapter was divided into four sections that explained the methodology and results for each test. The sections include:

- Accuracy Test
- Dynamic Range Test
- Repeatability Test
- Application Test



The end-of-the-chapter summarises the results of the four tests. Through the summary, the researcher is able to determine the effectiveness and performance of the sensory glove. The performance was measured against current sensory gloves that have been researched and developed.

## 5.2 Accuracy Test

This test aimed to determine the accuracy of the angular measurement obtained from the sensory glove, while the hand was in a desired orientation. This methodology of testing the glove began by creating a 3D printed model of a human hand. This model was created by 3D printing a similar hand model, that was used in the control system of the project, which can be seen in Chapter 4. Minor modifications were made to the design to incorporate the joints between the phalanges in the system. This was done to print the hand as a single object. This approach decreased the cost of printing. The assembled hand can be seen in Figure 5-1 below.



Figure 5-1: 3D printed hand and Goniometer

With the hand model printed, five predetermined hand orientations were established. These hand orientations had specific relative angle values to validate the accuracy of the sensory glove over a range of values. These angular values varied between the minimum and maximum values that the sensors could compute on the glove. The hand orientations consisted of different forms between the flat phase and the clench phase of a hand. The hand orientations were designed by using modelling clay so the

forms remained consistent between trials. Two of the predetermined hand orientations can be seen in Figure 5-2 below.

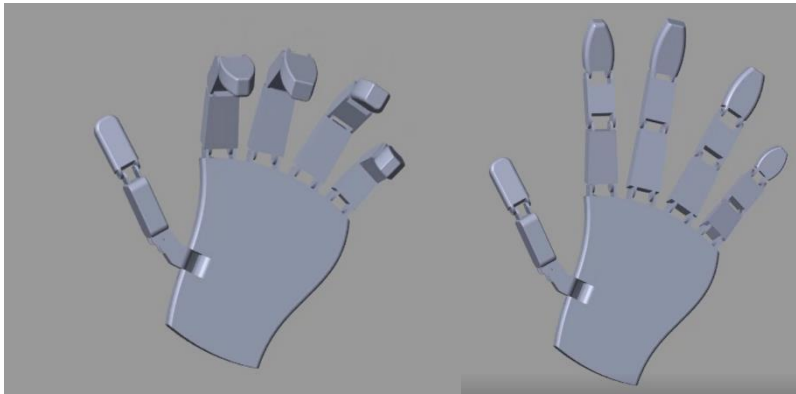


Figure 5-2: Flat hand orientation Phase (Right) and Clench hand orientation Phase (Left)

In order to perform the test, the following procedure was established:

- Firstly, the predetermined orientation was set on the 3D printed hand model of the hand with the use of modelling clay to keep it in position during testing.
- With the use of a Goniometer, the relative angular displacement (in degrees) was measured between adjacent phalanges on the hand model.
- These values were recorded and tabulated for each finger on the hand model.
- The hand was placed into the sensory glove and placed in the same predetermined orientation with the use of the modelling clay.
- The relative angular displacement, in degrees, between adjacent phalanges were recorded from the sensory glove and the values were tabulated for each finger.
- The above approach was repeated for five different predetermined orientations.
- Pearson's correlation coefficient for the Goniometer and sensory glove values were calculated to determine the strength of the relationship between the values.
- The 'Limit of Agreement' technique was calculated and a Bland-Altman agreement graph was drawn.
- A conclusion on the performance of the sensory glove was drawn.

A Goniometer was chosen as it was the most frequently used assessment tool in hand finger joint in clinical practice (Williams, et al., 2000). This test was repeated for different relative angles between each finger joint. A series of five tests were performed, with varying configurations of the hand to ensure a valid conclusion was drawn. The same testing process, as mentioned above, was followed throughout the five tests.

The results of the test can be seen in Table 5-1 overleaf. The table shows the measured relative angular value using the Goniometer, as well as the simulated values from the sensory glove for the index finger. The analysis of the index finger was chosen at random. Pearson's correlation coefficient indicated that

there was a strong linear relationship between the two sets of data ( $R > 0.92$ ). Pearson's correlation coefficient was calculated for each joint and can be seen in Table 5-2 below.

Table 5-1: Measured relative angular value using the Goniometer as well as the simulated values from the sensory glove for the index finger

Data Type	Trial	1	2	3	4	5
Goniometer Values	Relative Proximal Joint Value	1.0	4.0	9.0	28.0	60
	Relative Middle Joint Value	4.0	13.0	19.0	40.0	42
	Relative Distal Joint Value	1.0	1.0	3.0	8.0	32
Sensory Glove Values	Relative Proximal Joint Value	1.1	4.3	9.3	28.4	60.5
	Relative Middle Joint Value	3.9	13.2	18.8	40.4	42.5
	Relative Distal Joint Value	1.2	1.3	3.3	8.4	32.5

Table 5-2: Pearson's Co-efficient for Index Finger Joint Values

Digit	Relative Proximal Joint	Relative Middle Joint	Relative Distal Joint
Pearson's Coefficient	0.9205	0.9259	0.9423

Pearson's correlation coefficient doesn't provide enough evidence that the two values are statistically comparable. Therefore, the 'Limit of Agreement' technique was used (Bland & Altman, 1986). Figure 5-3 overlaid showed a Bland-Altman agreement graph that used the theory from the 'Limit of Agreement' on the Index finger values. It was used to verify if the Sensory glove values were comparable to the Goniometer values measured. The horizontal dotted lines indicate the Lower and Upper Limit of Agreement. The solid line indicates the bias of all the values.

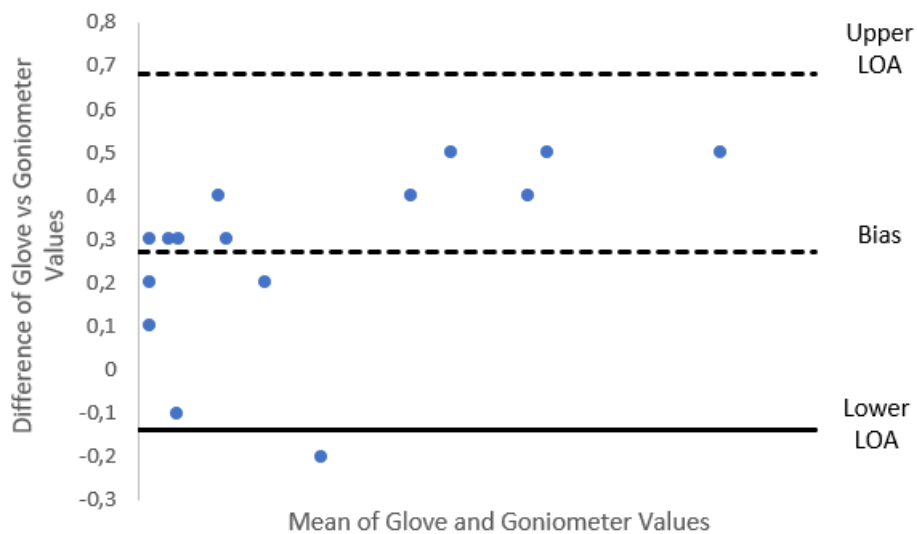


Figure 5-3: A Bland-Altman agreement graph that uses the theory from the 'Limit of Agreement' on the Index finger values

With the high Pearson correlation coefficient for the joints on the index finger, it implies that the sensory values and goniometer values are comparable. The Bland-Altman agreement graph further supports this conclusion as ninety-five percent of all the values obtained and calculated were within the 'Limit of Agreement'. Therefore, the sensory glove provided an effective and accurate solution, when determining the orientation of the human hand.

### 5.3 Dynamic Range Test

The aim of the test was to establish the ability of the system to track rapid finger movements. This would allow the researcher to establish the speed and reliability of the system. The test also enabled the researcher to understand how the sensory glove could improve the manufacturing environment's safety. With safety as a constraint in the development of the HRC systems, it had the potential to act as a catalyst in the field of research.

This test was performed by repeating thirty flexion-extension movements with all joints on the hand. This did not track the abduction of the joints due to the design requirements of the system. The flexion-extension action had to be consistent, each time the test was performed. In order to achieve this, modelling clay was used to create a cast to ensure that the same hand motion occurred, each time the test was performed. The use of a Metronome device was used to ensure the speed of the motion was kept constant. A Metronome is a mechanical instrument that makes repeated clicking or beeps at an adjustable speed (Dictionary.com, 2020). The Metronome tempo was set at approximately 116 BPM. The cast and the Metronome can be seen in Figure 5-4 overleaf.



Figure 5-4: Set-up of Dynamic Range Test with a metronome, sensory glove and clay model cast

During the test, the relative angles between adjacent joints were measured. All fingers performed a motion that experienced little, to no, abduction motion. In the beginning of the test, the researcher's hand was required to be flat and perpendicular to the surface of the earth. The procedure of the test was as follows:

- Firstly, the predetermined orientation was set using the 3D printed model of the hand with the use of a modelling clay. Once set, the 3D printed hand was removed
- The researcher initially positioned his hand in an upright position, perpendicular to the ground.
- The researcher's secondary hand provided support of the clay cast to ensure that the position remained constant during testing.
- The Metronome device was set to a predefined speed, which initiated the start of the test.
- The researcher began the motion of the hand at the start of each click to ensure consistent movement was recorded.
- As the Metronome device clicked at the predefined speed, the hand moved from the flat phase to the clench phase at each click.
- The above approach was repeated thirty times.
- The readings from the sensory glove were recorded and tabulated to validate and verify the results.

With all the finger motion being analysed during the test, the index finger motion was focused on. This was done to perform an extensive analysis of the responsive nature of the system. The results are shown in Figure 5-5 overleaf.

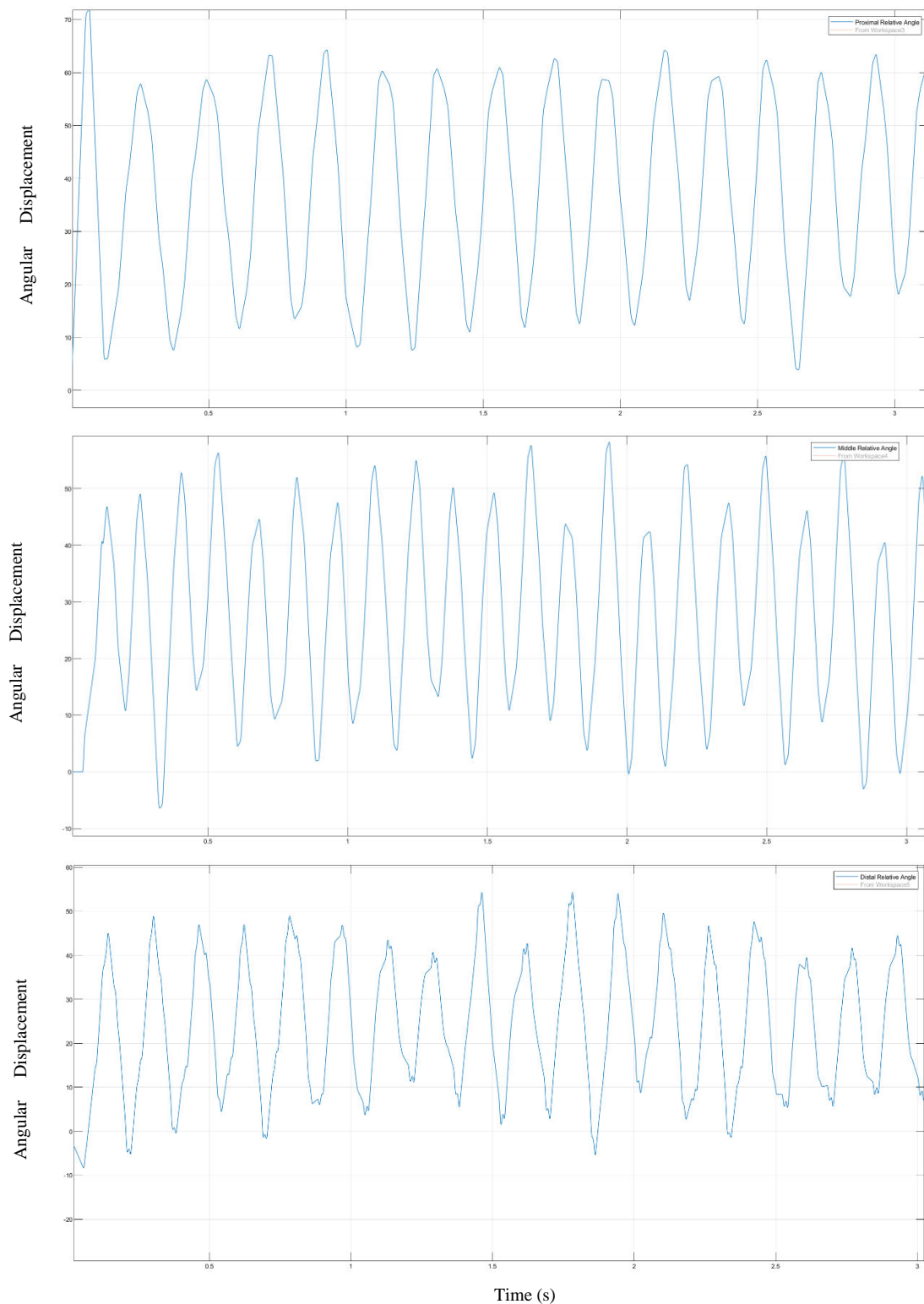


Figure 5-5: Dynamic Range of the Proximal Joint (Top), Middle Joint (Middle) and Distal Joint (Bottom) on the Sensory Glove.

It was noted that in order to approximate the dynamic range of the finger joints, the reconstruction of each joint cycle occurred when the derivative of the angular velocity was zero. Therefore, the dynamic range calculated between the time interval of two consecutive points, where the derivative of the angular velocity is zero. The bandwidth of the filter was large enough to track the rapid movements of the

system, however, the metronome tempo was not at the correct speed to capture all the motion. The tempo was chosen based on the sampling time of the filter. The problem was that since three sensors were connected to a finger and they were read individually, there was a time delay between reading the first sensor on the proximal phalange on the finger structure and the last sensor on the distal phalange. Therefore, the tempo had to be slower. Due to this, the metronome's tempo was reduced by approximately a third of the original value.

The results showed each joint's dynamic range on the index finger, during the first three seconds in the experiment. The dynamic range of proximal, middle and distal joint was approximately fifty degrees, forty degrees and forty degrees respectively. The dynamic range of the sensors was significantly less than the static constraints on the respective finger joints of the Index finger that are outlined by (Chen Chen, et al., 2011).

#### 5.4 Repeatability Test

The aim of the test was to study the repeatability of the sensory glove. The test was divided up into two phases. The first phase was known as the flat phase. The user's hand would be in the upright position with all the fingers straight and perpendicular to the ground. The second phase was known as the flexion phase. The user's hand would move their hand from the flat hand orientation to a clench hand orientation. Modelling clay was used to keep the clench hand phase constant through the test. Figure 5.6 below shows the 3D printed hand model in the flat phase and the clench hand phase.



Figure 5-6: Flat hand Phase (Left) and Clench hand Phase (Right)

The average range and standard deviation of all joint angles between the two phases, were tested during the experiment. The average range refers to the mean difference between the minimum and maximum angular displacement when in a specific orientation during each trial. These values were compared to various other sensory gloves in the field that have been researched and developed. This comparison allowed the researcher to compare the performance of the sensory glove with similar products. The procedure of the test was as follows:

- Firstly, the researcher used modelling clay to set a mold to ensure that a constant clench hand phase was achieved throughout the test.
- Once set, the user placed the glove on their hand and powered it on.
- The user's hand stalted in the flat phase for five seconds to ensure the conect orientation was captured.
- The user's hand perfolmed a flexion motion into the mold to achieve the hand's desired form and orientation. The abduction motion was minimal due to the design requirements of the glove.
- The clench folm was held for five seconds to ensure the conect orientation was captured.
- The average range and standard deviation between all joint angles during the two phases were recorded and tabulated
- This test was repeated six times to achieve accurate and reliable results.
- The results were averaged and compared to similar sensoly gloves that were in the field of data capturing.

The results of the test can be seen in Table 5-3 below. The table shows the dynamic range (in angular displacement) between the joints and standard deviation (in angular displacement) of each tiial's joint angles. The mean value for all the ti-ials was calculated in order to compare the results to existing sensoly gloves. It also displayed the same infoMation about similar sensoly gloves that have been researched and developed by various companies. This provided a method of comparing the performance of the sensoly glove with existing ones.

*Table 5-3: Results of Repeatability Analysis*

<i>Trails</i>	<b>Flat Phase</b>		<b>Flexion Phase</b>	
	<b>Range</b> (deg)	<b>Standard Deviation</b> (deg)	<b>Range</b> (deg)	<b>Standard Deviation</b> (deg)
<i>1</i>	1.1	0.5	3.8	1.2
<i>2</i>	1.5	0.4	<b>3.5</b>	1.3
<i>3</i>	1.7	0.5	3.7	1.5
<i>4</i>	1.0	0.3	3.6	1.2
<i>5</i>	1.1	0.5	3.9	1.4
<i>Mean Value</i>	1.3	0.4	3.7	1.3
<i>Dataglove</i>	4.5	1.6	6.5	2.6
<i>Humanglove</i>	<b>3.8</b>	1.2	7.5	2.4
<i>Shadow monitor</i>	1.5	0.5	<b>5.2</b>	1.6
<i>WUglove</i>	<b>2.6</b>	0.9	6.1	1.9
<i>Hand Kinematics Glove</i>	1.1	0.4	1.7	0.6

*Note: All Sensory Glove results by the competitors are referenced from (Korhier, Slmiter, Roetenberg, & Veltink, 2018).*



Based on the results, as seen in the table above, the repeatability range was 13 degrees, with a standard deviation of 0.4 degrees. This showed that the glove had greater performance than most of the competitor's sensory gloves but did not come out on top. This was due to the cost factor as the goal of the project was to create a low-cost glove. Table 5-3 above displayed that the range and spread of the angular values when the glove was in the clench hand phase was greater. The greater the motion required, the greater the mean drift velocity of the sensors. This was caused by the mean drift velocity of the sensors. The result showed that the sensory glove had adequate performance in terms of the cost of development.

### 5.5 Application Test

The aim of this test was to validate the application of the sensory glove, in a Human-Robot Collaboration environment. With the application of the project centred around the Human-Robot Collaboration, it was important to ensure that this device had the ability to be used in a real-world environment. This test was performed with a robotic arm. Robotic arms are standard pieces of equipment that are found on manufacturing and production floors.

The robot arm chosen for this test, was the Ufactory xAim Lite 5 (see in Figure 5-7 below). The xAim 5 Lite is a five-degree of freedom, low-cost manufacturing/production robot. It is a multifunctional robot that could perform tasks such as milling, screwing parts or moving objects from an adjacent production line. It has a three-kilogram payload and 0.1 mm repeatability. The robot is lightweight and consists of powerful joints in the form of brushless servomotors, which give the robot the ability to have accurate and precise movement. The robot has a built-in collision avoidance system that locks the servos of the joints if any unexpected force were acting on the servos while in operation. The robot has an open-source software platform that allows the robot to be integrated with multiple devices such as the sensory glove.

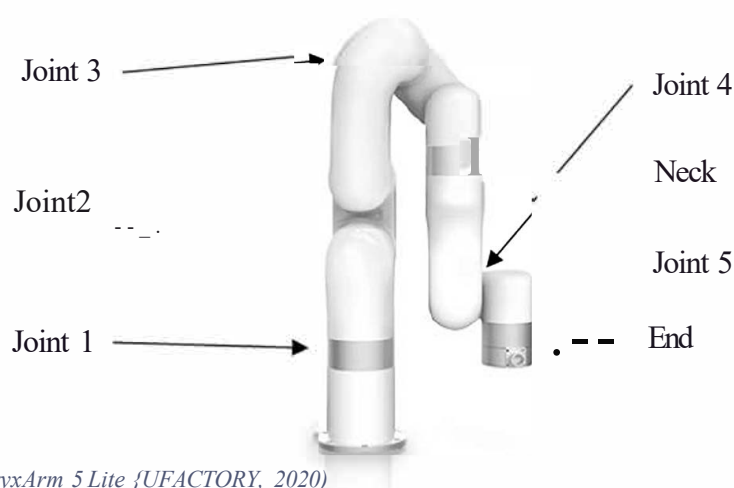


Figure 5-7: UfactoryxArm 5 Lite (UFACTORY, 2020)

The application test was centred around the ideology of a Human-Robot Collaborative environment. This test focused on mass-customized manufacturing plants, as it was an objective of the project. Research showed that in order for industry 4.0 to be achieved, extensive research and development was focused on building mass-customized factories (O'Marah, 2020). These factories meant that customers could customize their products, such as cars or home appliances, on the factory floor while it was on the production line. In order to create this environment, the use of robots that had the ability to collaborate with humans was recognized. Research showed that human labour would be at the centre of factories of the future (O'Marah, 2020). This would enable highly productive and efficient production lines as robots were built to be linear machines. As outlined in the literature review, the presence of a human added flexibility and problem-solving elements to an HRC system in a cost-effective solution.

Apart from safety, the cost factor of robot systems that had these features was high. Therefore, the sensory glove would provide a cost-effective and competitive solution for achieving a mass-customized factory for all businesses. The application of the sensory glove would be to enable Human-Robot Collaboration systems in mass-customized factories. There are multiple ways that the sensory glove could be used in Human-Robot Collaboration systems. From advanced collision avoidance systems, to collaboration operations with a robot, the forms of collaboration are extensive.

The application test details began by identifying a scenario where humans could enhance the mass-customized environment, on a production floor. Since robots could perform linear tasks to great accuracy and precision, it was not always feasible to replace them with humans. Through this process, it was realized that robots would have difficulty in recognizing new tasks that needed to be performed without the use of complex and expensive visual systems. Identifying and adapting a robot to perform new tasks on a flexible production line, was an important goal towards achieving factories of the future. Robot's ability to seamlessly adapt and change their function, based on a product in front of them, is a core ideology of mass customization. The researcher believed that with the sensory glove, this feature could be achieved through an economical and effective solution.

The test aimed to validate the use of the sensory glove on a flexible production line. This was validated by working in collaboration with a robotic arm, xArm 5 Lite. The test showed the sensory glove could seamlessly control the robot in order to achieve a flexible production line. This was verified using the sensory glove to change the start/end position of the robot arm based on the part received by the robot. The standard process of performing such a task was to manually control the robot with a computer between each part received. The original process increased production time and decreased quality control as the worker needed to estimate the robot's exact position to work on the product. The use of the sensory glove significantly reduced the time taken to operate the robot while providing a greater degree of accuracy when positioning the robot.

The worker physically took control of the robot and positioned it correctly before the task began. The robot remained in the waiting phase until the worker indicated that it was ready to collaborate. The following process details how the robot collaborated with the worker:

- The robot moved into a neutral location awaiting the control of the human (Waiting phase). The robot's joints were locked in place to ensure no movement while in that phase.
- The worker gripped the neck of the robot. An integrated algorithm, designed by the researcher, read the orientation sensor data from the sensory glove. If the orientation sensor data matched the predetermined orientation sensor data, the algorithm unlocked the robot's joints and allowed the robot to be positioned (Unlock phase).
- If at any time the orientation data from the sensory glove changed (with a predetermined range) while the robot was being positioned, the robot locked its joints.
- Once the robot was moved into position, the worker released the robot and the joints locked in place. To confirm that the robot was in the final position, the sensory glove presented a predetermined hand orientation to the robot. The sensor data was unique, so the algorithm could distinguish between the Unlock phase and the Operation phase. Figure 5-8 below demonstrates the flow chart operation of the algorithm.

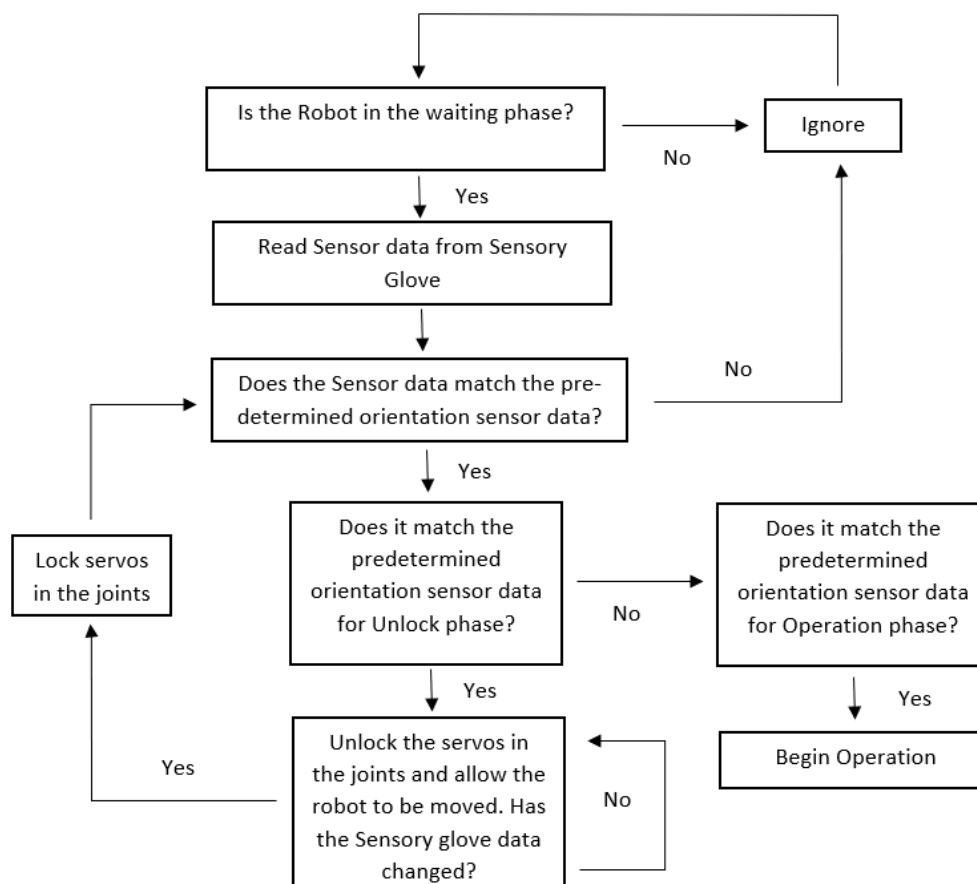


Figure 5-8: Flowchart of the designed Algorithm

To test this, ten trials took place to confirm if the algorithm did unlock the robot joints when in the predetermined orientation and if the algorithm did resume the robot's operation when in the predetermined orientation. Table 5-4 below shows the results of the test and the efficiency of the sensory glove. Efficiency was used as a parameter, as it gave an indication to the performance of the glove.

Table 5-4: Results from HRC Application Test

Trails	1	2	3	4	5	6	7	8	9	10	Efficiency (%)
Did the Joints Unlock?	Yes	Yes	Yes	Yes	Yes	Yes	Yes	Yes	Yes	Yes	100
Did Operation Resume?	Yes	Yes	Yes	Yes	Yes	Yes	Yes	Yes	Yes	Yes	100

Table 5-4 showed that the robot joints were unlocked and the robot resumed operation, every time the collected predetermined orientation was recognized on the sensory glove. This resulted in a 100% efficiency of the system and the designed algorithm, by the researcher. This showed that the glove could be integrated into a Human-Robot Collaboration environment. The sensory glove could provide a safe working environment for work in terms of the application. Figure 5-9 and Figure 5-10 below shows the Sensory glove and xArm 5 Lite in Collaboration together using the above testing procedure.



Figure 5-9: xArm 5 Lite in the waiting Phase (Left) & xArm 5 Lite in waiting Phase as Sensory glove approaches the neck of the robot (Right).



*Figure 5-10: Sensory gloves unlocks the joints of the xArm robotic arm to enter the Unlock phase (Left) & the Sensory glove moves the robotic arm into its final position (Right). Once the Sensory glove releases the neck, the xArm 5 Lite will be in Operation phase*

## 5.6 Conclusion

In order to determine the performance of the sensory glove, the four tests, as mentioned above, were conducted. Each test was designed to determine the different performance characteristics of the device. These performance characteristics were analysed using statistical analysis and comparing it's performance to current devices with similar functionalities. Since the sensory glove's primary objective was low-cost, the researcher needed to establish a relationship between performance and cost.

The accuracy test was aimed at determining the angular measurement accuracy of the device, while in operation. This was done with a statistical analysis approach. The results showed that the Pearson's correlation coefficient between the sensory glove and measured values was  $R > 0.92$ . A Bland-Altman agreement graph was drawn up to ensure that the data recorded was accurate and comparable. The 'Limit of Agreement' method supported the Pearson's correlation co-efficient as it represented an accurate system.

The dynamic range test aimed to determine the ability of the sensory glove system to rapidly track the hand's movement. This was conducted by performing 30 flexion-extension movements at a constant rapid tempo. The tempo was initially set based on the sampling time of the filter. The device was unable

to capture the motion of the sensory glove at this tempo due to sensory glove hardware and configuration. The tempo of the flexion-extension movement was reduced by a third in order to capture adequate data from the device. This test highlighted that further work needed to be conducted on the glove design and implementation.

The repeatability test aimed at analysing the repeatability of sensory glove. It was conducted to determine the reliability of the device when positioned in two predetermined orientations. The researcher captured each joint's dynamic range and standard deviation on the sensory glove for six trials. The results of the test were averaged and compared to the performance of existing sensory gloves. The results showed that the dynamic range and standard deviation between the Flat phase joints were smaller than the dynamic range in the Clench phase joints. When compared to existing sensory gloves, it performed well as it had the second-best performance values. It was identified that better performance could be achieved through the refinement of the system and high-cost components.

The final test conducted, validated the application objective of the sensory glove. This was centred around HRC systems. The researcher used a robotic arm, known as the xArm 5 Lite, to simulate the possible collaboration that would occur in an HRC environment. The researcher designed an algorithm that enabled the robotic and sensory glove systems to collaborate. With this algorithm, the test results showed that the robot was able to collaborate with the worker, every time the need for collaboration arose. The test was performed over multiple trials and collaboration was proven successful.

## 6. DISCUSSION AND FURTHER DEVELOPMENTS

### 6.1 Introduction

The purpose of the study was to find the answer to the following research question:

*'Could a low-cost mechatronic sensory glove be designed and developed to enable humans and robots to collaborate in a highly customizable environment in Advanced Manufacturing Systems?'*

In order to achieve this, the project was divided into five objectives. These objectives ensured that the research focused on the core concepts of the project. The objectives were as follows:

- Research technology and methodologies that enabled current sensory gloves that have the ability to provide Human-Robot Collaboration.
- Review and understand the role of humans and robots in the manufacturing environment in order to provide a safe environment.
- Design and develop a mechatronic sensory device for use in a Human-Robot Collaborative environment.
- Test and validate the performance of the glove versus the cost of the glove
- Conclude and discuss potential improvements of the sensory glove.

This chapter will showcase the information and results that the researcher obtained when achieving the five objectives of the project. Based on the following analysis of each objective, a conclusion was made in order to answer the above-mentioned research question.

### 6.2 Technology & Methodologies

In order to understand how sensory gloves operated, extensive research was done on the state of sensory gloves. This included identifying that a sensory glove was modelled as a mechatronic system that included mechanical, electrical, electronic, computer and control elements (See Figure 6-1 overleaf). The mechanical element of the system was the design of the glove and the associated components. The electrical and electronic elements were the IMU sensors and associated wiring of the circuitry. The Arduino<sup>®</sup> microcontroller acted as the controller element. The user-based algorithm, designed on Simulink<sup>®</sup>, acted as the mechatronic system's computer and control element.

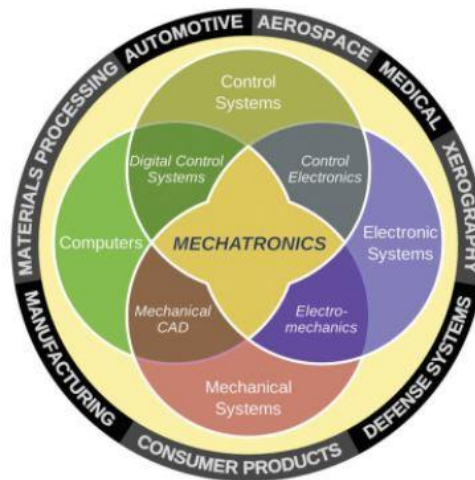


Figure 6-1: The Fundamental Components of a mechatronic System (Brown, 2011)

The key aspect of a mechatronic system is integration. All the components mentioned above required extensive integration to create a synergistic relationship between them. This had to be achieved to create an efficient and economical solution.

Extensive research has been conducted on current sensory gloves and it shows two methods of motion tracking. Some sensory gloves are designed and developed with resistive bend and optical fibre sensors. These types of sensors are advantageous as they can capture the orientation of the hand to a considerable degree of accuracy but have cumbersome calibration methods. In contrast, other sensory gloves have IMU sensors, which are made up of gyroscopes and accelerometers. These devices are integrated into a single chip, which allows for a smaller, less complex solution. The IMU sensors also enabled sensory gloves, to have a greater degree of freedom and were therefore chosen for the project.

In order to mathematically model the human hand, research showed that the hand could be modelled as a single kinematic chain structure. With the use of Simulink<sup>®</sup> and Simscape Multibody, the researcher had the ability to model a human hand. The modelling of the hand in Simulink<sup>®</sup> provided an integrated platform where all the components of the project were well-integrated to produce a robust system. A filtering process was introduced into the system to create greater accuracy and efficiency. The filtering system ensured an effective yet low-cost solution was established.

Multiple sensory gloves have been researched and developed and were used as the foundation of the project. With none of the current gloves focused on HRC systems, they all had the ability to track the motion and orientation of the human hand. (Weber, Reuckert, Calandra, Peters, & Beckerle, 2016) showed the limitations of using flex sensors when tracking the orientation of a human hand. The restrictions included complex calibration procedures and sensor displacement errors. (Baldi, Scheggi, Meli, Mohammadi, & Prattichizzo, 2017) used IMU sensors in the sensory glove and the results



represented an improved system. The glove's drawback was the absence of a Kalman filter design and IMU sensors on the hand's distal phalanges.

(Kortier, Sluiter, Roetenberg, & Veltink, 2018) designed a sensory glove to assess hand kinematics while evaluating hand functionality. The glove had sixteen IMU sensors, which consisted of an accelerometer, gyroscopes and magnetometer. It featured a robust extended Kalman filter for improved accuracy and precision. The sensory glove's performance made it the good solution to use as a reference point for the project. The only issue was that magnetometers in the IMU sensors that would malfunction in a robotic environment due to the electronic components and magnets that are commonly found in them.

### 6.3 Human Robot Collaboration

The application of this sensory glove focused on Human-Robot Collaborative environments. The sensory glove had to provide a safe way for humans and robots to collaborate on a single part on a manufacturing or production line. The type of collaboration was based on the worker positioning or guiding the robot before the operation began. The manufacturing or production line would be in a Flexible Manufacturing Environment, that could create multiple iterations of the same part, based on customer requests. These types of factories are one of the critical aspects of Industry 4.0.

To create a safe working space where humans and robots could collaborate, the researcher needed to understand the different levels of interaction in the HRC systems. (De Luca & Flacco, 2012) defined the broad ideology that Human-Robot Collaboration focused on safety, co-existence and collaboration. This ideology explained that HRC systems only existed if the worker's absolute safety was ensured. (Bauer, Wollherr, & Buss, 2008) explained that HRC systems were built on the foundation that humans and robots worked towards a common goal. This highlighted the fact that robots were not implemented to replace humans but to aid them in the manufacturing or assembly process

Through this understanding, an HRC environment needs to ensure that the robot can assist the worker during the operation and work independently on a single part while the human performs an alternate operation. The robot would perform tasks that were not physically possible for a human. The robot had a degree of accuracy, precision, and efficiency that humans did not possess. All of these tasks had to be performed with the safety of the worker in mind.

The main limitations of a robot are problem-solving. FMS environments exist as every part is not the same. Different hole sizes for drilling or a different position for a fuel injector would be the difference between adjacent parts on the line. Therefore, robots have to adapt when presented with a slightly different tasks or operations. The introduction of humans collaborating with robots added a problem-

solving element that can be cost-effective, reliable, and efficient. The human would need to have the ability to reposition, change tools and work with the robot.

Research has been done on these types of environments by researchers (Michalos, et al., 2014). These researchers focused on creating a seamless HRC system in a safe environment to achieve factory 4.0. The project was known as ROBO-PARTNER and showed that human skill was the main driver towards high added-value products, while integrating a robot's precision, repeatability and strength would improve it. The project highlighted the concept of creating sensor-based devices that would allow for workers and robots to collaborate safely and efficiently.

BMW have installed collaborative robots, known as the Universal Robot UR10, which collaborated with workers to seal doors on BMW vehicles in their factories. In contrast, a VW automation plant have integrated an UR-5 robot to insert glow plugs into various VW engines' cylinder heads. The level of collaboration was basic as the workers guide the robot through the operation. These examples laid the groundwork for people to be more open in accepting robots in the workspace, as workers don't only need to be safe, but feel safe. These initiatives showed that robots could work with humans in a secure, yet productive environment.

The above scenarios on HRC systems showed that humans can enter a partnership when collaborating with robots. The workers provided problem solving and flexibility to the task, while the robot provided accuracy, repeatability and precision. It created a synergistic relationship between the robot and the worker, while the worker remained in a safe working environment.

#### 6.4 Design and Development of Sensory Glove

Based on the mechatronic design approach, three conceptual designs were formulated for the sensory glove. The key feature that these designs shared, was the level of integration. The level of integration was important, as it is a key component in a mechatronic system.

Concept One was built with flex sensor technology, to track the worker's hand motion and orientation. While the design provided an efficient and integrated system, it was limited due to the flex sensors' level of accuracy and precision. Concept Two introduced IMU sensor technology, to track the motion and orientation of the workers' hand. An Extended Kalman filter was established to reduce the orientation estimation error of the system. IMU sensors significantly increased the system's accuracy, while the extended Kalman filter created a more computationally expensive solution. The third concept design used IMU sensor technology, but an Averaging filter was used. An Averaging filter is less computationally expensive and could be performed externally on the microcontroller. The potential application of the sensory glove required it to operate in real-time application.

The conceptual designs were analysed through a decision matrix and based on multiple key factors, such as degree of repeatability, accuracy, system integration and cost-effectiveness, the third concept was used as the foundation for the final mechatronic design. The final mechatronic design was divided into the four elements of a mechatronic system.

The electrical and electronic system consisted of fifteen MPU6050s and a custom-built PCB board. The PCB board was the operational circuit, that connected the MPU6050s to the microcontroller. The PCB board design went through multiple iterations, due to hardware and serial communication limitations. The board consisted of resistors, multiplexers, input/output pins and conductive line tracing. LEDs were installed to validate the operation of the circuit, when the algorithm was operational.

The computer system of the project consisted of the Simulink<sup>®</sup> hand model. The hand model was modelled in Solidworks<sup>®</sup> and imported into Simulink<sup>®</sup> using the Simscape Multibody tool. The Solidworks<sup>®</sup> model was based on the average human hand dimensions and joint constraints documented by (Chen Chen, et al., 2011). The tool modelled the hand as a single kinematic chain system, based on the Denavit-Hartenberg approach. The Simulink<sup>®</sup> tool also created the equations of motion of the human hand. It enabled the researcher to integrate the model into the project's control system. The Simulink<sup>®</sup> platform was used to import the model as it had the capability to integrate all the mechatronic design systems. This resulted in a less computationally expensive and efficient system to operate.

The control system of the project consisted of the data acquisition and the post-processing algorithm. Both systems were designed in Simulink<sup>®</sup> and integrated with the elements of the sensory glove. The data acquisition algorithm extracted the raw data from all the IMUs and configured the data to represent each sensor's roll and pitch. An Arduino<sup>®</sup> Due acted as the microcontroller due to the robust integration software with Simulink<sup>®</sup> and the mechatronic system's operational voltage. The sampling frequency achieved was two hundred hertz due to the serial communication limitations between the sensor and the microcontroller.

The control system's post-processing algorithm involved configuring each sensor on the sensory glove to the respective phalange on the Simulink<sup>®</sup> hand model. This was done to capture and validate the orientation of the sensory glove while in operation. This was the preliminary test that showed that the glove could capture the motion of a human hand. The model was then used to determine the sensory glove's performance, which is discussed later in the chapter. An average filter was implemented before the values were fed to the hand model. The averaging filter was used to smoothen the signals and reduce high-frequency noise from the sensors. The filter was ideal as it enabled the device to potentially be used in real-time applications due to its low computational cost. The control system provided an efficient system that could integrate with all the elements of the project. It was designed for high efficiency and low computational cost. The control system could be used in real-time applications; however, that was not the project's objective.

The system's mechanical element consisted of a low-cost glove, with which the sensory glove could be built around. The glove was made from a light and durable material to ensure easy operation in a manufacturing environment. The glove was versatile, as the hardware needed to be integrated onto the glove. The IMU sensors required a custom-built sensor housing as these components were attached to the glove during operation. Therefore, a protective housing for the sensor was designed by the researcher on Solidworks<sup>e</sup>. The housings were 3D printed with polylactic acid. The 3D printing process provided a flexible manufacturing method as the holders required a specific size and shape. It provided the holders with high strength while protecting the components during operation. Since it was 3D printed, the holders were a cost-effective solution.

Each element of the mechatronic system was designed and implemented to ensure an efficient, well-integrated and cost-effective solution was created. The final product of the sensory glove can be seen in Figure 6-2 below.

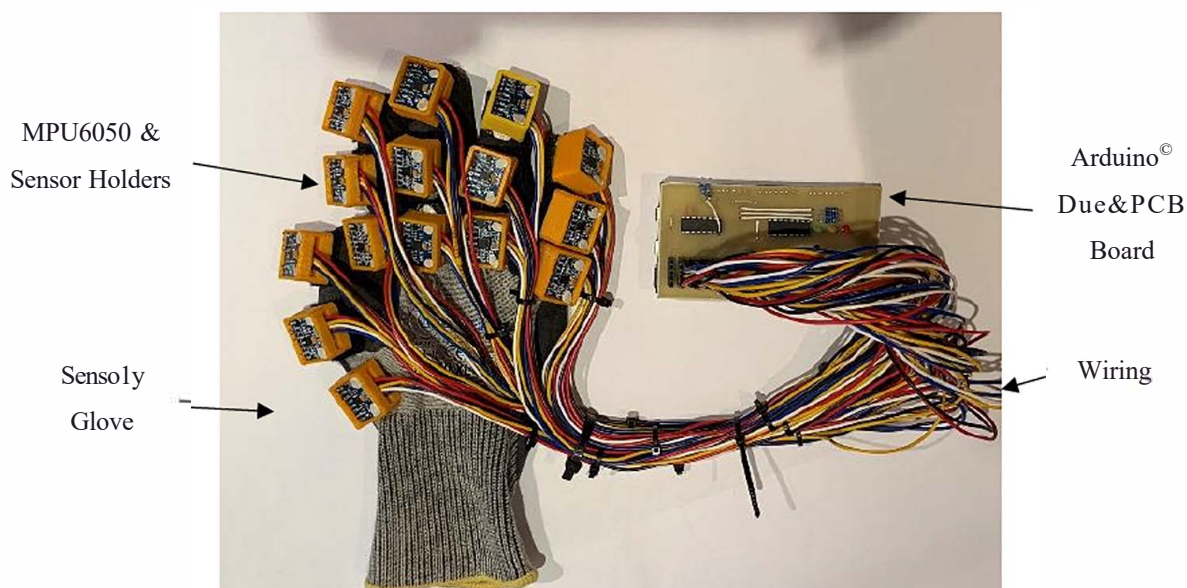


Figure 6-2: Final product of the sensory glove

### 6.5 Testing and Validation of Sensory Glove

In order to test the performance of the sensory glove, tests were conducted on the following parameters of the sensory glove:

- Accuracy
- Dynamic Range
- Repeatability
- Application

Each test was designed to determine the glove's overall performance and how the sensory glove could be compared to current devices that had similar functionalities. With the primary focus of the sensory

glove being low-cost, the researchers needed to establish a relationship between gloves' performance versus cost. For the first three tests, statistical analysis was used to analyse the results of the sensory gloves. The final test was based on the sensory glove's efficiency when performing the associated actions while in operation.

The accuracy test aimed to determine the angular measurement accuracy obtained from the sensory glove while the hand was in the desired orientation. The results, which can be seen in Chapter 5, showed that Pearson's correlation coefficient between the sensory glove values and the actual measured values was high ( $R > 0.92$ ). This displayed a relatively strong relationship between the two values. This parameter was not enough to yield if the sensory glove was accurate as the values could be incomparable. Therefore, a Bland-Altman agreement graph was drawn up and it showed that the two methods were comparable as ninety-five percent of all the values fell within the 'Limit of Agreement'. This supported the correlation value and showed that the system was accurate and could effectively track the orientation of a human hand. Further work can be done to improve this with an advanced Extended/Unscented Kalman filter. This would only be useful if the computation cost of these filtering solutions were optimized for real-time application.

The dynamic range test was conducted to establish the system's ability to rapidly track the motion of the sensory glove. The dynamic range of proximal, middle and distal joints were significantly less than the static constraints for the average human hand documented by (Chen Chen, et al., 2011). The hand movement's tempo was set based on the sampling frequency of the system. The system was unable to capture the correct data at the predefined tempo. This was due to the hardware and system constraints. With fifteen sensors involved in the system and the hand's rapid motion, the sensory glove was unable to capture the correct orientation at the predefined tempo. A more advanced microcontroller with multiple I2C communication lines could resolve the issue, and further work could be conducted on the structure of the IMU sensor's serial communication network. However, when the tempo was reduced by a third, the system could capture the motion of the sensory glove.

The repeatability test aimed to analyse the repeatability of the sensory glove. The test focused on determining if the sensory glove could repeatably capture the sensory glove's orientation when positioned in two phases. The joint's dynamic range and standard deviation of all the joints were captured for each trial. The test results showed that the dynamic range between the joints in the flat phase was smaller than the dynamic range in the clench phase. This showed that the sensory glove had a greater repeatability when in the flat position versus the clench position. This observation was also noted in the accuracy test as the sensory glove values had less effectiveness when working with greater flexion angles. This was due to the limitations of the sensors as they experienced sensor drift while in operation. However, the sensory glove performed well compared to other sensory gloves performing similar operations (See Table 5-3 in Chapter 5). With better IMU sensors, such as the ADXL 345, and

fine-tuning of the control algorithm, a greater repeatability, higher accuracy and dynamic range could be achieved. This was identified as the limiting factor in the project due to the cost requirements of the project.

Further research and development could be done on an IMU sensor for the sensory glove. With the tests highlighting that the IMU sensors are a limitation on the glove's performance, an improved IMU could significantly improve the performance. Research suggests that a magnetometer integrated into the IMUs provided significant improvement as it reduces sensor bias drift. Sensor bias drift is one of the major noise issues that affected IMU sensors. Magnetometers are sensitive devices that are affected by external magnet fields. In an FMS environment with multiple robotic arms and advanced machinery, these devices tend to have their own magnets and magnetic fields. Therefore, a magnetic shielding device would need to be installed on the IMU to ensure the most accurate data was captured. This significantly increases the cost of the solution and it would need to be investigated if the increase in cost justifies the improvements in the performance.

The final test consisted of validating if the sensory glove could be used in an HRC environment. The researcher acquired an advanced low-cost manufacturing robot, known as the xArm 5 Lite. Since the robot was used in a manufacturing environment, the researcher could simulate the possible interaction and collaboration between a worker and the robot. A test was done to validate a collaboration between the worker and a robot. The efficiency of the collaboration was analysed. This was performed by simulating possible scenarios where a robot would collaborate with the worker. An algorithm was designed by the researcher and implemented into the system to perform the test. The test results showed that the robot was able to collaborate with the worker every time the need for collaboration arose. Multiple trials were performed, and the efficiency of the collaboration was one hundred percent. This demonstrated the potential impact that the sensory glove could make if implemented in an FMS environment. Further research could allow for a greater degree of collaboration with complex tasks that would have the robot and human work hand-in-hand.

## 6.6 Conclusion

The design of the sensory glove focused on the use of IMU sensors. These IMU sensors were used as they provided a high-performance versus cost solution to track the worker's hand accurately. The design took the foundation of (Kortier, Sluiter, Roetenberg, & Veltink, 2018) sensory glove and focused on a low-cost device. The sensory glove was developed with the mechatronic design approach as it focused on the four key elements of the project. One of the major differences was the filtering system implemented in the project as it was required for a real-time application system. This was important as HRC systems require real-time applications.

The project's application focused on creating a safe environment for a worker to collaborate with a worker in a flexible manufacturing environment. The sensory glove needed to have high performance to ensure a safe working environment for the worker. Four tests were conducted on the sensory glove to validate the performance. The tests showed that results had a high Pearson's correlation coefficient for accuracy ( $R > 0.92$ ) while the system performed better when in a uniform position (flat hand position). These limitations were concluded due to the low-cost components and the system architecture of the device. The researcher highlighted that further research and development could be conducted on improving the filtering system and IMU devices to better the glove's performance.

## 7. CONCLUSION

Research of current sensory gloves created the foundation for the study. Different technologies have been tried and tested by multiple researchers to establish an effective method of tracking the human hand's orientation. (Weber, Reuckert, Calandra, Peters, & Beckerle, 2016) showed the limitations of using flex sensors on sensory gloves. These limitations included complex calibration processes and sensor displacement errors. (Baldi, Scheggi, Meli, Mohammadi, & Prattichizzo, 2017) designed a sensory glove with IMU sensors but without a comprehensive filtering process, the project lacked the accuracy and precision that could be achieved with such devices.

Through multiple readings, researchers agreed with the notion that IMU sensors provided the most effective and cost-effective solution to tracking a human hand's orientation, such as (Kortier, Sluiter, Roetenberg, & Veltink, 2018). These researchers concluded that IMU sensors were a promising solution when performing such an operation provided a well-designed filter was implemented. Filtering was an essential part of the system as it enabled the system to reduce noise in serial communication and improve the accuracy of the sensory glove. This conclusion was based on the field of research and the trend that these devices were becoming less costly and smaller in size (Kortier, Sluiter, Roetenberg, & Veltink, 2018). Through this research, the project's first objective was achieved as the researcher had built an in-depth knowledge of the state of research of sensory gloves and its associated technologies.

The second major research principle involved understanding the role of humans and robots in the manufacturing environment. The purpose of this was to create a safe working environment where humans and robots could collaborate. The sensory glove's application enabled and empowered workers on FMS environments to effectively and safely collaborate with robots. Through the research presented, it was clear that robots had two constraints while operating in an FMS environment. This included problem-solving skills and flexibility that humans pose. A small percentage of industrial-grade robots have this capability but at a high cost. This research aimed to establish an efficient and cost-effective method to achieve an FMS environment in HRC systems.

Humans possess the problem solving and flexible capabilities that most industry robots lack. The key idea behind HRC systems was that robots and humans would work together towards a common goal. This is evident by the researchers (Michalos, et al., 2014) who focused on creating a seamless HRC system in a safe environment to achieve industry 4.0. The project was known as ROBO-PARTNER and highlighted that sensor-based equipment was an efficient and sustainable method of potentially creating a productive and safe HRC environment. Automotive companies, such as VW and BWM, had also implemented collaborative robots on their manufacturing/assembly floors but with limited capabilities.



This research showed that a synergistic relationship between the robot and the worker was the goal of any HRC environment. Therefore, through this research, the project's second objective was achieved as a comprehensive understanding of a human and robot role in an HRC environment was established.

The sensory glove design focused on the mechatronic approach as the device encompassed its four elements. Three conceptual designs were developed for the project. Once the conceptual designs were complete, each design went through a decision matrix to establish the best and well-rounded approach to the project. The decision matrix focused on multiple design features, such as performance, level of integration, size and cost. These features were important as it was aligned with the objectives and research question of the project. A detailed design of the mechanical, computer, control, electrical and electronic systems was established from the final concept design. A key criterion of the individual systems was ensuring a high level of integration existed between them. This was important as mechatronic systems are based on the effective integration of their individual systems.

Fifteen IMU sensors and the custom-built PCB board made up the project's electrical and electronic system. The IMUs were used based on their performance versus cost capabilities. Extensive design and development of IMU gloves, seen in Chapter 2, represented an effective device for the application. The custom-built PCB board ensured a neat and compact design for the circuitry of the system. With multiple iterations and the addition of LEDs, the PCB board was the ideal solution for this project. The computer system of the project was the Simulink<sup>®</sup> hand model. A hand model was created in Solidworks<sup>®</sup> and imported into Simulink<sup>®</sup> using the Simscape Multibody tool. This allowed the equations of motion of the hand and the mathematical hand model to be created in Simulink<sup>®</sup>. It was an alternate approach that was taken in comparison to other sensory gloves that were developed. The mathematical approach was the same, but Simscape Multibody had the ability to optimize the model. The hand model results showed that it was an effective way to mathematically model the human hand. It also allowed seamless integration with the other elements of the project due to Simulink<sup>®</sup>'s robust capabilities.

The control system consisted of two algorithms that focused on data acquisition from the IMU sensors and post-processing of the data. The data acquisition algorithm captured the data from the sensors and configured the data to represent the individual sensor's roll and pitch values. The pitch values were not used in the second process, but it proved to be a validation test for the system in the early development stage. The roll and pitch values were calculated based on the accelerometer data as there were serial communication limitations when dealing with the gyroscopic data. This was identified and could be further worked on with the use of an advanced microprocessor and fine-tuning of the control algorithm. The post-processing algorithm focused on configuring each sensor on the sensory glove to the respective phalanges on the Simulink<sup>®</sup> model. An averaging filter was implemented to smoothen the data signals and reduce high-frequency noise from the sensors. A preliminary test showed that the

introduction of the averaging filter provided significant improvements to the system. This was all designed and built in Simulink<sup>®</sup> with its MATLAB<sup>®</sup> coder and filter design software.

The project's mechanical system consisted of a low-cost glove for the sensory glove to be built-on. The gloved was durable, malleable and cost-effective to achieve the goals of the project. Protection holders for the sensors were designed and manufactured using 3D printing technology as complex shapes were required. 3D printing the holders provided a cost-effective solution. All the systems were designed and developed to ensure that it had high integration while remaining cost-effective. Therefore, the third objective was achieved by designing and developing a mechatronic sensory device.

In order to test the performance of the designed sensory glove, four tests were conducted on various parameters. These parameters gave an overall operational performance of the sensory glove. The first test aimed at determining the accuracy of the sensory glove while in operation. Pearson's correlation coefficient and Bland-Altman agreement graph showed that the glove was accurate and could be used to track the orientation of a human hand effectively. The dynamic range test focused on establishing the system's ability to track the motion of the sensory glove rapidly. The system could not capture the hand's motion accurately at the pre-determined tempo due to hardware constraints. These constraints could be resolved through a more advanced microprocessor and further improvements to the I2C communication network.

The repeatability test analysed the repeatability of the sensory glove. The test focused on two orientation forms (Flat and Clench phase). The test results showed that the sensory glove was more effective when in the flat phase than in the clench phase. However, when compared to similar sensory gloves, it performed second best. Improvements, such as high-performance IMUs, such as the ADXL 345, and fine-tuning of the control algorithm could improve the device's repeatability. The Application test focused on validating if the sensory glove could be used in an HRC environment. The sensory glove was integrated into a simulated HRC environment to verify if it could collaborate with a robot. A testing algorithm was built and it showed that the sensory glove was able to collaborate with a one hundred percent efficiency. Through these results, the fourth objective of the project was achieved.

The project achieved the four objectives defined at the beginning of the project and answered the research question. The research, design and results showed that it was possible to develop a low-cost mechatronic sensory glove to enable humans and robots to collaborate in a customized environment in an Advanced Manufacturing system. The results also show that safety can be achieved with further improvements in the algorithm design, filtering solution and hardware. This demonstrated the potential impact of the sensory glove if implemented in an FMS environment.

## 8. REFERENCES

1. Adendorff. (2020, November 10). *Adendorff*. Retrieved from MAC AFRIC Working Gloves (Size 10): <https://www.adendorff.co.za/product/mac-afric-working-gloves-size-10/>
2. Adorno, B. V. (2017, April 14). <https://hal.archives-ouvertes.fr/hal-01478225/>. Retrieved from Robot Kinematic Modeling and Control Based on Dual Quaternion Algebra --- Part I: Fundamentals.: <https://hal.archives-ouvertes.fr/hal-01478225/>
3. Baldi, T., Scheggi, S., Meli, L., Mohammadi, M., & Prattichizzo, D. (2017). GESTO: A Glove for Enhanced Sensing and Touching Based on Inertial and Magnetic Sensors for Hand Tracking and Cutaneous Feedback. *IEEE Transactions on Human-Machine Systems*, 1066-1076.
4. Bauer, A., Wollherr, D., & Buss, M. (2008). HUMAN-ROBOT COLLABORATION: A SURVEY. *International Journal of Humanoid Robotics*, 47-66.
5. Bland, J. M., & Altman, D. G. (1986). STATISTICAL METHODS FOR ASSESSING AGREEMENT BETWEEN TWO METHODS OF CLINICAL MEASUREMENT. *THE LANCET*, 307-310.
6. Bradley, D. (2000). Mechatronics - An established discipline or a concept in need of direction. *Proceedings of the 7th Mechatronics Forum International Conference*.
7. Brown, A. S. (2011, August 12). *Mechatronics and the Role of Engineers*. Retrieved from The American Society of Mechanical Engineers: <https://www.asme.org/topics-resources/content/mechatronics-and-the-role-of-engineers>
8. Chen, F., Favetto, A., Mousavi, M., Ambrosio, E., Appendino, S., Battezzato, A., . . . Bona, B. (2011). Human Hand: Kinematics, Statics and Dynamics. *International Conference on Environmental Systems*, (pp. 1-10). Portland, Oregon.
9. Cherubini, A., Passama, R., Crosnier, A., Lasnier, A., & Fraitse, P. (2016). Collaborative manufacturing with physical human-robot interaction. *Robotics and Computer-Integrated Manufacturing*, 1-13.
10. Cobos, S., Ferre, M., Sanchez, M., Ortegom, J., & Pena, C. (2008). Efficient Human Hand Kinematics for Manipulation Tasks. *IEEE/RSJ International Conference on Intelligent Robots and Systems Acropolis Convention Center*. Nice, France,: IEEE.
11. Components101. (2018, March 20). *Arduino Due*. Retrieved from Components101: <https://components101.com/microcontrollers/arduino-due>
12. CyberGlove Systems Inc. (2020, April 15). *CyberGlove III: Overview*. Retrieved from CyberGlove Systems: <http://www.cyberglovesystems.com/cyberglove-iii/>
13. De Luca, A., & Flacco, F. (2012). Integrated control for pHRI: Collision avoidance, detection, reaction and collaboration. *The Fourth IEEE RAS/EMBS International Conference on Biomedical Robotics and Biomechanics* (pp. 288-295). 2012: IEEE.

14. Dictionary.com. (2020, September 29). *Metronome*. Retrieved from Dictionary.com: <https://www.dictionary.com/browse/metronome>
15. Gonzalez-Barajas, J., & Montenegro, D. (2016). Average Filtering: Theory, Design and Implementation. In J. Zhang, *Digital Signal Processing (DSP): Fundamentals, Techniques and Applications*. Hauppauge: Nova Science Publisher.
16. Hansard, M., Lee, S., Choi, O., & Horaud, R. P. (2013). *Time-of-Flight Cameras: Principles, Methods and Applications*. London: Springer-Verlag London.
17. Hayes, A. (2019, September 12). *Flexible Manufacturing System (FMS)*. Retrieved from Investopedia: <https://www.investopedia.com/terms/f/flexible-manufacturing-system.asp>
18. Integrated, M. (2020, August 17). *GLOSSARY DEFINITION FOR PRINTED-CIRCUIT-BOARD*. Retrieved from maxim integrated: <https://www.maximintegrated.com/en/glossary/definitions.mvp/term/Printed-Circuit-Board/gpk/973>
19. Kim, S. Y., Soh, S. B., & Lee, S. (2005). A new wearable input device: SCURRY. *IEEE Transactions on Industrial Electronics*, 1490-1499.
20. Kim, Y., & Bang, H. (2018). Introduction to Kalman Filter and Its Applications. In *Introduction and Implementations of the Kalman Filter* (pp. 1-18). IntechOpen.
21. Knez, L., Slavic, J., & Boltezar, M. (2017). A Sequential Approach to the Biodynamic Modeling of a Human Finger. *Shock and Vibration*, 1-12.
22. Kortier, H., Sluiter, V., Roetenberg, D., & Veltink, P. (2018). *ASSESSMENT OF HAND KINEMATICS AND INTERACTIONS WITH THE ENVIRONMENT*. Enschede: University of Twente.
23. Kucuk, S., & Bingul, Z. (2006). Robot Kinematics: Forward and Inverse Kinematics. In S. Cubero, *Industrial Robotics: Theory, Modelling and Control* (pp. 118-148). Austria: Pro Literatue Verlag.
24. Leber, J. (2013, September 09). *At Volkswagen, Robots Are Coming Out Of Their Cages*. Retrieved from FastCompany: <https://www.fastcompany.com/3016848/at-volkswagen-robots-are-coming-out-of-their-cages>
25. Liu, H., & Wang, L. (2018). Gesture recognition for human-robot collaboration: A review. *International Journal of Industrial Ergonomics*, LXVIII(2), 355-367.
26. Lotz, V., Himmel, S., & Ziefle, M. (2019). You're My Mate - Acceptance Factors for Human-Robot Collaboration in Industry. *International Conference on Competitive Manufacturing* (pp. 405-410). Cape Town: Stellenbosch University.
27. Manus VR. (2020, April 15). *Optitrack: Hybrid Glove*. Retrieved from Manus VR: <https://manus-vr.com/prime-xsens-gloves/>
28. MathworksInc. (2020, June 15). *Simulink*. Retrieved from Mathworks: <https://www.mathworks.com/products/simulink.html>

29. McCall, M. (2020, April 21). *First Robot Collaborates Directly with Employees at Volkswagen Plant*. Retrieved from Businesswire: A Berkshire Hathaway Company: <https://www.businesswire.com/news/home/20130829005825/en/Robot-Collaborates-Employees-Volkswagen-Plant>
30. Mehrabi, N., & MePhee, J. (2019). Chapter Four - Model-Based Control of Biomechatronic Systems. In J. Segil, *Handbook of Biomechatronics* (pp. 95-126). Academic Press.
31. Michalos, G., Makris, S., Spiliotopoulos, J., Misios, I., Tsarouchi, P., & Chryssolouris, G. (2014). ROBO-PARTNER: Seamless Human-Robot Cooperation for Intelligent, Flexible and Safe Operations in the Assembly Factories of the Future. *Confernece on Assembly Technology and Systems* (pp. 71-76). Dresden: Elsevier B.V.
32. Michalos, G., Makris, S., Tsarouchi, P., Guasch, T., Kontovrakis, D., & Chryssolouris, G. (2015). Design consideration for safe human-robot collaborative workplaces. *CIRPe 2015 - Understanding the life cycle implications of manufacturing* (pp. 248-253). N/A: Elsevier B.V.
33. Moreira, A., Queiros, S., Fonseca, J., Rodrigues, P., Rodrigues, N., & Vilaca, J. (2014). Real-time hand tracking for rehabilitation and character animation. *2014 IEEE 3rd International Conference on Serious Games and Applications for Health (SeGAH)* (pp. 1-8). Rio de Janeiro: IEEE.
34. Nanayakkara, V., Cotugno, G., Vitzilaios, N., Venetsanos, D., Nanayakkara, T., & Sahinkaya, M. (2017). The Role of Morphology of the Thumb in Anthropomorphic Grasping: A Review. *Frontiers in Mechanical Engineering*, 1-22.
35. O'Marah, K. (2020, October 13). *Mass Customization and the Factory of the Future*. Retrieved from IndustryWeek: <https://www.industryweek.com/supply-chain/article/22008141/mass-customization-and-the-factory-of-the-future>
36. Oshana, R. (2006). Overview of Digital Signal Processing Algorithms. In R. Oshana, *DSP Software Development Techniques for Embedded and Real-Time Systems* (pp. 59-121). Newnes.
37. Pacchierotti, C., Prattichizzo, D., & Kuchenbecker, K. (2015). Cutaneous feedback back of fingertip deformation and vibration for palpation in robotic surgery. *IEEE Transactions on Biomedical Engineering*, 278-287.
38. Patel, D., Nayak, S., & Venkatkrishna, A. (2018). Design of a wearable sensor glove to measure human hand movement. *Interntaional Journal of Pure and Applied Mathematics*, 547-553.
39. Pedersen, M., Nalpantidis, L., Andersen, R., Schou, C., Bogh, S., Kruger, V., & Madsen, O. (2016). Robot skills for manufacturing: From concept to industrial deployment. *Robotics and Computer-Integrated Manufacturing*, 282-291.
40. Rhadamanthys76. (2016, October 24). *Help modelling palm of a prosthetic hand*. Retrieved from Eng-Tips: <https://www.eng-tips.com/viewthread.cfm?qid=416158>
41. Silva, C. (2005). *Mechatronics: An Intergrated Approach*. Boca Raton: CRC Press.

42. Smith, S. (1999). *The Scientist and Engineer's Guide to Digital Signal Processing*. California: California Technical Publishing.
43. Spiegel, R. (2017, September 21). *Is All Engineering Mechatronics Now?* Retrieved from DesignNews: <https://www.designnews.com/automation-motion-control/all-engineering-mechatronics-now>
44. StatisticsSolution. (2020, September 24). *Pearson's Correlation Coefficient*. Retrieved from Statistics Solutions: <https://www.statisticssolutions.com/pearsons-correlation-coefficient/>
45. TexasInstruments. (2016, September). *SNx4HC138 3-Line To 8-Line Decoders/Demultiplexers*. Dallas, Texas, USA: Texas Instruments Incorporated.
46. UFACTORY. (2020, October 01). *xArm 5 Lite*. Retrieved from UFACTORY: <https://store.ufactory.cc/products/xarm-5-lite-2020>
47. Villani, V., Pini, F., Leali, F., & Secchi, C. (2018). Survey on human–robot collaboration in industrial settings: Safety, intuitive interfaces and applications. *Mechatronics*, 248-266.
48. Weber, P., Reuckert, E., Calandra, R., Peters, J., & Beckerle, P. (2016). A Low-cost Glove with Vibrotactile feedback and Multiple Finger Joint and Hand Motion Sensing for Human-Robot Interaction. *Robot and Human Interactive Communication (RO-MAN)* (pp. 99-104). New York: IEEE.
49. Weisstein, E. W. (2020, November 28). *Euler Angles*. Retrieved from From MathWorld--A Wolfram Web Resource: <https://mathworld.wolfram.com/EulerAngles.html>
50. Williams, N. W., Penrose, M. T., Caddy, C. M., Barnes, E., Hose, D. R., & Harley, P. (2000). A GONIOMETRIC GLOVE FOR CLINICAL HAND ASSESSMENT. *Journal of Hand Surgery (British and European Volume, 2000)*, 200-207.
51. Zanchettin, A., Ceriani, N., Rocco, P., Ding, H., & Matthias, B. (2016). Safety in Human-Robot Collaborative Manufacturing Environments: Metric and Control. *IEEE Transaction on Automation Scirnce and Engineering*, 882-893.

## 9. APPENDIX

### A Arduino<sup>®</sup> Code and Results

#### A.1 Arduino<sup>®</sup> Code for Data Extraction (MPU6050)

```
#include <I2Cdev.h>

#include <MPU6050.h>

#if I2CDEV_IMPLEMENTATION == I2CDEV_ARDUINO_WIRE
#include "Wire.h"
#endif

// class default I2C address is 0x68

// specific I2C addresses may be passed as a parameter here

// AD0 low = 0x68
// AD0 high = 0x69

MPU6050 accelgyro1(0x68);

int16_t ax_0, ay_0, az_0;

int16_t gx_0, gy_0, gz_0;

#define OUTPUT_READABLE_ACCELGYRO

#define LED_PIN 13

bool blinkState = false;

//Defining time variables

float elapsedTime, time, timePrev;
```

```
//Mux control pins

int s0 = 10;

int s1 = 9;

int s2 = 8;

//Mux in "SIG" pin

int SIG_pin = 0;

const int MPU=0x68;

void setup() {

    pinMode(s0, OUTPUT);

    pinMode(s1, OUTPUT);

    pinMode(s2, OUTPUT);

    #if I2CDEV_IMPLEMENTATION == I2CDEV_ARDUINO_WIRE

        Wire.begin();

    #elif I2CDEV_IMPLEMENTATION == I2CDEV_BUILTIN_FASTWIRE

        Fastwire::setup(400, true);

    #endif

    // initialize serial communication

    Serial.begin(38400);
```





```
accelgyro1.initialize();

Serial.println("Testing device connections #0 ...");

Serial.println(accelgyro1.testConnection() ? "MPU6050 connection #0 successful" : "MPU6050
connection #0 failed");

delay(5);

pinMode(LED_PIN, OUTPUT);

}

void loop() {

// ===== MPU: 0 =====

digitalWrite(s0, LOW);

digitalWrite(s1, LOW);

digitalWrite(s2, LOW);

delay(20);

accelgyro1.getMotion6(&ax_0, &ay_0, &az_0, &gx_0, &gy_0, &gz_0);

#ifdef OUTPUT_READABLE_ACCELGYRO

    Serial.print("#0\t a/g:\t");

    Serial.print("aX = "); Serial.print(ax_0/4096.0); Serial.print("\t");

    Serial.print("aY = "); Serial.print(ay_0/4096.0); Serial.print("\t");

    Serial.print("aZ = "); Serial.print(az_0/4096.0); Serial.print("\t");

    Serial.print("gX = "); Serial.print((gx_0/32.8)); Serial.print("\t");

    Serial.print("gY = "); Serial.print((gy_0/32.8)); Serial.print("\t");

    Serial.print("gZ = "); Serial.println((gz_0/32.8));
```

```

#endif

delay(20);

// blink LED to indicate activity

blinkState = !blinkState;

digitalWrite(LED_PIN, blinkState);

}

```

## A.2 Results for Single MPU6050 from Arduino® IDE

```

COM5
MPU6050 connection #0 successful
#0 a/g: aX = -0.13 aY = -6.20 aZ = 4.22 gX = -26.80 gY = 6.04 gZ = -8.90
#0 a/g: aX = -0.14 aY = -6.21 aZ = 4.24 gX = -27.23 gY = 5.18 gZ = -9.24
#0 a/g: aX = -0.14 aY = -6.20 aZ = 4.22 gX = -26.62 gY = 5.76 gZ = -8.96
#0 a/g: aX = -0.15 aY = -6.23 aZ = 4.20 gX = -26.80 gY = 5.61 gZ = -9.15
#0 a/g: aX = -0.11 aY = -6.24 aZ = 4.26 gX = -26.77 gY = 5.15 gZ = -9.18
#0 a/g: aX = -0.14 aY = -6.20 aZ = 4.24 gX = -26.40 gY = 5.46 gZ = -9.30
#0 a/g: aX = -0.16 aY = -6.22 aZ = 4.25 gX = -26.83 gY = 4.51 gZ = -9.24
#0 a/g: aX = -0.13 aY = -6.22 aZ = 4.23 gX = -26.74 gY = 5.82 gZ = -8.78
#0 a/g: aX = -0.15 aY = -6.22 aZ = 4.23 gX = -26.68 gY = 5.52 gZ = -9.15
#0 a/g: aX = -0.13 aY = -6.21 aZ = 4.25 gX = -26.62 gY = 4.66 gZ = -8.48
#0 a/g: aX = -0.12 aY = -6.22 aZ = 4.25 gX = -26.74 gY = 5.27 gZ = -9.09
#0 a/g: aX = -0.14 aY = -6.21 aZ = 4.25 gX = -26.40 gY = 5.15 gZ = -8.78
#0 a/g: aX = -0.13 aY = -6.23 aZ = 4.24 gX = -26.89 gY = 5.85 gZ = -8.63
#0 a/g: aX = -0.16 aY = -6.21 aZ = 4.23 gX = -26.55 gY = 5.21 gZ = -8.90

```

Figure A-1: Results for Single MPU6050 from Arduino® IDE

## B Data Sheets

B.1 Data Sheet pages for MPU6050 (TexasInstruments, 2016)

**Gyroscope Specifications**VDD = 2.375V-3.46V, VLOGIC (MPU-6050 only)= 1.8V±5% or VDD, T<sub>A</sub> = 25° C

Table B-1: Gyroscope Specifications (TexasInstruments, 2016)

PARAMETER	CONDITIONS	MIN	TYP	MAX	UNITS	NOTES
<b>GYROSCOPE SENSITIVITY</b>						
Full-Scale Range	FS_SELFO		±250		°/s	
	FS_SELFI		±500		°/s	
	FS_SELFI2		±1000		°/s	
	FS_SELFI3		±2000		°/s	
Gyroscope ADC Word Length			16		bits	
Sensitivity Scale Factor	FS_SELFO		131		LSBI(°/s)	
	FS_SELFI		655		LSBI(°/s)	
	FS_SELFI2		32.8		LSBI(°/s)	
	FS_SELFI3		16.4		LSBI(°/s)	
Sensitivity Scale Factor Tolerance	25 C	-3		+3	%	
Sensitivity Scale Factor Variation Over Temperature			±2		%	
Nonlinearity	Best fit straight line; 25 C		0.2		%	
Cross-Axis Sensitivity			±2		%	
<b>GYROSCOPE ZERO-RATE OUTPUT (ZRO)</b>						
Initial ZRO Tolerance	25 C		±20		°/s	
ZRO Variation Over Temperature	-40 C to +85 C		±20		°/s	
Power-Supply Sensitivity (1-10Hz)	Sine wave, 100mVpp; VDD=2.5V		0.2		°/s	
Power-Supply Sensitivity (10 - 250Hz)	Sine wave, 100mVpp; VDD=2.5V		0.2		°/s	
Power-Supply Sensitivity (250Hz - 100kHz)	Sine wave, 100mVpp; VDD=2.5V		4		°/s	
Linear Acceleration Sensitivity	Static		0.1		°/g	
<b>SELF-TEST RESPONSE</b>						
Relative	Change from factory trim	-14		14	%	1
<b>GYROSCOPE NOISE PERFORMANCE</b>	FS_SEL=0					
Total RMS Noise	DLPCFG=2 (100Hz)		0.05		°/s <sub>rms</sub>	
Low-frequency RMS noise	Bandwidth 1Hz to 10Hz		0.033		°/s <sub>rms</sub>	
Rate Noise Spectral Density	At 10Hz		0.005		°/s/√Hz	
<b>GYROSCOPE MECHANICAL FREQUENCIES</b>						
X-Axis		30	33	36	kHz	
Y-Axis		27	30	33	kHz	
Z-Axis		24	27	30	kHz	
<b>LOW PASS FILTER RESPONSE</b>						
	Programmable Range	5		256	Hz	
<b>OUTPUT DATA RATE</b>						
	Programmable	4		8,000	Hz	
<b>GYROSCOPE START-UP TIME</b>	DLPCFG=0					
ZRO Settling (from power-on)	to ±1°/s of Final		30		ms	

Please refer to the following document for further information on Self-Test: *MPU-6000/MPU-6050 Register Map and Descriptions*

## Accelerometer Specifications

2.375V-3.46V, VLOGIC (MPU-6050 only)= 1.8V

Table B-2: Accelerometer Specifications (TexasInstruments, 2016)

PARAMETER	CONDITIONS	MIN	TYP	MAX	UNITS	NOTES
<b>ACCELEROMETER SENSITIVITY</b>						
Full-Scale Range	AFS_SELFO		±2		g	
	AFS_SELFI		±4		g	
	AFS_SELFI2		±8		g	
	AFS_SELFI3		±16		g	
ADC Word Length	Output in two's complement format		16		bits	
Sensitivity Scale Factor	AFS_SELFO		16,384		LSB/g	
	AFS_SELFI		8,192		LSB/g	
	AFS_SELFI2		4,096		LSB/g	
	AFS_SELFI3		2,048		LSB/g	
Initial Calibration Tolerance			±3		%	
Sensitivity Change vs. Temperature	AFS_SELFO, -40 C to +85 C		±002		%/C	
Nonlinearity	Best Fit Straight Line		0.5		%	
Cross-Axis Sensitivity			±2		%	
<b>ZERO-G OUTPUT</b>						
Initial Calibration Tolerance	X and Y axes		±50		mg	1
	Z axis		±80		mg	
Zero-G Level Change vs. Temperature	X and Y axes, 0 C to +70 C		±35		mg	
	Z axis, 0 C to +70 C		±60		mg	
<b>SELF TEST RESPONSE</b>						
Relative	Change from factory trim	-14		14	%	2
<b>NOISE PERFORMANCE</b>						
Power Spectral Density	@10Hz, AFS_SELFO & ODR=1kHz		400		μg <sup>2</sup> /Hz	
<b>LOW PASS FILTER RESPONSE</b>						
	Programmable Range	5		260	Hz	
<b>OUTPUT DATA RATE</b>						
	Programmable Range	4		1,000	Hz	
<b>INTELLIGENCE FUNCTION INCREMENT</b>			32		mg/LSB	

1. Typical zero-g initial calibration tolerance value after MSL3 preconditioning
2. Please refer to the following document for further information on Self-Test: *MPU-6000/MPU-6050 Register Map and Descriptions*

## Electrical and Other Common Specifications

2.375V-3.46V, VLOGIC (MPU-6050 only)= 1.8V

Table B-3: Electrical and Other Common Specifications (TexasInstruments, 2016)

PARAMETER	CONDITIONS	MIN	TYP	MAX	Units	Notes
<b>TEMPERATURE SENSOR</b>						
Range			-40 to +85		C	
Sensitivity	Untrimmed		340		LSB/ C	
Temperature Offset	35•c		-521		LSB	
Linearity	Best fit straight line (-40 C to +85 C)		±1		C	
<b>VDD POWER SUPPLY</b>						
Operating Voltages		2.375		3.46	V	
Normal Operating Current	Gyroscope+ Accelerometer+ DMP		3.9		mA	
	Gyroscope+ Accelerometer (DMP disabled)		3.8		mA	
	Gyroscope+ DMP (Accelerometer disabled)		3.7		mA	
	Gyroscope only (DMP & Accelerometer disabled)		3.6		mA	
	Accelerometer only (DMP & Gyroscope disabled)		500		µA	
Accelerometer Low Power Mode Current	1.25 Hz update rate		10		µA	
	5 Hz update rate		20		µA	
	20 Hz update rate		70		µA	
	40 Hz update rate		140		µA	
Full-Chip Idle Mode Supply Current			5		µA	
Power Supply Ramp Rate	Monotonic ramp. Ramp rate is 10% to 90% of the final value			100	m s	
<b>VLOGIC REFERENCE VOLTAGE</b>	MPU-6050 only					
Voltage Range	VLOGIC must be VDD at all times	1.71		VDD	V	
Power Supply Ramp Rate	Monotonic ramp. Ramp rate is 10% to 90% of the final value			3	m s	
Normal Operating Current			100		µA	
<b>TEMPERATURE RANGE</b>						
Specified Temperature Range	Performance parameters are not applicable beyond Specified Temperature Range	-40		+85	C	

## B.2 Pinout Diagram of the Arduino<sup>®</sup> Due (Components101, 2018)

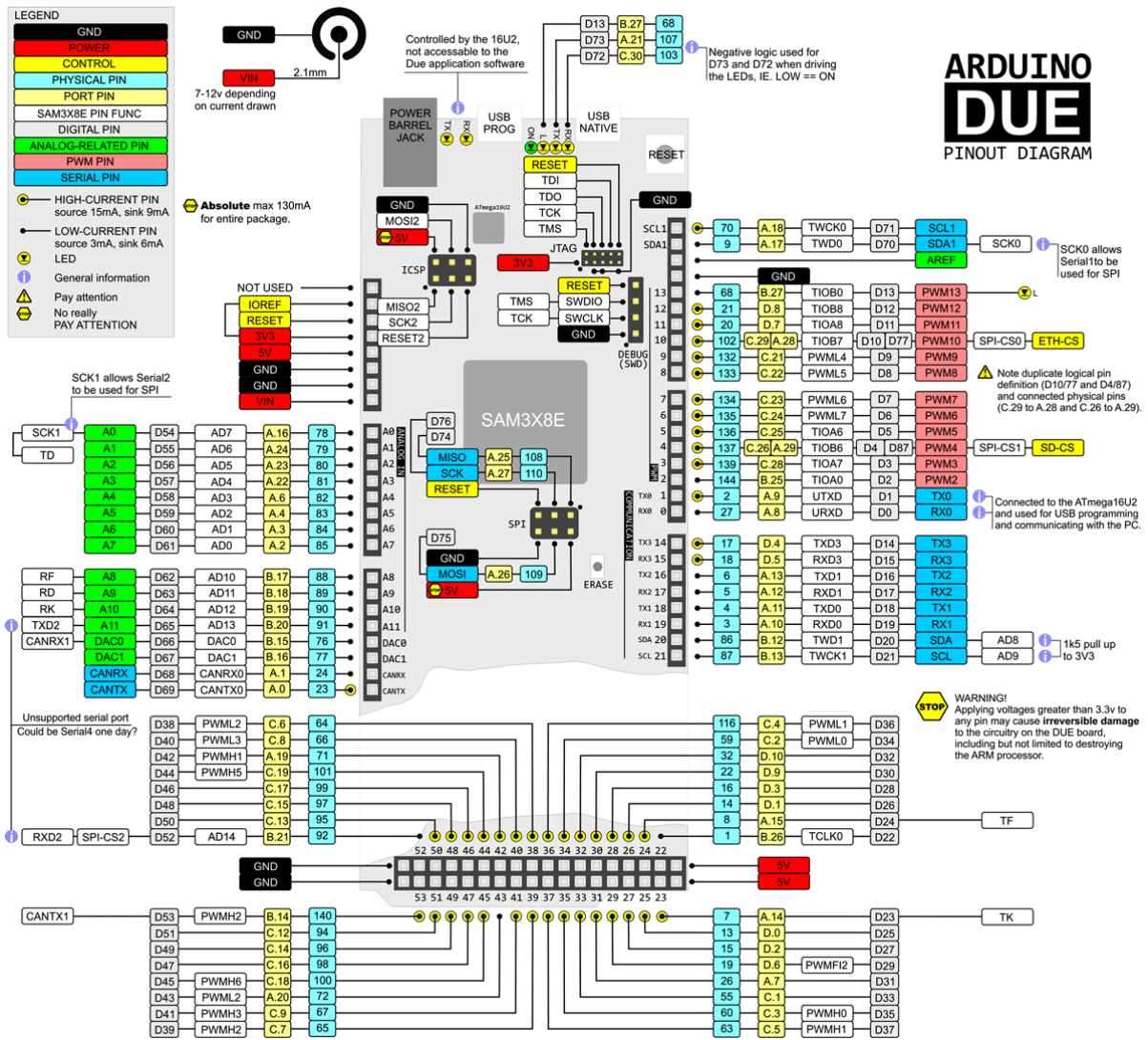


Figure B-1: Arduino<sup>®</sup> Due Pinout Diagram (Components101, 2018)

C Solidwork® CAD Drawings

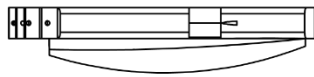
C.1 Human Hand Model

ITEM NO.	PART NUMBER	QTY.
1	PALM	1
2	UPPER SMALL	1
3	MIDDLE SMALL	1
4	LOWER SMALL	1
5	UPPER THIRD	1
6	MIDDLE THIRD	1
7	LOWER THIRD	1
7	UPPER MIDDLE	1
9	MIDDLE MIDDLE	1
10	LOWER MIDDLE	1
11	UPPER INDEX	1
12	MIDDLE INDEX	1
13	LOWER INDEX	1
14	UPPER THUMB	1
15	MIDDLE THUMB	1
16	LOWER THUMB	1

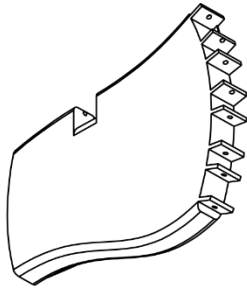
UNLESS OTHERWISE STATED GENERAL TOLERANCES : ± 0.4 mm ANGLES : ± 0.5 °		SCALE: 1:2		No. REQ.: 1		No.: 1	
UNIVERSITY OF KWAZULU-NATAL		STUDENT NAME: T Bright		CHECKED		PROJECT: Human Hand Model	
SCHOOL OF ENGINEERING		STUDENT No.: 215024209		DATE		TITLE: Low-cost Sensory Glove for HRC	
MECHANICAL ENGINEERING		E-MAIL:		PROJECT SUPERVISOR		No.:	
		TEL. No.:		WORKSHOP TECHNICIAN		No.:	
				TECHNICAL OFFICER		No.:	



C.2Palm Model



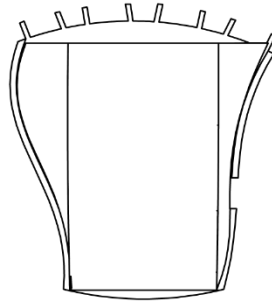
Front View



Isometric View



Top View



Left Side View

UNLESS OTHERWISE STATED GENERAL TOLERANCES :  $\pm 0.4$  mm ANGLES :  $\pm 0.5^\circ$

UNIVERSITY OF KWAZULU-NATAL  
SCHOOL OF ENGINEERING  
MECHANICAL ENGINEERING

MAT.: Polylactic Acid

PROJECT SUPERVISOR

WORKSHOP TECHNICIAN

TECHNICAL OFFICER

DATE

No. REQ.: 1

CHECKED

SCALE: 1:2

STUDENT NAME: T Bright

STUDENT No.: 215024209

E-MAIL:

TEL. No.:

UNITS: mm

PROJECT: Palm of Human Hand Model


TITLE: Low-cost Sensory Glove for HRC

No.:

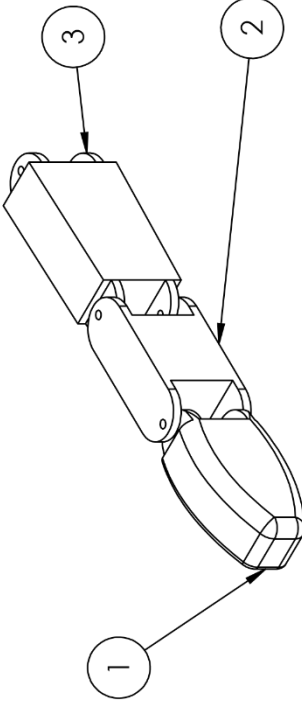
2



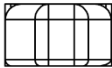
### C.3 Index Finger Assembly



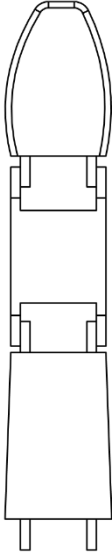
Front View



Isometric View




Top View



Left Side View

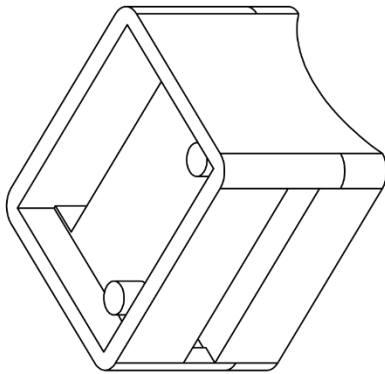
ITEM NO.	PART NUMBER	QTY.
1	UPPER INDEX	1
2	MIDDLE INDEX	1
3	LOWER INDEX	1

PROJECT: Index Finger Assembly TITLE: Low-cost Sensory Glove for HRC	No.: 3 
SCALE: 1:1 STUDENT NAME: T Bright STUDENT No.: 215024209 E-MAIL: TEL. No.:	No. REQ.: 1 CHECKED
MAT.: Polylactic Acid DATE	No. REQ.: 1 CHECKED
PROJECT SUPERVISOR WORKSHOP TECHNICIAN TECHNICAL OFFICER	No. REQ.: 1 CHECKED

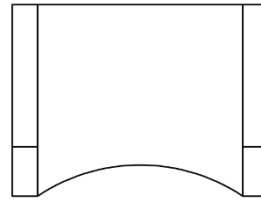
UNLESS OTHERWISE STATED GENERAL TOLERANCES : ± 0.4 mm  
 ANGLES : ± 0.5 °

UNIVERSITY OF KWAZULU-NATAL  
 SCHOOL OF ENGINEERING  
 MECHANICAL ENGINEERING

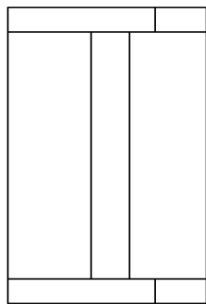
C.4 Sensor Holder



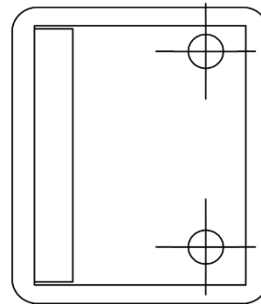
Isometric View



Left Side View



Front View



Top View

UNLESS OTHERWISE STATED GENERAL TOLERANCES:  $\pm 0.4$  mm ANGLES:  $\pm 0.5$

UNIVERSITY OF KWAZULU-NATAL		MAT.: <b>Polylactic Acid</b>		No. REQ.: <b>15</b>	SCALE: <b>2:1</b>	UNITS: mm	PROJECT: <b>Sensor Holder</b>	No.: <b>4</b>
SCHOOL OF ENGINEERING		PROJECT SUPERVISOR	STUDENT NAME: <b>T Bright</b>	CHECKED				
MECHANICAL ENGINEERING		WORKSHOP TECHNICIAN	STUDENT No.: <b>215024209</b>				TITLE: <b>Low-cost Sensory Glove for HRC</b>	
		TECHNICAL OFFICER	E-MAIL:					
			TEL. No.:					

## D MATLAB<sup>®</sup> Code

### D.1 Simulink<sup>®</sup> Write Function

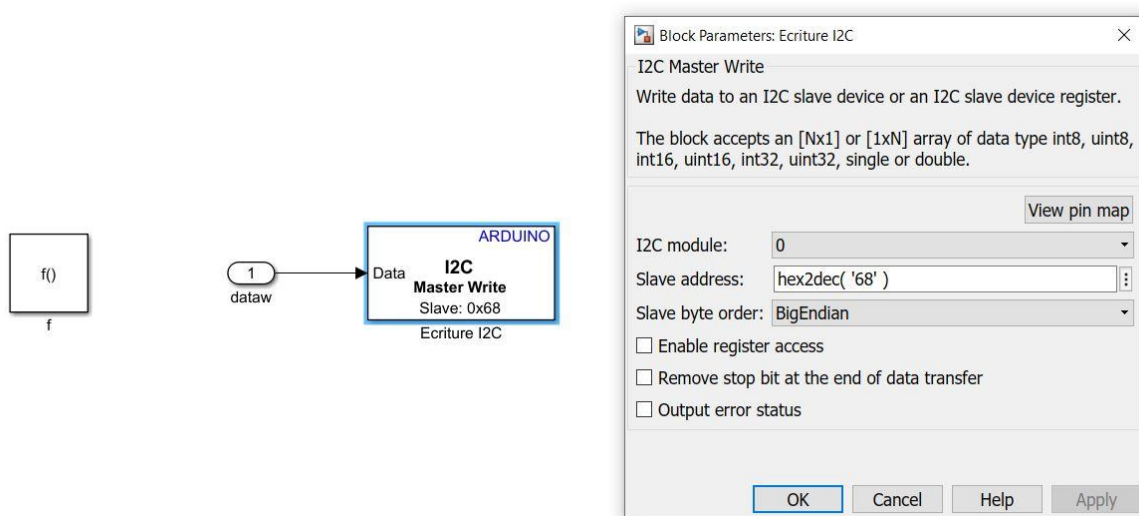


Figure D-1: Simulink<sup>®</sup> Write Function

### D.2 Simulink<sup>®</sup> Read Function

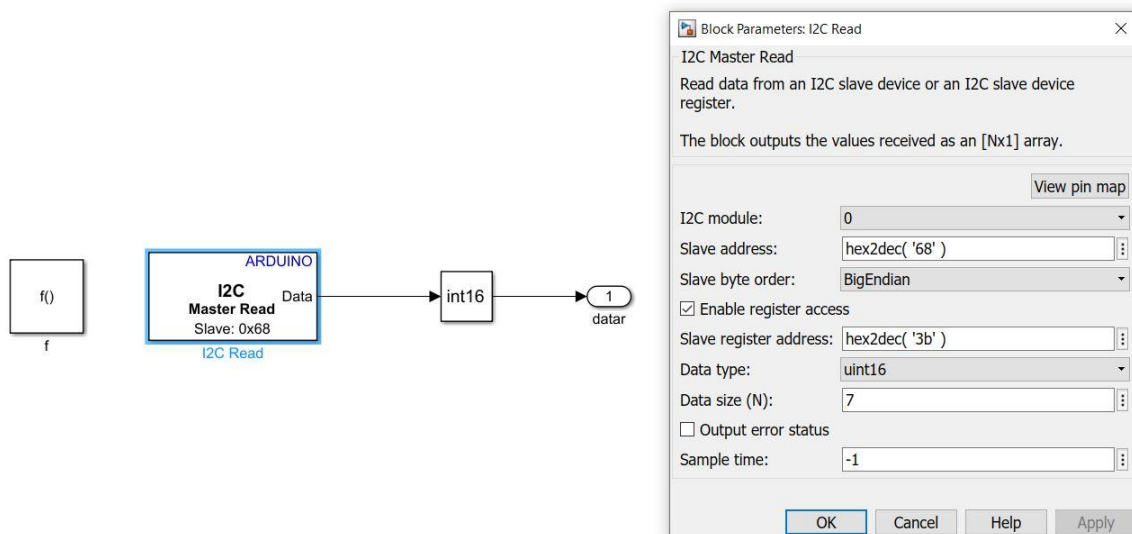


Figure D-2: Simulink<sup>®</sup> Read Function

### D.3 Roll and Pitch Estimation Function

```
function [roll, pitch] = rollAndPitchEstimation(x, y, z)
```

```
pitch = atan2d(-1*y, sign(z)*sqrt(z^2));
roll = atan2d(-1*x, sign(z)*sqrt(z^2));
```

```
end
```

#### D.4 Frequency Spectrum Analysis Function

```

SetupPaths;
applycleaning

for i = 1:5
    func = ['computeFrequencySpectrum(pitchDataDist' num2str(i) ');
    run(func)
    title(['pitchDataDist' num2str(i)])
    func = ['computeFrequencySpectrum(pitchDataMid' num2str(i) ');
    run(func)
    title(['pitchDataMid' num2str(i)])
    func = ['computeFrequencySpectrum(pitchDataProx' num2str(i) ');
    run(func)
    title(['pitchDataProx' num2str(i)])
end

```

#### D.5 Cleaning Function

```

load('C:\Users\user\Documents\MATLAB\SimulinkAndArduinoIntegration\Results for Testing
Section\Test 2 - Dynamic Range\Test for Graph 3.mat')

[pitchDataProx1, pitchDataMid1, pitchDataDist1] = DataPrepOneFinger(out.Pitch, out.Pitch1,
out.Pitch2);

[pitchDataProx2, pitchDataMid2, pitchDataDist2] = DataPrepOneFinger(out.Pitch3, out.Pitch4,
out.Pitch5);

[pitchDataProx3, pitchDataMid3, pitchDataDist3] = DataPrepOneFinger(out.Pitch6, out.Pitch7,
out.Pitch8);

[pitchDataProx4, pitchDataMid4, pitchDataDist4] = DataPrepOneFinger(out.Pitch9, out.Pitch10,
out.Pitch11);

[pitchDataProx5, pitchDataMid5, pitchDataDist5] = DataPrepOneFinger(out.Pitch12, out.Pitch13,
out.Pitch14);

```

## D.6 Data Prep Function

```
figure;
```

```
plot(pitch)
```

```
pitchData(:,1) = double(pitch.Time);
```

```
pitchData(:,2) = double(pitch.Data);
```

```
negInd = pitchData(:,2) > -180 & pitchData(:,2) < -50;
```

```
pitchData(negInd,2) = pitchData(negInd,2) + 360;
```

```
figure
```

```
plot(pitchData(:,2))
```